# ABSTRACT

Title of Dissertation: PATTERNS OF REACTIVITY OF
LANTIBIOTICS SUBTILIN AND NISIN
WITH MOLECULAR TARGETS IN
*Bacillus cereus* AND *Bacillus subtilis* 168

Srilatha Kuntumalla, Doctor of Philosophy, 2005

Dissertation Directed By: Professor J. Norman Hansen
Department of Chemistry and Biochemistry

Subtilin and nisin belong to a unique class of antibiotics called lantibiotics that contain unusual dehydro and lanthionine amino acid residues. The gene-encoded antimicrobial peptides subtilin and nisin exhibit bactericidal effects against several Gram-positive bacteria and also inhibit bacterial spore outgrowth.

Subtilin and nisin are structural analogs and possess similar mechanisms of antimicrobial action. Although nisin is very stable, subtilin previously isolated was highly unstable with loss of biological activity observed during storage. Subtilin isolated in this work using hydrophobic interaction chromatography was very stable, with biological activity retained for at least a few months after isolation.

The possibility that specificity of subtilin and nisin towards sensitive Gram-positive bacteria is due to interaction of these lantibiotics with specific target proteins in susceptible bacteria was explored in this work. Phage display experiments performed to detect peptides interacting with subtilin identified a 12-mer peptide with a KTTLL motif found in ATP binding proteins such as ABC transporters and protein synthesis initiation

factor IF-2 (~78 kDa). Binding of subtilin to specific ABC transporters in bacterial cell membrane would contribute to its specificity. Binding of subtilin to IF-2 would result in inhibition of protein synthesis suggesting an alternative mechanism of action for subtilin.

Experiments performed to determine the nature of interaction of subtilin and nisin with bacterial cellular proteins detected both covalent and non-covalent interactions. The covalent interactions between bacterial proteins and subtilin or nisin were stable on boiling in SDS and analyzing by SDS-PAGE. These stable covalent adducts indicated that the electrophilic dehydro residues of subtilin and nisin were probably involved in covalent attachment with specific nucleophilic groups in bacterial protein targets. Covalent attachment of an antibiotic to its bacterial target has been previously observed with only a few antibiotics.

Sites of nisin attachment to bacterial spores as visualized by electron microscopy showed nisin binds to highly localized regions on spore surfaces. Attempts to identify bacterial protein targets of subtilin and nisin using monomeric avidin and anti-FITC columns, respectively, resulted in isolation of proteins in ~70-80 kDa range. Further characterization of these proteins should help in understanding the specificity and antimicrobial mechanism of action of nisin and subtilin.

PATTERNS OF REACTIVITY OF
LANTIBIOTICS SUBTILIN AND NISIN
WITH MOLECULAR TARGETS IN
*Bacillus cereus* AND *Bacillus subtilis* 168


By


Srilatha Kuntumalla


Dissertation submitted to the Faculty of the Graduate School of the
University of Maryland, College Park, in partial fulfillment
of the requirements for the degree of
Doctor of Philosophy
2005


Advisory Committee:

Professor J. Norman Hansen, Chair
Associate Professor Ibrahim Z. Ades
Associate Professor Douglas A. Julin
Research Professor J. Frederic Mushinski
Associate Professor Judd O. Nelson

Dedications


To Mr. Chinnaiah, my grandfather

For your immense encouragement and innumerable sacrifices

Wish you were here now

To Vijay Shankar, my brother

Miss you very much

To Dr. Konappa and Mrs. Padmavathi, my parents

For being there, for letting me pursue my dreams

No matter how hard it was for you

To Mr. Sainath and Mrs. Lakshmi, my uncle and aunt

Without your moral and financial support, I wouldn't be here

Thanks for believing in me

And to Yogitha, my sister

For not giving up

Acknowledgements

I would like to express my thanks to my research advisor, Dr. J. Norman Hansen, for his guidance and patience through the years.

I would also like to thank all of my advisory committee members for their advice and encouragement, including Dr. Ibrahim Z. Ades, Dr. Douglas A. Julin, Dr. Jason D. Kahn, Dr. Ian H. Mather, Dr. J. Frederic Mushinski and Dr. Judd O. Nelson.

I would like to thank Dr. Dorothy Beckett for instructing me in using the analytical ultracentrifuge. I would also like to thank Dr. Tim Maugel for teaching me about electron microscopy.

I would like to thank all the past and present members of this laboratory. From the past, I would like to thank Dr. Martha Ligon Dang, Dr. Brian Balgley, Dr. Amer Villaruz, Dr. Leena Paul, Dr. Virginia Rodriguez, Faiza Malik, Dr. Sun Paik, Monika Sharma, Gaobo Zhou and Dr. Sahru Yuksel. In particular, I would like to thank Mimi, Faiza and Brian for their friendship and support. I would also like to thank Amer for teaching me lab techniques. From the present, I thank William Shadrick and Mike Thomas for their friendship. I would also like to thank all of my friends, in particular, Suresh Chellapilla, Dr. Sandeep Krishnan, Dr. Vikas Anathy and Dr. Suvarna Sathe, for their encouragement, help and moral support. I am greatly indebted to my large family of parents, uncles and aunts for their patience, encouragement and support all throughout these long years of doctoral studies. I would also like to acknowledge and thank NIH and JIFSAN for supporting this research.

Table of Contents

vi

List of Figures

List of Tables

## List of Abbreviations

| | |
|---|---|
| Ab | antibody |
| Abs | absorbance |
| AP | alkaline phosphatase |
| APS | ammonium persulfate |
| BCIP | 5-bromo-4-chloro-3-indolyl-phosphate |
| BSA | bovine serum albumin |
| *cat* | chloramphenicol transacetylase gene |
| $cm^{10}$ | chloramphenicol (10 µg/ml) |
| Da | daltons |
| $ddH_2O$ | distilled deionized water |
| Dha | dehydro alanine |
| Dhb | dehydro butyrine |
| DMF | N, N - dimethyl formamide |
| dNTP (dATP, dTTP, dCTP, dGTP) | deoxyribonucleoside triphosphate |
| ddNTP (ddATP, ddTTP, ddCTP, ddGTP) | dideoxyribonucleoside triphosphate |
| DTT | dithiothreitol |
| EDTA | ethylenediaminetetraacetic acid |
| EtBr | ethidium bromide |
| FITC | fluorescein iso thio cyanate |
| HPLC | high performance liquid chromatography |
| h | hour |

| | |
|---|---|
| IPTG | isopropyl-β-thiogalactopyranoside |
| kDa | kilodalton |
| Lan | lantibiotic |
| LB | Luria-Bertani medium |
| L | liter |
| MALDI-TOF-MS | matrix-assisted laser desorption/ionization – time of flight mass spectrometry |
| 2-ME | 2-mercaptoethanol |
| Me-Lan | β-methyl lanthionine |
| μg | microgram |
| μl | microliter |
| μM | micromolar |
| μm | micrometer |
| ml | milliliter |
| mM | millimolar |
| M | molar |
| min | minute |
| MS/MS | mass spectrometry/mass spectrometry |
| mV | millivolt |
| MW | molecular weight |
| $m/z$ | mass/charge |
| NBT | nitro blue tetrazolium chloride |
| NC membrane | nitrocellulose membrane |

| | |
|---|---|
| ng | nanogram |
| nM | nanomolar |
| PAB | Penassay broth (antibiotic medium 3) |
| PAGE | polyacrylamide gel electrphoresis |
| PBS | phosphate buffered saline |
| PEG | polyethylene glycol |
| pfu | plaque forming units |
| rpm | revolutions per min |
| RT | room temperature |
| sec | second |
| ss | single-stranded |
| SDS | sodium dodecyl sulfate |
| TBE | Tris-borate EDTA |
| TBST | Tris-buffered saline - Tween 20 |
| TEMED | N, N, N',N', tetramethylenediamine |
| TFA | trifluoroacetic acid |
| Tris | Tris (hydroxylmethyl) aminomethane |
| wt | weight |
| w/v | weight/volume |
| X-Gal | 5-bromo-4-chloro-3-indolyl-$\beta$-galactoside |

**Introduction**

Part I. Antibiotics and the problem of bacterial resistance.

Antibiotics are chemical compounds synthesized by microorganisms that can inhibit the growth of or kill other microorganisms (74). Antibiotics can be classified as non-peptide antibiotics like tetracycline or peptide antibiotics like gramicidin S (32), (83). Peptide antibiotics can be synthesized by multienzyme complexes (penicillin) or by ribosomal mechanisms as seen in lantibiotics (83). Modes of action of antibiotics include interference with DNA replication, transcription, translation, cell wall biosynthesis and cell membrane integrity (53) by forming pores or ion channels in membrane bilayers and inhibiting enzyme reactions (29).

Antibiotics are the primary agents used to treat microbial infections. Unfortunately, bacterial resistance to the antibiotics in use has been steadily increasing. Measures taken to combat this problem have involved improving the currently available antibiotics, discovering new antibiotics or inventing new antibiotics. However, modification of existing antibiotics like penicillin has not been able to ward off bacterial infections for long and has led to the evolution of bacteria resistant to the modified penicillins (34). In addition, designing variants of enzyme-synthesized antibiotics like penicillin involves organic synthesis, which limits the number of structural variants that can be synthesized and tested.

Also, screening of microorganisms for new antibiotics over the past several years has not been very successful as it involves screening a multitude of microorganisms. The few new substances that could be found are likely to belong to an already known antibiotic class which would therefore not be very effective for long (82). It is easier to

alter the reactivity and specificity of already known and effective antibiotics that are gene-encoded in order to invent new antibiotics. The advantage that gene-encoded antibiotics have over conventional enzyme-synthesized antibiotics is that it is possible to make a great variety of mutants by site-directed mutagenesis to generate analogs that exhibit enhanced antimicrobial activity.

Part II. Lantibiotics: unusual peptide antibiotics.

Lantibiotics produced by Gram-positive bacteria form an example of gene-encoded peptide antibiotics (52). Lantibiotics are so named because of the presence of lanthionine rings (Fig. 1). Lanthionine formation is a result of posttranslational modification and involves the reaction of a dehydrated serine or threonine with cysteine residues through thioether linkages (Fig. 2) resulting in the formation of lanthionine (Ala-S-Ala) or β-methyl lanthionine (Aba-S-Ala), respectively (24), (83). The presence of these unusual residues, their influence on structure and activity of the peptides and their unique biosynthetic pathways have caused them to be targets of research (62). Lantibiotics can be classified into types A, B and C according to their structural features (Fig. 3). Type A lantibiotics are linear, cationic peptides which include nisin, subtilin and sublancin. Type B such as cinnamycin are less cationic or neutral, while type C lantibiotics like mersacidin are small and neutral (24).

Part III. Type A lantibiotics – nisin and subtilin.

Two well-studied type A lantibiotics are nisin and subtilin produced by *Lactococcus lactis* ATCC 11454 and *Bacillus subtilis* ATCC 6633, respectively. Nisin

**Figure 1. Structures of dehydro residues and lanthionine residues.**

The unusual dehydro residues and lanthionine residues observed in lantibiotics are formed as a result of post-translational modifications of naturally occurring amino acids (Sahl, *et al.*, 1995).
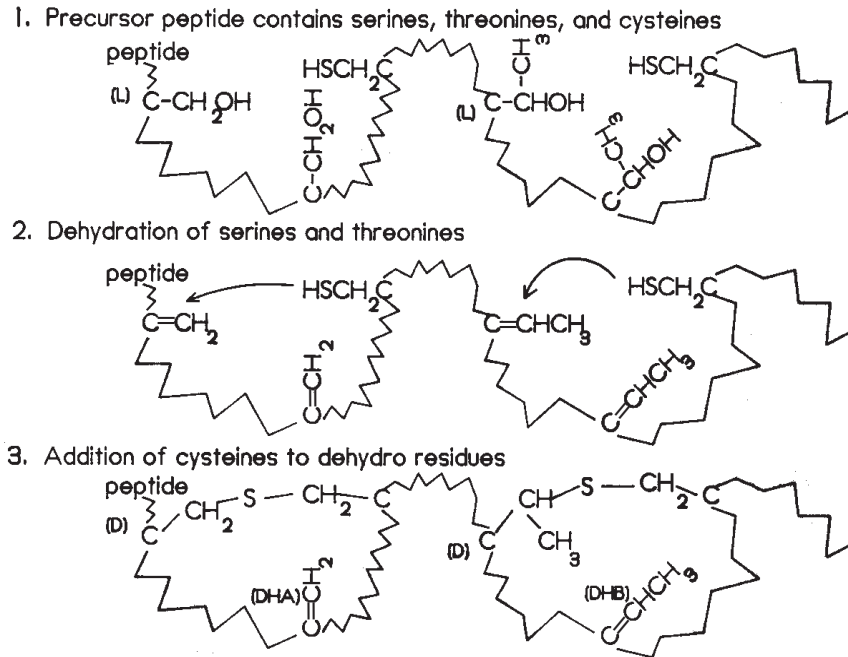
**Figure 2. Formation of dehydro and lanthionine residues.**

Enzyme-catalyzed dehydration of serines and threonines during posttranslational modifications results in the formation of dehydroalanine (Dha) and dehydrobutyrine (Dhb), respectively. Nucleophilic addition of the sulfhydryl group of cysteine to Dha and Dhb leads to the formation of lanthionine and β-methyl lanthionine, respectively (Hansen, J.N., 1993).

4
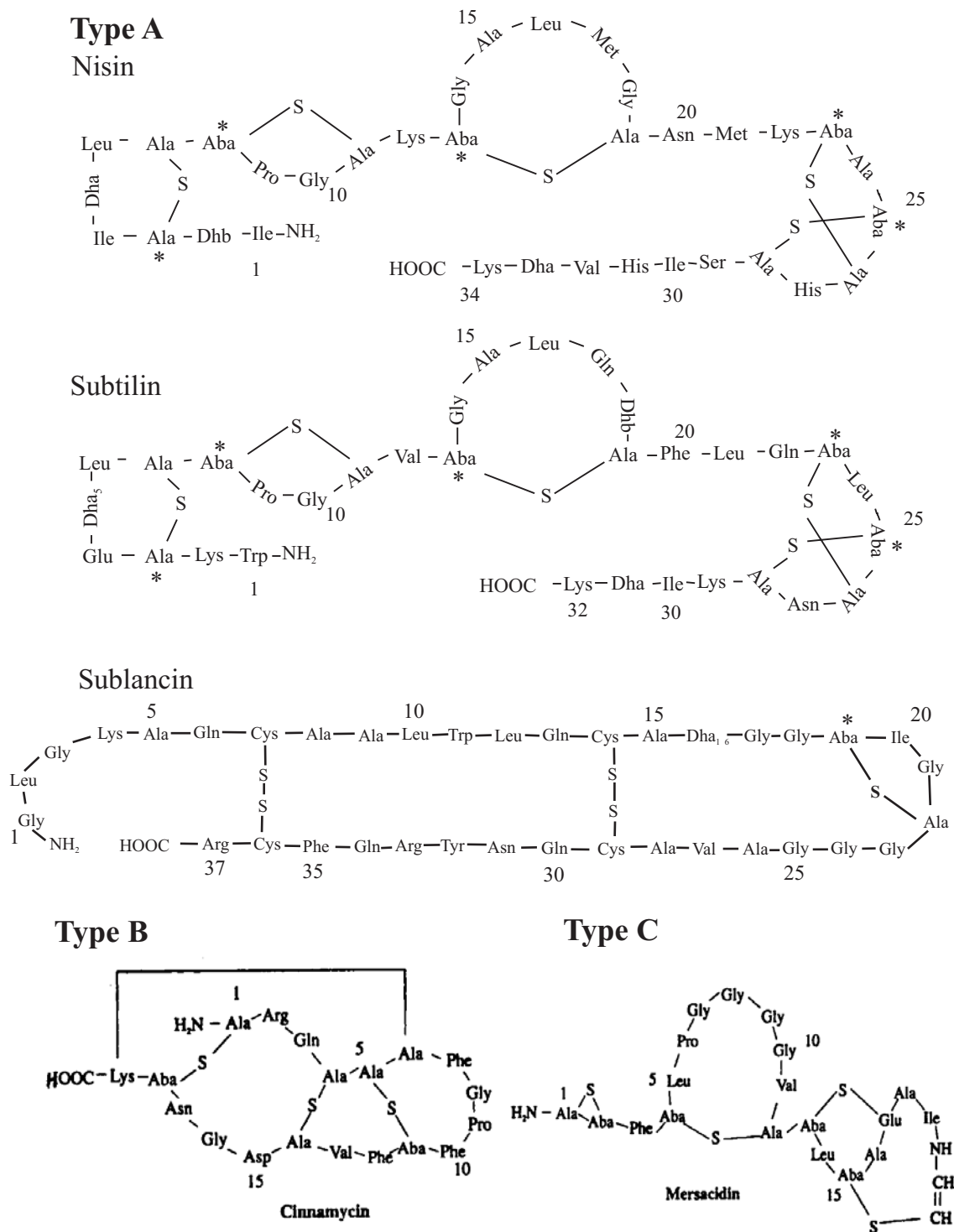
**Figure 3. Structures of few type A, type B and type C lantibiotics.**

Lantibiotics are classified into type A, type B and type C based on their structural features. Nisin, subtilin and sublancin belong to type A (nisin-like) lantibiotics. Cinnamycin is a type B (duramycin-like) lantibiotic, and mersacidin is a type C lantibiotic (Hansen, J.N., 1997).

5

and subtilin are structural analogs exhibiting 60% identity in their amino acid residues (22). Nisin is a peptide of 34 amino acids while subtilin has 32 amino acids. Both peptides possess three dehydro residues - two Dha and one Dhb, and five lanthionine rings (31), (42). The lanthionine rings are named alphabetically with ring A at the amino terminus. Another type A lantibiotic is sublancin with 37 amino acid residues, including a Dha residue and a lanthionine ring. Sublancin differs from other lantibiotics in exhibiting the presence of disulfide bridges, instead of the thioether linkages seen in other lantibiotics (57).

Subtilin and nisin are synthesized as precursor peptides with leader peptides at the N terminus comprising 24 and 23 amino acid residues, respectively, that must be cleaved to give the mature lantibiotic. Biosynthesis of subtilin involves multiple genes arranged in a cluster on the *B. subtilis* ATCC 6633 chromosome, comprising the *spaBTCSIFGRK* gene cluster. The subtilin structural gene, *spaS,* is located in the middle of the gene cluster. Enzyme SpaB is responsible for dehydration of serines and threonines whereas SpaC is involved in lanthionine ring formation. The SpaT protein exhibits characteristics of ATP-binding cassette (ABC) transporters and participates in transport of subtilin. SpaIFG proteins appear to participate in immunity against secreted subtilin. SpaK and SpaR are involved in the regulation of subtilin synthesis (2), (28). In contrast to the subtilin gene cluster, the nisin genes are located on a conjugative transposon comprising the *nisABTCIPRKFEG* gene cluster (69). Nisin is synthesized as a prepropeptide from the *nisA* gene and then modified posttranslationally by a membrane localized enzyme complex consisting of the NisB and NisC proteins. The modified prepeptide is then transported through the cellular membrane by the NisT protein. The mature peptide is

then released into the extracellular medium after being proteolytically cleaved by NisP (Fig. 4). Immunity to the mature nisin molecule is possibly provided by the NisI lipoprotein, which could interact with the extracellular nisin and prevent it from binding to the cell membrane (65). Alternatively, the ABC transporter system comprising of proteins NisE, NisF and NisG may participate in the active transport of mature nisin into the cell which is subsequently degraded to protect the cell from mature nisin (13), (16).

Part IV.  Applications of lantibiotics.

Nisin has found application as a food preservative after being granted GRAS (generally recognized as safe) status in 1988 (23). Nisin is the only antibiotic approved by the FDA for use as a food preservative. Nisin has also been approved as a food preservative in 50 countries worldwide. Specifically, nisin is used to increase the shelf-life of dairy products such as cheese and ice cream as it inhibits not only bacterial spore outgrowth but also vegetative bacterial cells. Nisin is also used in meat products, and is being considered as an alternative to the potentially carcinogenic nitrite used as a food preservative. Use of nisin in beer and wine is another growing application (24).

Lantibiotics exhibit a broad spectrum of action against Gram-positive bacteria. With the exception of *Neisseria gonorrhoeae* (49), lantibiotics are generally not active against Gram-negative bacteria unless the lipopolysaccharide layer has been treated with chelating agents such as EDTA (71). Nisin has been shown to inhibit several Gram-positive bacteria such as *Enterococcus faecalis* ssp. *liquefaciens* ATCC 27959, *Staphylococcus aureus* ATCC 29740, *Staphylococcus epidermidis* ATCC 14990, several species of *Streptococcus* and *Bacillus*, and a few species of *Clostridium* (23). Nisin also
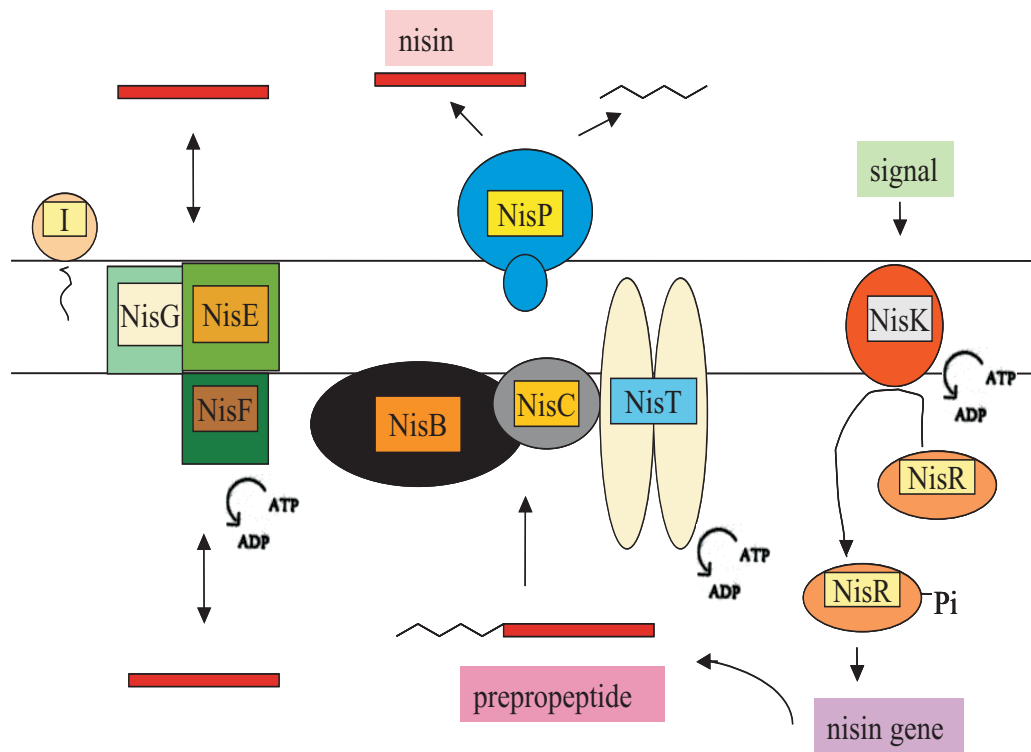
**Figure 4. Model for nisin biosynthesis.**

Activation of the sensor histidine kinase NisK protein by a signal leads to the activation of the response regulator NisR protein. NisR then activates the nisin gene to produce the nisin prepropeptide which undergoes specific dehydrations and thioether modifications. The modified prepeptide is then transported through the cell membrane by the NisT protein. The leader peptide is cleaved by NisP to release the mature nisin peptide. NisI and NisGEF provide immunity to mature nisin (Entian, *et al.*, 1996).

8

inhibits *Bacillus cereus* spores as well as vegetative *B. cereus* cells. *Bacillus cereus* is an opportunistic human pathogen causing contamination problems in dairy products leading to food poisoning. The genomes of *Bacillus cereus* and *Bacillus anthracis* exhibit a close similarity, suggesting that they could be considered as belonging to the same species, with the functional differences arising as a result of genes carried on different plasmids in the two organisms (25). The spore-forming *B. anthracis* causes the lethal disease anthrax and is therefore of concern as a possible agent in biological warfare. *Bacillus cereus* and *B. anthracis* are genetically very closely related, and therefore, nisin could potentially be used to combat *B. anthracis*. Coughlin *et al.* showed that formulations containing nisin, chelator, detergent, and alcohol inhibited growth of spores and vegetative cells of a test strain of *B. anthracis* (11).

Other lantibiotics that have been studied include epidermin and mersacidin. Epidermin, a type A lantibiotic, has been used in the treatment of skin diseases such as acne (30). Mersacidin, a type C lantibiotic, was shown to be effective in treating systemic staphylococcal infections by affecting a target that is not attacked by the current drugs (5). This offers hope in developing new antimicrobial substances that are active against methicillin-resistant staphylococci or vancomycin-resistant enterococci. An example of a modified antibiotic with increased antimicrobial activity is E4I subtilin, which exhibited enhanced biological activity and stability when Glu4, a residue adjacent to Dha5, was altered to Ile4. The mutant E4I subtilin exhibited a three-fold increase in antimicrobial activity and a 60-fold increase in chemical stability mainly on account of changing the amino acid environment around Dha5 (44).

Lantibiotics therefore form interesting objects of study on account of the unique amino acid residues and the high amount of amino acid modifications. The lanthionine rings confer local rigidity, protease stability and increased temperature insensitivity while the dehydro residues are important in antimicrobial activity (30). Deciphering the structure-function relationship of these residues could aid in the development of newer antibiotics targeted against resistance-developing pathogens.

Part V.  Antimicrobial mechanism of type A lantibiotics subtilin and nisin.

This points to the importance of understanding the mechanism of the antimicrobial effect of these lantibiotics. Two modes of bacterial growth inhibition have been suggested for type A lantibiotics, one which involves the pore-forming ability of the lantibiotics in vegetative bacterial cells and another in which the dehydro residue plays an important role in inhibition of spore outgrowth. Type B lantibiotics affect enzyme function while type C lantibiotics inhibit cell wall biosynthesis in susceptible bacteria (29), (62).

Part V-1.  Pore forming mechanism in bacterial vegetative cells.

The mechanism of pore formation by type A lantibiotics has been thoroughly studied, mainly using nisin as a model. Pore formation involves diffusion of nisin through the cell wall, association of nisin with the cell membrane surface, followed by insertion of nisin aggregates into the membrane in the presence of a sufficiently high transnegative membrane potential (62) or a transmembrane pH gradient (inside alkaline) resulting in pores. Experiments involving the activity of nisin on bacterial cells artificially energized

10

by valinomycin speculated a range of –50 mV to -80 mV as the threshold potential ($\Delta\Psi$) required for nisin to form pores (63). In the absence of $\Delta\Psi$, nisin can form pores when the pH gradient is alkaline inside the cell (19), (48).

Nisin forms pores with a diameter of approximately 1 nm while subtilin pores are approximately 2 nm in diameter (62), (67). Nisin and subtilin exhibit subtle differences in the mechanism of pore formation. Subtilin forms more stable pores which are larger in size compared to nisin (67), (33). This has been explained to be due to the absence of charged amino acids in the central domain of subtilin (residues 5-28), which increase the hydrophobicity of subtilin that could facilitate membrane insertion and therefore, lead to the formation of more stable pores. The affinity of nisin is strongly dependent on the presence of negatively charged phospholipids and based primarily on electrostatic interactions, while subtilin may partially penetrate into membranes with its hydrophobic central domain (33).

Nisin and subtilin are thought to consist of two domains connected by a flexible hinge. Lanthionine rings A, B and C in the N-terminus form one domain while rings D and E in the C-terminus form the other domain with the hinge region composed of amino acids 20-22 (62). Intact rings A and C have been shown to be essential for antibacterial activity of nisin (8). This evidence supports the wedge model (Fig. 5) proposed by Moll *et al*. for the formation of pores by nisin in the bacterial membrane which postulates that the N-terminal part of nisin, comprising rings A and C, is responsible for binding of nisin to the membrane and/or its oligomerization, while the more cationic C-terminal part of the molecule plays a significant role in pore formation. The flexible hinge region is thought to act as a twist that allows nisin to bend the lipid surface, giving rise to a wedge-
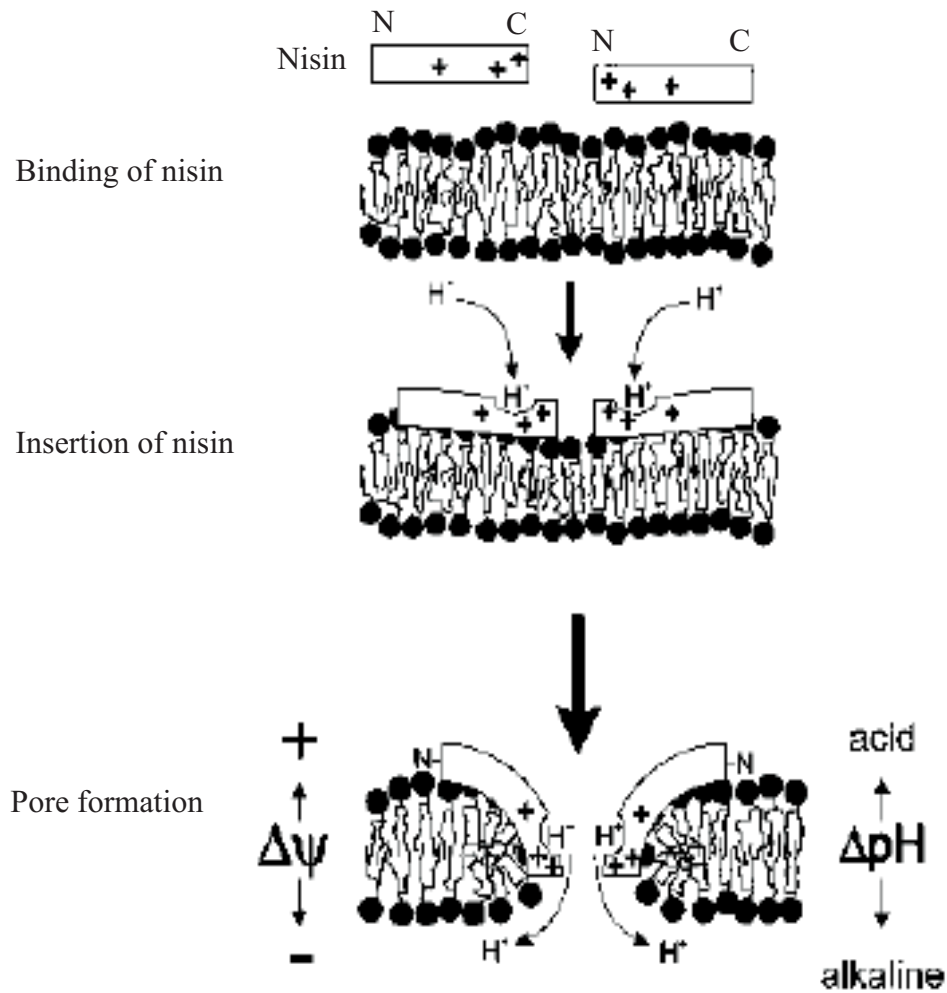
**Figure 5.  Wedge model of pore formation by nisin.**

In the wedge model, pore formation by nisin involves three steps - binding of nisin to the cell membrane, followed by insertion of nisin into the cell membrane which subsequently results in wedge-like pore formation. Binding of nisin leads to perturbation of the bilayer surface. A transnegative membrane potential or a pH gradient (inside alkaline) can induce the insertion of nisin into the cell membrane. Coinsertion of bound phospholipids together with the C-terminus of nisin results in bending of the lipid surface, leading to a wedge-like pore (Moll, *et al*., 1997).

like pore. Nisin is considered to be amphipathic in the pores and oriented with its hydrophobic side towards the membrane and with its hydrophilic side towards the water-filled channel (76). The adhesion of the amphiphilic molecules to the surface of the cell membrane causes destabilization of the bilayer structure by disturbing the lipid dynamics near the phospholipid polar headgroup-water interface (14). The presence of a transnegative membrane potential above a threshold or transmembrane pH gradient (inside alkaline) may change the orientation of nisin in the membrane relative to the plane of the membrane and drive the membrane insertion of the phospholipid surface-bound molecules (14), (48). The carboxyl terminal residues carrying a net positive charge, together with the bound lipids, are then drawn across the membrane forming a wedge to form a water-filled pore. Pore formation leads to an efflux of ions, amino acids and ATP resulting in cell death. Nisin exhibits no selectivity for charge and size of the efflux, as the efflux velocity remains unchanged for small ions like $Rb^+$ and for larger positively or negatively charged amino acids. This suggests that nisin causes a generalized membrane perturbation rather than a channel with finite size (61). Transient, multi-state pores are formed by nisin and subtilin, which require the aggregation of several peptide molecules in a transmembrane orientation (33).

The wedge model proved to be a good model to illustrate the effect of nisin on model membranes. However, the wedge model failed to explain the observation that micromolar concentrations of nisin were required for pore formation in model membranes, whereas nanomolar concentrations of nisin were sufficient to inhibit living bacterial cells (79). This effect was explained by proposing a model involving the role of lipid II as a docking molecule for nisin (Fig. 6). The lipid II-mediated nisin pore

13
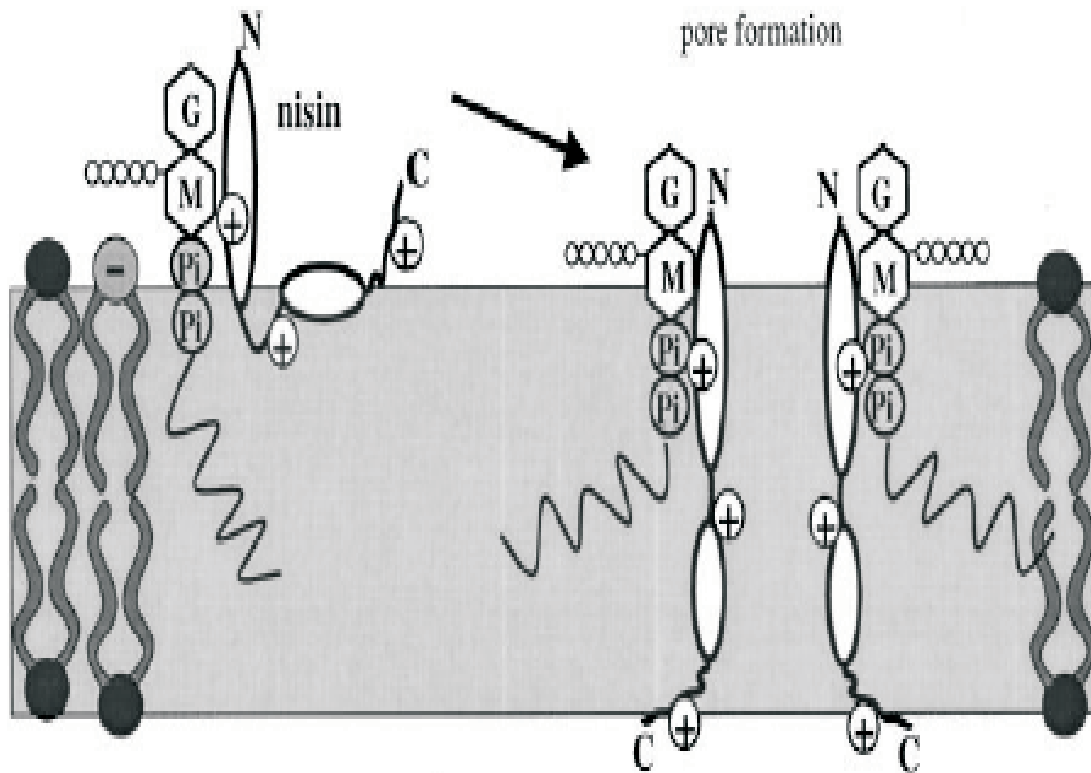
**Figure 6. Lipid II-mediated model of pore formation by nisin.**

The lipid II-mediated model of pore formation by nisin proposes that lipid II, a peptidoglycan precursor acts as a docking molecule for nisin. Nisin first binds to the carbohydrate moiety of lipid II through its N-terminal segment. The C-terminal part of nisin then translocates across the cell membrane. Interaction of nisin with lipid II may stabilize the transmembrane orientation of nisin. Several nisin-lipid II complexes assemble together to form a functional pore resulting in the efflux of metabolites and cell lysis (Wiedemann, *et al*., 2001).

formation model proposed that nisin uses lipid II as a docking molecule for subsequent pore formation. Lipid II is a precursor of peptidoglycan, which comprises the bacterial cell wall. The model proposed that nisin first binds to the carbohydrate moiety of lipid II in a 1:1 stoichiometry through its N-terminal segment. The C-terminal part of nisin then translocates across the cell membrane. Interaction of nisin with lipid II may stabilize the transmembrane orientation of the nisin molecule. Several such nisin-lipid II complexes assemble to form a functional pore resulting in the efflux of metabolites from the cell and eventual cell lysis (79).

Part V-2. Mechanism of inhibition of bacterial spore outgrowth.

The second mechanism of antimicrobial action of nisin and subtilin involves their ability to inhibit bacterial spore outgrowth probably by covalent modification. The electrophilic dehydro residues are speculated to react with nucleophilic sulfhydryl groups on the surface of germinating spores. This was supported by experiments which showed that covalent modification of a nucleophilic sulfhydryl group in germinating spores by iodoacetate resulted in inhibition of *B. cereus* spore outgrowth (50). Further, nisin was shown to compete with iodoacetate, which modifies membrane sulfhydryl groups, for binding to germinated spores (51). The spore inhibiting activity has been critically linked to Dha5 in ring A. Mutation of Dha5 to Ala in subtilin (44) and nisin (8) resulted in loss of inhibition of spore outgrowth but had no effect on the ability to cause cell lysis of vegetative cells. Thus, it can be summarized that the antimicrobial action of nisin and subtilin on vegetative cells and germinated spores occurs by two different mechanisms (45).

Part VI.  Research objectives.

The wedge model of pore formation by type A lantibiotics in bacterial vegetative cells has postulated that the pore forming ability of type A lantibiotics does not require specific receptors in the cell membrane since they act on artificial phospholipid bilayers although the overall charge of the bilayer may assist in attracting and accumulating the peptides at the membrane surface (47). However, the lipid II-mediated model of nisin pore formation requires binding of nisin to lipid II which acts as a docking molecule and thereby enhances the antimicrobial effect of nisin. Both the wedge model and the lipid II model do not satisfactorily explain the high specificity of nisin towards certain Gram-positive bacteria. The phospholipid composition of the bacterial cell membrane is fairly similar amongst a wide spectrum of Gram-positive bacteria, with the differences arising mainly from the presence of different cell membrane proteins. Also, lipid II is a precursor of peptidoglycan that forms the bacterial cell wall. All Gram-positive and Gram-negative bacteria possess a bacterial cell wall formed from peptidoglycan. Therefore, although lipid II might function as a docking molecule to enable nisin binding, the possibility that the specificity of nisin towards susceptible Gram-positive bacteria is due to the result of its interaction with specific, and as yet, unidentified protein targets in the bacterial cell membrane cannot be ruled out.

Also, the two models that were proposed to explain type A lantibiotic pore formation contrast with the mechanism of action of a number of other antibacterial peptides, such as lactococcin A, a bacteriocin produced by *Lactococcus lactis* (75), and carnocin UI49, a type A lantibiotic produced by *Carnobacterium piscicola* UI49 (73), which are thought to interact with specific membrane-bound receptor proteins that

16

mediate the specificity of these antibacterial peptides. Carnocin UI49 shows bactericidal activity against many lactic acid bacteria (LAB) including the nisin-producing *L. lactis* subsp. *lactis*, which are 10-fold more sensitive to carnocin UI49 than other LAB. Experiments involving testing several transformed *L. lactis* subsp. *lactis* strains carrying a fragment of the nisin gene cluster for their sensitivity to carnocin UI49 suggested that NisP, one of the membrane associated proteins involved in the production of active nisin by cleaving off the leader peptide, acts as a receptor for carnocin UI49. NisP may facilitate the binding and/or insertion of carnocin UI49 into the cytoplasmic membrane thus increasing the efficiency of its bactericidal activity (72).

Since protein-protein interactions are highly specific, this work explored the possibility that specificity of subtilin and nisin is conferred by their initial recognition and binding to specific protein targets in the bacterial cell membrane and not merely due to their interaction with membrane lipids. The phage display technique was therefore employed to identify potential peptide targets of subtilin by allowing subtilin to select for specific peptide structural motifs from random peptide libraries displayed on the surface of M13 bacteriophage. This research also attempted to isolate and identify bacterial protein targets of subtilin and nisin in susceptible bacterial vegetative cells to correlate the results obtained from phage display with the biological targets of subtilin and nisin. Isolation and identification of bacterial protein targets of subtilin and nisin will not only help in understanding the specificity of subtilin and nisin but also provide an insight into understanding how the specificity contributes to the mechanism of antimicrobial action.

Further, a research goal in this lab has been to determine whether covalent attachment of nisin and subtilin with their biological targets can occur. Previous experiments involving E4I/Dha5A subtilin, in which Glu4 was changed to Ile and dehydroalanine5 (Dha5) was changed to Ala, revealed that E4I/Dha5A subtilin lost its ability to inhibit spore outgrowth in *B. cereus* spores. However, E4I/Dha5A subtilin was capable of inducing cell lysis in vegetative *B. cereus* cells (45). A similar result was seen with Dha5A nisin (8), indicating that both subtilin and nisin exert their antimicrobial effects against bacterial spores and vegetative cells by different mechanisms. It is possible that the mechanism of bacterial spore outgrowth by subtilin and nisin involves covalent modification of nucleophilic sulfhydryl groups on the surface of germinating spores by the electrophilic dehydro residues since an intact Dha5 is required to inhibit spore outgrowth. Experiments were therefore performed to determine the nature of interaction of subtilin and nisin with bacterial protein targets in bacterial vegetative cells to examine whether subtilin and nisin could interact covalently with specific bacterial protein targets in bacterial vegetative cells. Detection of a covalent linkage would indicate that the electrophilic dehydro residues are involved in bond formation with specific nucleophilic groups in the protein target. Detection of covalent attachment of subtilin and nisin to protein targets in bacterial vegetative cells would also pave the way towards understanding alternative mechanisms of action of subtilin and nisin in bacterial vegetative cells, in addition to pore formation. This knowledge will aid in the design of structural variants of antibiotics by introducing reactive groups such as dehydro residues (35) to create newer antibiotics more effectively targeted against bacterial pathogens.

## Materials and Methods

Part I.  Material sources

Part I-1.  Reagents and chemicals

| | |
|---|---|
| Acetic Acid, Glacial | Baker Inc., Phillipsburg, NJ |
| Acetonitrile, HPLC grade | Fisher Scientific Co., Fair Lawn, NJ |
| Acrylamide | Bio-Rad Laboratories, Hercules, CA |
| Agarose | Gibco BRL, Gaithersburg, MD |
| Amino acids | Sigma Chemical Company, St. Louis, MO |
| Ammonium hydroxide (30%) | Baker Inc., Phillipsburg, NJ |
| Ammonium persulfate | Baker Inc., Phillipsburg, NJ |
| Ammonium phosphate, dibasic | Sigma Chemical Company, St. Louis, MO |
| $[\alpha\text{-}^{35}S]$-dATP | New England Nuclides, Boston, MA |
| BCIP | Gibco BRL, Gaithersburg, MD |
| Biotin disulfide NHS ester | Sigma Chemical Company, St. Louis, MO |
| Bisacrylamide | Bio-Rad Laboratories, Hercules, CA |
| Bovine serum albumin | Sigma Chemical Company, St. Louis, MO |
| Bromophenol blue | Sigma Chemical Company, St. Louis, MO |
| Calcium chloride | Fisher Scientific Co., Fair Lawn, NJ |
| Cellulose, non ionic powder | Bio-Rad Laboratories, Hercules, CA |
| Citric acid monohydrate | Fisher Scientific Co., Fair Lawn, NJ |
| $\alpha$-Cyano-4-hydroxycinnamic acid | Sigma Chemical Company, St. Louis, MO |
| N, N, - dimethylformamide | Fisher Scientific Co., Fair Lawn, NJ |

| | |
|---|---|
| Dithiothreitol | Sigma Chemical Company, St. Louis, MO |
| Ethanol | Aaper Chemical Co., Shelbyville, KY |
| Ethidium bromide | Gibco BRL, Gaithersburg, MD |
| Ferric chloride | Acros Organics, NJ |
| Glycerol | Fisher Scientific Co., Fair Lawn, NJ |
| Glycine | Fisher Scientific Co., Fair Lawn, NJ |
| Guanidine hydrochloride | Sigma Chemical Company, St. Louis, MO |
| Hydrochloric acid (38%) | Baker Inc., Phillipsburg, NJ |
| N-hydroxy succinimide fluorescein | Pierce Biotechnology Inc., Rockford, IL |
| IPTG | Gibco BRL, Gaithersburg, MD |
| Isobutanol | Baker Chemical, Phillipsburg, NJ |
| Isopropanol | Fisher Scientific Co., Fair Lawn, NJ |
| Manganous chloride tetrahydrate | Baker Inc., Phillipsburg, NJ |
| Magnesium chloride hexahydrate | Fisher Scientific Co., Fair Lawn, NJ |
| Magnesium sulfate | Baker Inc., Phillipsburg, NJ |
| 2-mercaptoethanol | Baker Inc., Phillipsburg, NJ |
| Methanol | Fisher Scientific Co., Fair Lawn, NJ |
| NBT | Gibco BRL, Gaithersburg, MD |
| Phosphoric acid | Fisher Scientific Co., Fair Lawn, NJ |
| Polyethylene glycol-8000 | Fisher Scientific Co., Fair Lawn, NJ |
| Potassium chloride | Baker Inc., Phillipsburg, NJ |
| Potassium phosphate, monobasic | Fisher Scientific Co., Fair Lawn, NJ |
| Potassium phosphate, dibasic | Fisher Scientific Co., Fair Lawn, NJ |

| | |
|---|---|
| 1-Step™ NBT/BCIP | Pierce Biotechnology Inc., Rockford, IL |
| Sinapinic acid | Sigma Chemical Company, St. Louis, MO |
| Sodium bicarbonate | Fisher Scientific Co., Fair Lawn, NJ |
| Sodium chloride | Fisher Scientific Co., Fair Lawn, NJ |
| Sodium dodecyl sulfate | Fisher Scientific Co., Fair Lawn, NJ |
| Sodium hydroxide | Fisher Scientific Co., Fair Lawn, NJ |
| Sodium iodide | Baker Inc., Phillipsburg, NJ |
| Sodium phosphate, monobasic | Baker Inc., Phillipsburg, NJ |
| Sodium phosphate, dibasic | Baker Inc., Phillipsburg, NJ |
| Sodium sulfate | Fisher Scientific Co., Fair Lawn, NJ |
| Sucrose | Fisher Scientific Co., Fair Lawn, NJ |
| TEMED | Sigma Chemical Company, St. Louis, MO |
| Thiamine | Sigma Chemical Company, St. Louis, MO |
| Toyopearl™ Butyl-650M HIC resin | Tosohaas, Montgomeryville, PA |
| Tricine | Sigma Chemical Company, St. Louis, MO |
| Trifluoroacetic acid | Acros Organics, NJ |
| Tris base | Fisher Scientific Co., Fair Lawn, NJ |
| Tween-20 | Sigma Chemical Company, St. Louis, MO |
| Urea | Fisher Scientific Co., Fair Lawn, NJ |
| X-Gal | Gibco BRL, Gaithersburg, MD |
| Zinc Chloride | Fisher Scientific Co., Fair Lawn, NJ |

Part I-2.  Antibodies, enzymes and kits

Goat Anti-rabbit IgG-alkaline phosphatase    Pierce Biotechnology Inc., Rockford, IL

Ph.D.-7 Phage Display Peptide Library Kit    New England Biolabs, Boston, MA

Ph.D.-12 Phage Display Peptide Library Kit   New England Biolabs, Boston, MA

PlusOne$^{TM}$ Silver Staining Kit                   Pharmacia Biotech, Uppsala, Sweden

Immobilized Monomeric Avidin Kit             Pierce Biotechnology Inc., Rockford, IL

ImmunoPure Protein A IgG Orientation Kit    Pierce Biotechnology Inc., Rockford, IL

Rabbit anti-FITC antibody                          Biodesign International, Saco, ME

Rabbit anti-subtilin antibody                       Research Genetics, Huntsville, AL

Seize Classic (A) Immunoprecipitation Kit    Pierce Biotechnology Inc., Rockford, IL

Seize X Protein A Immunoprecipitation Kit   Pierce Biotechnology Inc., Rockford, IL

Sequenase version 2.0 DNA sequencing kit    U. S. Biochemicals, Cleveland, OH

Streptavidin-alkaline phosphatase                Gibco BRL, Grand Island, NY

Trypsin                                                     Sigma Chemical Company, St. Louis, MO


Part I-3.  Media and antibiotics

Bacto agar                                               Difco, Detroit, MI

Bacto tryptone                                         Difco, Detroit, MI

Chloramphenicol                                      Sigma Chemical Company, St. Louis, MO

Penassay broth (PAB) antibiotic medium 3   Difco, Detroit, MI

Nisin                                                       Aplin Barrett, Trowbridge, Wilts UK (?)

Yeast extract                                            Becton Dickinson, Sparks, MD

Part I-4.  Apparatus

| | |
|---|---|
| Air and water incubating shakers | New Brunswick Scientific, New Brunswick |
| Centrifuge, Avanti J25-I | Beckman Instruments Inc., Palo Alto, CA |
| Centrifuge bottles | VWR Scientific, Baltimore, MD |
| Corex glass centrifuge tubes, 30 ml | VWR Scientific, Baltimore, MD |
| Digital photo documentation system | Eastman Kodak Company, Rochester, NY |
| DNA sequencing apparatus | American Bionuclear, Emeryville, CA |
| DNA sequencing glass plates and spacers | VWR Scientific, Baltimore, MD |
| ESI-Mass Spectrometer (LCQ) | Finnigan, San Jose, CA |
| HIC chromatography Econo-Columns | Bio-Rad Laboratories, Hercules, CA |
| HIC peristaltic pump | Gilson Medical Electronics, WI |
| HPLC column, Microsorb | Rainin Instrument Co. Inc., Woburn, MA |
| HPLC | Hewlett-Packard Company, Avondale, PA |
| Eppendorf microcentrifuge tubes | VWR Scientific, Baltimore MD |
| French pressure cell | Aminco Inc., Silver Spring, MD |
| French pressure cell power supply | Enerpac, Butler, WI |
| Gel dryer, Model 583 | Bio-Rad, Hercules, CA |
| Gel electrophoresis vertical units | Bio-Rad Laboratories, Hercules, CA |
| Gel electrophoresis vertical unit glass plates | Bio-Rad Laboratories, Hercules, CA |
| Immobilon$^{TM}$-NC nitrocellulose membrane | Millipore Inc., Bedford, MA |
| Kapak pouches | VWR Scientific, Baltimore, MD |
| Kapak pouch sealer | Kapak Corporation, Minneapolis, MN |
| MALDI-TOF MS | Bruker Instruments, Manning Park, MA |

| | |
|---|---|
| MALDI-TOF MS sample stages | Bruker Instruments, Manning Park, MA |
| Microscope | Nikon, Japan |
| Petri dishes | VWR Scientific, Baltimore, MD |
| pH meter, Accumet AB15 | Fisher Scientific Co., Fair Lawn, NJ |
| Pipetman, P20, P200, P1000 | Rainin Instruments Co. Inc., Woburn, MA |
| Power supply, Model 494 | ISCO, Lincoln, NE |
| Power supply, Model EC105 | E-C Apparatus, St. Petersburg, FL |
| Snakeskin pleated dialysis tubing | Pierce Biotechnology Inc., Rockford, IL |
| SpeedVac concentrator | Savant Instruments Inc., Farmingdale, NY |
| Spore spray unit | Sigma Chemical Company, St. Louis, MO |
| Storm 860 Imager | Amersham Biosciences, Piscataway, NJ |
| Syringes, 60 ml | VWR Scientific, Baltimore, MD |
| Syringe filters, 0.2 μm, 0.45 μm | Pall Corporation, Ann Arbor, MI |
| Syringe needles, 18G1½ | VWR Scientific, Baltimore, MD |
| UV transilluminator | Fotodyne Inc., New Berlin, WI |
| UV-VIS Spectrophotometer | Hewlett-Packard Company, Avondale, PA |
| X-Omat XAR-5 X-ray films | VWR Scientific, Baltimore, MD |
| Water bath | Precision Scientific, Chicago, IL |
| Whatman 3MM filter paper | VWR Scientific, Baltimore, MD |
| X-ray film developer | Konica, Newark, NJ |

Part II.  Methods

Part II-1.  Stock solutions, buffers and growth media

1-1.  Stock Solutions

Acrylamide/bis-acrylamide:   Several acrylamide:bis-acrylamide stock solutions were prepared for use in SDS-PAGE of proteins and DNA sequencing. For tricine-SDS-PAGE of peptides, two stock solutions of varying acrylamide:bis concentrations were prepared (66). The first stock solution of acrylamide and bis (49.5%T, 3%C) was prepared by dissolving 48 g of acrylamide and 1.5 g of bis-acrylamide in 70 ml of ddH$_2$O, and then adjusting the volume to 100 ml with ddH$_2$O. The second stock solution of acrylamide and bis (49.5%T, 6%C) was prepared by dissolving 46.5 g of acrylamide and 3 g of bis-acrylamide in 70 ml of ddH$_2$O. The volume was then adjusted to 100 ml with ddH$_2$O. Both solutions were filtered through a 0.45 μm filter and stored at 4°C in lightproof bottles.

A stock solution of acrylamide:bis (29:1) for Laemmli SDS-PAGE of proteins was prepared by dissolving 29 g of acrylamide and 1 g of bis-acrylamide in 70 ml of ddH$_2$O. After adjusting the volume to 100 ml with ddH$_2$O, the solution was filtered through a 0.45 μm filter and stored at 4°C in a lightproof bottle.

For DNA sequencing, a 40% acrylamide:bis (19:1) solution was prepared by dissolving 38 g of acrylamide and 2 g of bis-acrylamide in 70 ml of ddH$_2$O. The volume was adjusted to 100 ml with ddH$_2$O and the solution filtered through a 0.45 μm filter. The solution was stored at 4°C in a lightproof bottle.

Ammonium persulfate (APS):  A 10% stock solution of APS was prepared by dissolving 0.5 g of APS in 5 ml of ddH$_2$O. The solution was stored at 4ºC for upto a month.

Chloramphenicol:  A 10 mg/ml stock solution was prepared by dissolving 10 mg of chloramphenicol in 1 ml of 95% ethanol. The stock solution was stored at -20ºC for upto a month.

Dithiothreitol (DTT):  A 1 M stock solution of DTT was prepared by dissolving 1.54 g of DTT in 10 ml of 10 mM sodium acetate, pH 5.2. The solution was filter sterilized through a 0.2 μm filter and stored in 1 ml aliquots at –20°C.

EDTA:  A 0.5 M stock of EDTA was prepared by adding 9.3 g of Na$_2$EDTA·2H$_2$O to 40 ml of ddH$_2$O. The pH was adjusted to 8.0 with 1 N NaOH to dissolve all of the EDTA. The volume was adjusted to 50 ml with ddH$_2$O and the solution stored at RT.

Isopropylthio-β-galactoside (IPTG):  A 0.1 M stock solution was prepared by dissolving 0.25 g of IPTG in 10.5 ml of ddH$_2$O. The solution was filter sterilized using a 0.2 μm filter and stored at –20°C in 0.5 ml aliquots.

Nisin:  A stock solution of 10 mg/ml was prepared by dissolving 10 mg in 1 ml of 0.05% TFA. The solution was stored at -20ºC for upto 3 months.

Sodium acetate:  A 1 M stock solution of NaOAc, pH 4.0 was prepared by adding 28.6 ml of glacial acetic acid to 400 ml of ddH$_2$O. The pH was increased to 4.0 with 10 N NaOH and the volume adjusted to 500 ml with ddH$_2$O. The solution was autoclaved at 121°C for 20 min and stored at 4°C.

Sodium chloride (NaCl):  A 5 M solution of NaCl was prepared by dissolving 146.1 g of NaCl in 400 ml of ddH$_2$O and then adjusting the volume to 500 ml with ddH$_2$O. The solution was stored at 4°C.

Sodium dodecyl sulfate (SDS):  A 10% stock solution was prepared by dissolving 1 g of SDS in 10 ml of ddH$_2$O by gentle inversion. The solution was stored at RT.

Tris-HCl:  A 1 M stock solution of Tris-HCl was prepared by dissolving 121.11 g of Tris base in 800 ml of ddH$_2$O. The pH was adjusted to the desired pH using concentrated HCl and the volume increased to 1 L with ddH$_2$O. A 1.5 M stock of Tris-HCl was also prepared by dissolving 18.16 g of Tris base in 80 ml of ddH$_2$O, adjusting to the desired pH with concentrated HCl, and the volume increased to 100 ml with ddH$_2$O. Stock solutions were autoclaved at 121°C for 20 min and stored at RT. The stock solutions were diluted to the desired working concentrations as specified in the appropriate methods.

5-bromo-4-chloro-3-indolyl-β-galactoside (X-Gal):  A 20 mg/ml stock solution was prepared by dissolving 200 mg of X-gal in 10 ml of dimethyl formamide. The solution was stored in the dark at –20°C in 0.5 ml aliquots.

1-2.  Solutions for peptide purification.

HIC equilibration/wash buffer:  The HIC equilibration buffer consisted of 0.05 M NaOAc, pH 4.0 and 1 M NaCl. A 1 L buffer solution was prepared by adding 50 ml of 1 M NaOAc, pH 4.0 and 200 ml of 5 M NaCl to 750 ml of ddH$_2$O.

HIC elution buffer:  The HIC elution buffer used to elute subtilin from the HIC column consisted of 50% CH$_3$CN in 0.05% TFA. 50 ml of elution buffer was prepared by

adding 500 µl of 5% TFA to 24.5 ml of ddH$_2$O and adjusting the volume to 50 ml with CH$_3$CN.

Solvent A for RP-HPLC:  500 ml of solvent A was prepared by adding 25 ml of CH$_3$CN, 500 µl of acetic acid and 50 µl of 100% TFA to ddH$_2$O and adjusting the volume to 500 ml with ddH$_2$O.

Solvent B for RP-HPLC:  500 ml of solvent B was prepared by adding 25 ml of ddH$_2$O, 500 µl of acetic acid and 50 µl of 100% TFA to CH$_3$CN and adjusting the volume to 500 ml with CH$_3$CN.

Solvent C for SEC-HPLC:  500 ml of solvent C (0.05 M KH$_2$PO$_4$, 0.1 M NaCl, pH 6.8) was prepared by dissolving 3.4 g of KH$_2$PO$_4$ and 2.92 g of NaCl in 400 ml of HPLC-grade water. The pH was adjusted to 6.8 using 1 N NaOH and the volume adjusted to 500 ml with water.

1-3.  Solutions for SDS-PAGE.

16.5% T, 6% C separating gel with 6 M urea:  The separating gel for Tricine-SDS-PAGE was prepared by dissolving 3.6 g of urea in 3.33 ml of gel buffer (3 M Tris, 0.3% SDS), 2 ml of ddH$_2$O, and 3.33 ml of 49.5% T, 6% C acrylamide/bisacrylamide solution. The volume was adjusted to 10 ml with ddH$_2$O (66).

10% T, 3% C spacer gel:  The spacer gel for Tricine-SDS-PAGE was prepared by adding 1 ml of 49.5% T, 3% C acrylamide/bis solution to 1.66 ml of gel buffer (3 M Tris, 0.3% SDS) and adjusting the volume to 5 ml with ddH$_2$O.

4% T, 3% C stacking gel:  The stacking gel for Tricine-SDS-PAGE was prepared by adding 0.33 ml of 49.5% T, 3% C acrylamide/bis solution to 1 ml of gel buffer (3 M Tris, 0.3% SDS) and adjusting the volume to 4.2 ml with ddH$_2$O.

12% resolving gel for Laemmli SDS-PAGE:  The resolving gel was prepared by adding 16 ml of 30% acrylamide/bis (29:1) solution, 10 ml of 1.5 M Tris at pH 8.8, 0.4 ml of 10% SDS and 13.2 ml of $ddH_2O$.

5% stacking gel for Laemmli SDS-PAGE:  The stacking gel was prepared by adding 1.7 ml of 30% acrylamide/bis (29:1) solution, 1.25 ml of 1 M Tris at pH 6.8, 0.1 ml of 10% SDS and 6.8 ml of $ddH_2O$.

Anode buffer:  A 5X anode buffer for Tricine-SDS-PAGE (1 M Tris) was prepared by dissolving 121.11 g of Tris base in 800 ml of $ddH_2O$. After adjusting the pH to 8.9 with concentrated HCl, the volume was adjusted to 1 L with $ddH_2O$.

Cathode buffer:  A 5X cathode buffer for Tricine-SDS-PAGE (0.5 M Tris, 0.5 M Tricine, 0.5% SDS) was prepared by dissolving 60.55 g of Tris base, 89.6 g of Tricine and 5 g of SDS in a total volume of 1 L of $ddH_2O$. The pH of this solution was around 8.25 and therefore, pH adjustment was not necessary. Both the cathode and the anode buffers were stored at RT.

Gel buffer:  A 3 M Tris, 0.3% SDS gel buffer for Tricine-SDS-PAGE was prepared by dissolving 36.33 g of Tris base and 0.3 g of SDS in 70 ml of $ddH_2O$. The pH was adjusted to 8.45 with concentrated HCl and the volume increased to 100 ml with $ddH_2O$.

A 5X stock of Tris-glycine electrophoresis buffer (125 mM Tris, 1.25 M glycine, 0.5% SDS) for Laemmli SDS-PAGE was prepared by dissolving 7.55 g of Tris base, 47 g of glycine and 2.5 g of SDS in 400 ml of $ddH_2O$. The pH of this solution was not adjusted since the pH of this solution was around 8.3. The volume was adjusted to 500 ml with $ddH_2O$ (64).

Gel-loading buffer:  5X gel-loading buffer (250 mM Tris-HCl at pH 6.8, 10% SDS, 50% glycerol and 0.5% bromophenol blue) was prepared by dissolving 2.5 ml of 1 M Tris-HCl at pH 6.8, 1 g of SDS, 5 ml of glycerol and 0.05 g of bromophenol blue in a total volume of 10 ml using ddH₂O.

1-4.  Solutions for Western blot transfer and blot development.

Alkaline phosphatase developing buffer:  A 1 L solution of 100 mM Tris-HCl at pH 9.5, 100 mM NaCl and 50 mM MgCl₂ was prepared by dissolving 12.11 g of Tris base, 5.84 g of NaCl, and 10.15 g of MgCl₂•6H₂O in 950 ml of ddH₂O. The pH was adjusted to 9.5 with concentrated HCl and the volume adjusted to 1 L with ddH₂O.

Blocking buffer:   Blocking buffer of 1% BSA in TBST was prepared by dissolving 0.5 g of BSA in 50 ml of TBST.

5-bromo-4-chloro-3-indolyl phosphate (BCIP):  A 15 mg/ml stock solution was prepared by dissolving 15 mg of BCIP in 1 ml of DMF. The stock solution was stored at –20°C for upto three months.

Nitro blue tetrazolium chloride (NBT):  A 30 mg/ml stock solution was prepared by dissolving 30 mg of NBT in 1 ml of 70% DMF. 1 ml of 70% DMF was prepared by adding 0.3 ml of ddH₂O to 0.7 ml of DMF. The NBT stock solution was stored at –20°C for upto three months.

TBST (Tris buffered saline - 0.05% Tween-20):  1 L of 10 mM Tris-HCl at pH 8 and 150 mM NaCl was prepared by dissolving 1.21 g of Tris and 8.76 g of NaCl in 950 ml of ddH₂O. The pH was adjusted to 8.0 with concentrated HCl. 500 μl of Tween-20 was added to get a final concentration of 0.05% and the volume adjusted to 1 L with ddH₂O.

Transfer buffer: For transfer of a Tricine-SDS-PAGE gel, a 3 L transfer buffer was prepared by dissolving 9.1 g of Tris and 43.2 g of glycine in 2 L of ddH$_2$O. 600 ml of methanol was added and the volume adjusted to 3 L with ddH$_2$O.

For transfer of a Laemmli gel, a 3 L transfer buffer was prepared by dissolving 17.4 g of Tris, 8.7 g of glycine and 1.11 g of SDS in 2 L of ddH$_2$O. 600 ml of methanol was added and the volume adjusted to 3 L with ddH$_2$O (64).

1-5. Solutions for Phage Display.

Blocking buffer: 100 ml of blocking buffer (0.1 M NaHCO$_3$ at pH 8.6, 5 mg/ml BSA, 0.02% NaN$_3$) was prepared by dissolving 0.5 g of BSA in 80 ml of 0.1 M NaHCO$_3$. 1 ml of 2% NaN$_3$ was added to obtain a final concentration of 0.02%, and the volume adjusted to 100 ml with NaHCO$_3$. The solution was filter sterilized using 0.2 μm filter and stored at 4°C for upto a week.

Coating buffer: 500 ml of coating buffer (0.1 M NaHCO$_3$, pH 8.6) was prepared by dissolving 4.2 g of NaHCO$_3$ in 450 ml of ddH$_2$O. The pH was adjusted to 8.6 with 1 N NaOH and the volume increased to 500 ml with ddH$_2$O. The solution was autoclaved and stored at RT.

Dithiothreitol (DTT) elution buffer: 10 ml of 20 mM DTT was prepared by adding 0.2 ml of 1 M DTT stock solution to 9.8 ml of 10 mM sodium acetate, pH 5.2.

Glycine-HCl elution buffer: 50 ml of 0.2 M Glycine-HCl at pH 2.2, 1 mg/ml BSA was prepared by dissolving 0.75 g of glycine in 40 ml of ddH$_2$O. The pH was adjusted to 2.2 with concentrated HCl and 0.05 g of BSA added. The volume was increased to 50 ml with ddH$_2$O and the solution stored at 4°C.

Iodide buffer:  50 ml of iodide buffer (10 mM Tris-HCl at pH 8, 1 mM EDTA, 4 M NaI) was prepared by dissolving 29.96 g of NaI in 25 ml of ddH$_2$O. 0.5 ml of 1 M Tris-HCl stock at pH 8 and 0.1 ml of 0.5 M EDTA stock were added and the volume increased to 50 ml with ddH$_2$O. The solution was stored at RT.

PEG/NaCl:  100 ml of PEG/NaCl (20% w/v polyethylene glycol-8000, 2.5 M NaCl) was prepared by dissolving 14.6 g of NaCl and 20 g of PEG-8000 in 80 ml of ddH$_2$O, and adjusting the volume to 100 ml with ddH$_2$O. This was autoclaved and stored at RT.

Streptavidin stock solution:  1 ml of streptavidin stock solution was prepared by dissolving 1.5 mg of lyophilized streptavidin in 1 ml of 10 mM sodium phosphate at pH 7.2, 100 mM NaCl, 0.02% NaN$_3$. The solution was stored at –20°C for upto 6 months.

TBS buffer:  A 1 L solution of TBS (50 mM Tris-HCl at pH 7.5, 150 mM NaCl) was prepared by dissolving 6.05 g of Tris and 8.76 g of NaCl in 950 ml of ddH$_2$O. The pH was adjusted to 7.5 with concentrated HCl and the volume adjusted to 1 L with ddH$_2$O. The solution was autoclaved and stored at RT. Tween-20 was added according to the required strength.

TBE buffer:  A 10X stock of TBE buffer (1 M Tris, 0.83 M boric acid, 10 mM EDTA) was prepared by dissolving 121.11 g of Tris, 51.4 g of boric acid, and 3.72 g of Na$_2$EDTA in 800 ml of ddH$_2$O. The pH was checked to be ~8.3 and the volume adjusted to 1 L with ddH$_2$O. The autoclaved solution was stored at RT. The working buffer of 0.5X TBE was prepared by diluting the 10X stock 1:19 with ddH$_2$O.

TE buffer:  10 ml of TE buffer (10 mM Tris-HCl at pH 8, 1 mM EDTA) was prepared from stocks of 1 M Tris-HCl, pH 8.0 and 0.5 M EDTA, pH 8.0 by adding 0.1 ml of 1 M Tris-HCl, pH 8 and 0.02 ml of 0.5 M EDTA, pH 8 to a final volume of 10 ml of ddH$_2$O.

1-6.  Growth Media.

Agarose Top:  500 ml of agarose top was prepared by dissolving 5 g of bacto tryptone, 2.5 g of yeast extract, 2.5 g of NaCl and 0.5 g of MgCl$_2$ in 400 ml of ddH$_2$O. 3.5 g of agarose was added and the volume adjusted to 500 ml with ddH$_2$O. The media was autoclaved at 121°C for 20 min and stored solid in 50 ml aliquots in sterile bottles at room temperature. The media was melted in a microwave as needed.

LB (Luria Bertani) media and plates:  LB media was prepared by dissolving 10 g of bacto tryptone, 5 g of yeast extract, and 5 g of NaCl in 800 ml of ddH$_2$O. The volume was adjusted to 1 L with ddH$_2$O and then autoclaved at 121°C for 20 min. The media was stored in a sterile bottle at room temperature. To make plates, the LB media was supplemented with 15 g of bacto agar and then autoclaved. For plates requiring IPTG and X-Gal, 20 μl of 0.1 M IPTG and 40 μl of 20 mg/ml X-Gal were added to the autoclaved media just before pouring onto the plates. The media was poured onto sterile 100 mm petri dishes (~15 ml/dish) in a sterile hood. Plates were allowed to solidify at room temperature and kept overnight for evaporation of excess moisture. Plates were then stored inverted at 4°C in the dark for upto one month without loss of IPTG/X-gal activity.

Medium A media and plates:  Medium A was prepared from four stock solutions. Solution I was prepared by dissolving 20 g of sucrose and 2 g of PAB medium in 780 ml of ddH$_2$O. To prepare solution II (5X), 11.7 g of citric acid, 4.2 g of (NH$_4$)$_2$HPO$_4$, 4 g of

33

Na$_2$SO$_4$, and 5 g of yeast extract were dissolved in 150 ml of ddH$_2$O. The pH was adjusted to 6.9 with 30% NH$_4$OH and the volume increased to 200 ml with ddH$_2$O. Solution III was prepared as a 100X stock by dissolving 7.62 g of KCl, 4.18 g of MgCl$_2$·6H$_2$O, 0.543 g of MnCl$_2$·4H$_2$O and 0.11 g of ZnCl$_2$, and the volume adjusted to 100 ml with ddH$_2$O. The autoclaved solutions I, II and III were stored at 4°C. Solution IV (100X) was prepared by dissolving 0.25 g of FeCl$_3$ in 100 ml of ddH$_2$O. This was sterilized by filtering through 0.2 µm and stored at 4°C. 1 L of medium A was prepared by adding 200 ml of solution II and 10 ml of solutions III and IV to 780 ml of autoclaved solution I just before inoculation with the *Bacillus subtilis* strain. The bacterial strain was cultured in 500 ml of medium A transferred to a 2 L baffled flask. To make plates, 1 L of medium A was supplemented with 15 g of bacto agar and then autoclaved.

Minimal plates:  500 ml of media for minimal plates was prepared by dissolving 3 g of Na$_2$HPO$_4$, 1.5 g of KH$_2$PO$_4$, 0.25 g of NaCl, 0.5 g of NH$_4$Cl, 1 ml of 1 M MgSO$_4$ and 50 µl of 1 M CaCl$_2$ in 400 ml of ddH$_2$O. 7.5 g of agar was added and the volume adjusted to 490 ml with ddH$_2$O. The solution was autoclaved and cooled to <50°C before adding 10 ml of filter sterilized 20% glucose and 0.5 ml of filter sterilized 10 mg/ml thiamine. The plates were stored at 4°C for upto a month.

Penassay Broth (PAB) media and plates:  PAB media was prepared by dissolving 17.5 g of dehydrated antibiotic medium 3 (PAB) in 800 ml of ddH$_2$O, and the volume adjusted to 1 L. For plates, 15 g of bacto agar was added to the solution. Autoclaving and storage of PAB media and plates were performed in the same manner as with LB. To make plates with chloramphenicol, 1 ml of 10 mg/ml chloramphenicol was added to the

autoclaved media and the media poured onto the petri dishes. The PAB/cm$^{10}$ plates were stored at 4°C in the dark and retained antibiotic activity for upto a month.

Part II-2.  Maintenance and growth of bacterial strains.

_Bacillus subtilis_ LH45:  Frozen stocks of _B. subtilis_ LH45 were maintained in PAB medium containing 15% of sterilized glycerol at –80°C, and working stocks were maintained on PAB/cm$^{10}$ plates at RT. For long-term storage, the LH45 strain was grown on a PAB/cm$^{10}$ plate at 37°C overnight to form a dense lawn. The bacterial lawn was suspended in 3 ml of PAB medium and 15% sterile glycerol. 1 ml of this solution was pipetted into each labeled cryotube. The cryotubes were flash frozen in an ethanol/dry ice bath and stored frozen at –80°C. To grow cells from the frozen archives, they were quickly streaked onto a PAB/cm$^{10}$ plate using a sterile inoculation needle. The working stock was then restreaked onto a fresh PAB/cm$^{10}$ plate every 3-4 weeks.

_Escherichia coli_ ER2537:  A frozen stock of _E. coli_ ER2537 in glycerol culture was maintained at –80°C. The ER2537 strain was supplied with the Phage Display kit to be used for M13 bacteriophage amplification. The ER2537 strain was streaked onto a minimal plate using sterile techniques. The plate was inverted and incubated at 37°C for 1-2 days. The plate was wrapped with parafilm and stored at 4°C for a maximum of one month. To culture ER2537 for M13 propagation, LB medium was inoculated with a single colony of ER2537 from the minimal plate.

Part II-3.  Isolation of subtilin from bacterial culture.

Subtilin was isolated from *Bacillus subtilis* LH45, a strain of *B. subtilis* 168 that was engineered to produce subtilin (43). The natural producer of subtilin is *B. subtilis* ATCC 6633 from which the chromosomal fragment (~40 kb) carrying the subtilin operon was isolated and integrated alongwith the *cat* gene into the chromosome of *B. subtilis* 168 to obtain *B. subtilis* LH45, a subtilin producing strain. A single colony of LH45 from a PAB/cm$^{10}$ plate was inoculated into 5 ml of PAB/cm$^{10}$ medium and grown overnight at 37°C at 250 rpm. The LH45 strain was then grown in 500 ml of medium A (17) by inoculating medium A/cm$^{10}$ with 5 ml of the overnight culture grown in PAB/cm$^{10}$. The medium A culture was grown for 27-30 hours at 37°C at 250 rpm, after which it was checked for change in color and pH. Cultures producing subtilin turned reddish-brown with pH decreasing from 6.9 to anywhere between 6.0-6.4. These cultures were acidified to a pH of 2.5 using 85% phosphoric acid and then centrifuged to pellet the cells. Subtilin and sublancin, both being secretory peptides, were present in the supernatant. Isolation of subtilin from LH45 also resulted in isolation of sublancin, since *B. subtilis* 168 is a natural producer of sublancin.

Part II-4.  Hydrophobic interaction chromatography (HIC).

The supernatant obtained after centrifugation of the LH45 culture (from Part II-3) was either loaded immediately on to a hydrophobic interaction column or stored at -20°C until used. A chromatographic Bio-Rad Econo-Column of 15 cm length and 1.5 cm diameter was packed with 20 ml of Tosohaas Toyopearl Butyl-650 resin (57). The column was equilibrated with 7 volumes of equilibrating/wash buffer comprising of

0.05 M sodium acetate, pH 4 and 1 M NaCl (see Part II-1, 1-3). The supernatant was also equilibrated with NAOAc (pH 4) and NaCl to a final concentration of 0.05 M and 1 M, respectively. The equilibrated supernatant was placed on ice and slowly loaded onto the column at a flow rate of 1.5-2 ml/min using a peristaltic pump. The column was then washed with 7 volumes of wash buffer. The less hydrophobic molecules were washed off the column using 2 volumes of 0.05 M NaOAc, pH 4. Subtilin, a more hydrophobic peptide, was eluted with 50% acetonitrile in 0.05% TFA and fractions collected every minute in microcentrifuge tubes. The collected fractions were tested for antimicrobial activity using halo assays.

Part II-5. Spore outgrowth inhibition assay (halo assay).

The antimicrobial activity of the lantibiotics subtilin, sublancin and nisin was assessed by their ability to inhibit the outgrowth of *B. cereus* T spores. The spores were prepared for the assay by heat shocking the spores. 250 mg of lyophilized *B. cereus* spores was suspended in 20 ml of sterile ddH$_2$O. The spores were thoroughly dispersed in a glass homogenizer. The homogenized spores were then heat shocked for 2 h at 65°C. The spore pellet was collected after centrifugation for 10 min at 4,000 rpm. The spores were resuspended in 50 ml of 10% ethanol prepared in sterile water and stored in a Sigma spray unit at RT. The same protocol of heat shocking *B. subtilis* 168 spores was followed in cases where biotinylated subtilin or biotinylated nisin was tested for antimicrobial activity against *B. subtilis* 168 spores.

The halo assay was performed on medium A plates pre-warmed at 37°C for 10-15 min. 10 μl of each fraction to be tested for antimicrobial activity was spotted onto a

37

pre-warmed medium A plate and allowed to air dry. The plate was sprayed either with heat shocked *Bacillus cereus* or *B. subtilis* 168 spores using a Sigma spray unit and the inverted plate was incubated at 37°C overnight for ~12 hours. Fractions with antimicrobial activity showed clear halos representing zones of growth inhibition amidst a lawn of bacterial cells.

Part II-6. Reversed phase high performance liquid chromatography (RP-HPLC).

Reversed phase high performance liquid chromatography was used to further purify the peptides obtained from the HIC purification. Reversed phase HPLC was performed on a Hewlett-Packard Ti Series 1050 equipped with a diode array detector system. The HPLC was interfaced to a Gateway 2000 computer running the HP Chemstation instrument and data acquisition software provided by the manufacturer.

Fractions collected from the HIC purification (see Part II-4) that exhibited antimicrobial activity were lyophilized in a SpeedVac and resuspended in 0.05% TFA. The resuspended fractions were pooled in a total volume of 1-2 ml, centrifuged to remove any insoluble matter and then purified using a reverse phase C-18 HPLC column. The column used was a Rainin Microsorb-MV C-18 column with 5 μm spherical particles and 300 Å pores, and was of 250 mm length and 4.6 mm internal diameter. Subtilin was eluted initially by a linear gradient going from 0-100% of solvent B (0.05% TFA in acetonitrile) from solvent A (0.05% TFA in water) over 30 min at a flow rate of 1.2 ml/min. Later, to optimize conditions for MALDI-TOF analysis of the collected fractions, solvent A was modified to 95% $ddH_2O$, 4.89% $CH_3CN$, 0.1% acetic acid and 0.01% TFA while solvent B consisted of 95% $CH_3CN$, 4.89% $ddH_2O$, 0.1% acetic acid, and 0.01% TFA. The column was first equilibrated for 20 min with solvents A and B

after which the sample was loaded onto the column. Non-specifically bound proteins were washed off the column by a linear gradient going from 0-25% of solvent B from solvent A over 5 min. The sample was then subjected to a mobile phase of 100% solvent A for 4 min, followed by a linear gradient of 0-100% solvent B for 21 min when sublancin eluted first followed by subtilin at a later time. The mobile phase was maintained at 100% solvent B for 3 min and then changed back to 100% solvent A over 2 min with the entire elution run lasting for 30 min. The elution profile was observed at 254 nm, 214 nm and 280 nm to monitor the absorbances of dehydro residues, peptide bond and aromatic residues, respectively. Fractions were collected every min and the fractions assayed for activity using halo assays (see Part II-5). Presence of subtilin in the active fractions was confirmed by MALDI-TOF mass spectrometry (see Part II-7). The active fractions containing subtilin were lyophilized and stored at -20°C.

RP-HPLC was also used to separate biotinylated subtilin or biotinylated nisin (see Part II-8) from the non-biotinylated peptide species. Fluorescein labeled nisin (see Part II-17) was also purified from unreacted nisin using RP-HPLC. After first equilibrating the column for 20 min with solvents A and B, the biotinylated peptide or fluorescein-nisin in 2 ml of the reaction solution was loaded onto the column. The labeled peptide was eluted over a 30 min elution run by a linear gradient of 0-100% solvent B for 21 min and the fractions corresponding to the labeled peptide collected.

Part II-7.  MALDI-TOF mass spectrometry.

Matrix-assisted laser desorption/ionization-time of flight mass spectrometry (MALDI-TOF MS) was employed to detect subtilin and sublancin in the various

biologically active fractions collected from RP-HPLC purification. CHCA (α-cyano-4-hydroxycinnamic acid) matrix was employed for mass spectroscopy analysis of peptides less than 10 kDa. The samples for MALDI-TOF MS analysis were crystallized on CHCA matrix by the 'sandwich method' as described by Kussmann *et al.* (37). The CHCA matrix was prepared by dissolving 0.02 g of CHCA in 1 ml of 0.1% TFA and 50% $CH_3CN$. Sample crystallization for mass spectrometry analysis was performed on a small metal disc about 2 cm in diameter with 10 numbered, etched circles (~2 mm in diameter) arrayed on the sample disc in a circular fashion for sample deposition. The sample disc was cleaned with 0.1% TFA, followed by methanol and rinsing with $ddH_2O$. The sample disc was dried before adding the sample onto the disc.

For each sample to be analyzed, 0.5 μl of CHCA matrix was pipetted onto a circle of the sample disc and allowed to air dry completely in a fume hood. The samples to be analyzed were either HPLC purified samples, or were dissolved in a low pH solution such as 0.05% TFA to facilitate ionization. 1 μl of each sample was then overlaid on top of the dried crystallized matrix and allowed to air dry completely. 0.5 μl of matrix was then deposited again on top of the dried sample to create a 'sandwich' of the sample to be analyzed. Peptides of known molecular mass such as nisin (MW = 3354 Da) were used as external standards for calibration during measurements. Samples were analyzed on a Bruker Proflex MALDI-TOF mass spectrometer which was interfaced to a Sun Solaris workstation. The relative power of the laser and the number of laser shots were adjusted to obtain the best possible spectra for each sample. The data was averaged over multiple laser shots by the machine. The external standard was always measured first so as to use

40

the mass peak of the standard for calibration. The mass spectra of the samples were then taken, which were depicted as the $m/z$ values of the resulting peaks.

Part II-8.  Biotinylation of subtilin and nisin.

Highly purified, lyophilized nisin was obtained from Aplin and Barrett (Trowbridge, Wilts UK). A 10 mg/ml stock solution of nisin was prepared by dissolving 1 mg of nisin in 1 ml of 0.05% TFA. Subtilin concentration was calculated in moles by comparing the peak area of subtilin obtained from RP-HPLC at $OD_{254}$ with that of the peak area of a known molar quantity of a nisin standard since subtilin and nisin share the same number of Dha (two) and Dhb (one) residues (24). The biologically active fractions containing subtilin were pooled and the concentration of subtilin was also determined in a uv-vis spectrophotometer at 254 nm using nisin dilutions to plot the standard curve.

Subtilin or nisin was biotinylated by reacting the peptide with the biotinylating agent biotin disulfide N-hydroxy succinimide ester (BDNHSE) in a 1:1 nanomolar ratio. Both subtilin and nisin have three lysine residues. A 1:1 ratio was therefore chosen to ensure that the peptide was biotinylated at only one of its three lysine residues. A fresh 1 mg/ml stock solution of BDNHSE was prepared by dissolving 1 mg of BDNHSE in 1 ml of $ddH_2O$ with vigorous vortexing for 15 min. 87 μl of the BDNHSE stock corresponding to an equimolar concentration of subtilin (151 μM) was added to 0.5 mg of subtilin or nisin and the volume adjusted to 2 ml with 100 mM $NaHCO_3$, pH 8. This was incubated on ice for 2 hours. The biotinylated peptide was purified using RP-HPLC as described in Part II-6, and fractions corresponding to the biotinylated peptide were collected. Halo assay was performed on the fractions to test whether the biotinylated

41

peptide retained antimicrobial activity (see Part II-5). The fractions with biological activity were lyophilized in a SpeedVac, pooled together in a 500 µl volume of 0.05% TFA and stored at –20°C. The presence of biotin was confirmed by resolving the biotinylated peptide on a 16.5% polyacrylamide gel (see Part II-9), followed by western blot analysis using streptavidin-conjugated alkaline phosphatase as a probe (see Part II-11, 11-1 and 11-2).

Part II-9.  SDS-PAGE analysis of peptides and proteins.

Analysis of proteins and peptides was performed by electrophoresing on SDS-PAGE. While larger proteins were resolved on a 12% gel using the Laemmli SDS-PAGE method, the Tricine-SDS-PAGE protocol was used for resolution of small peptides in the 5-20 kDa range (66). All the solutions used for SDS-PAGE are described in Part II-1, 1-1 and 1-3.

9-1.  Tricine-SDS-PAGE of biotinylated subtilin.

The biotinylated subtilin fractions purified by HPLC were run on a Tricine-SDS-PAGE gel. The Tricine-SDS-PAGE gel comprised of a separating gel, a spacer gel and a stacking gel. 14 cm x 16 cm gel plates were assembled with spacers of 1 mm thickness, and the edges and the bottom of the assembly were sealed with 1% molten agarose (in ddH$_2$O). 150 µl of 10% APS and 30 µl of TEMED were added to 10 ml of the separating gel solution and this was immediately poured into the plate assembly. The solution was overlaid with isobutanol and allowed to polymerize for 45-60 min. After polymerization was complete, the overlay was poured off and the top of the gel washed with ddH$_2$O several times. The spacer gel was then allowed to polymerize on top of the separating gel.

42

This was followed by polymerization of the stacking gel which occurred with the spacer comb in place. The comb and clamps were then removed from the assembly, and the gel assembly was placed into the electrophoretic apparatus. 400 ml of 1X cathode buffer (0.1 M Tris at pH 8.25, 0.1 M Tricine, 0.1% SDS) was added to the upper chamber of the gel apparatus, while the lower reservoir was filled with 400 ml of 1X anode buffer (0.2 M Tris, pH 8.9). 10 µl of the sample was diluted with an equal volume of 2X gel loading buffer. The samples were boiled for 3 min before being loaded on the gel. The gel was electrophoresed at a constant voltage of 100 mV until the bromophenol blue tracking dye had just migrated into the separating gel. The gel was then electrophoresed at 15 mV until the tracking dye had migrated to the bottom of the gel (~17-19 hr). The gel was stained using the silver stain protocol (see Part II-10). Alternatively, proteins resolved on the gel were electroblotted onto a nitrocellulose membrane for western blot analysis as described in Part II-11.

9-2. Laemmli SDS-PAGE of proteins.

Bacterial proteins bound either to biotinylated subtilin or to fluorescein-nisin were analyzed by resolving on a 12% polyacrylamide gel containing 0.1% SDS (38). 16 cm x 20 cm gel plates were assembled with spacers of 1.5 mm thickness and the glass plate sandwich was clamped on either side using two sandwich clamps. The assembled gel plate sandwich was then clamped upright in a Bio-Rad Protean II xi casting stand. 400 µl of 10% APS and 16 µl of TEMED were added to 40 ml of the separating gel, and this was allowed to polymerize for 45-60 min with an overlay of isobutanol. 100 µl of 10% APS and 10 µl of TEMED were then added to 10 ml of the stacking gel which was allowed to polymerize with a 1.5 mm 15-well comb in place. The comb was removed and

the gel assembly placed in a Protean II xi electrophoretic apparatus. The upper and lower buffer chambers were filled with a total volume of 2.5 L of 1X gel running buffer (25 mM Tris, 250 mM glycine, 0.1% SDS). 5% 2-ME and 5X gel buffer (250 mM Tris-HCl at pH 6.8, 10% SDS, 50% glycerol, 0.5% bromophenol blue) were added to 50-75 µl of the samples which were boiled for 3 min before being loaded on the gel. The gel was then electrophoresed at 100 V for 5-6 h. The gel was then either silver stained (see Part II-10) or transferred onto a nitrocellulose membrane for Western blot analysis (see Part II-11).

For samples analyzed on mini gels, the separating and stacking gels were polymerized in between 8 cm x 10 cm gel plates with 1 mm spacers clamped in a Hoefer Mini-Gel gel caster and 10-20 µl of the samples electrophoresed on the gel at 100 V for 90 min in a Hoefer Mini-Gel electrophoresis apparatus.

Part II-10.  Silver staining of proteins resolved by SDS-PAGE.

Silver staining was used to detect proteins which were less than 100 ng in quantity on the gel. Silver staining allowed detection of as little as 0.1-1 ng of protein bands. The gel was stained using a Pharmacia Biotech PlusOne$^{TM}$ Silver Staining Kit in accordance with manufacturer protocols. 250 ml of solutions were used for the 16 cm x 20 cm gels and 100 ml of solutions were used for the mini gels. The gel was fixed for 30 min in 40% $C_2H_5OH$ and 10% $CH_3COOH$ with gentle agitation. The gel was then sensitized in 30% $C_2H_5OH$, 0.125% glutardialdehyde, 0.2% sodium thiosulfate and 0.83 M sodium acetate for 30 min. The gel was washed thrice in dd$H_2O$ for 5 min each. The gel was then placed in the silver reaction solution comprised of 0.25% $AgNO_3$ and 0.015% HCHO for

20 min. The gel was washed twice in ddH$_2$O for 1 min before adding the developing solution comprised of 0.24 M Na$_2$CO$_3$ and 0.007% HCHO. Development was continued for several min until protein bands of the desired intensity were seen. The developing reaction was stopped by the addition of 0.04 M EDTA-Na$_2$ for 10 min. The gel was washed thrice in ddH$_2$O for 5 min and placed in a preserving solution of 30% C$_2$H$_5$OH and 4% glycerol. Silver stained protein bands were visualized on a fluorescent light box and photographed by a Kodak Photo Documentation and Analysis System running the Kodak Digital Science 1D LE computer software package.

Part II-11. Western blot detection of peptides/proteins resolved by SDS-PAGE.

Biotinylated subtilin electrophoresed on Tricine-SDS-PAGE and larger proteins resolved on Laemmli SDS-PAGE were detected by Western blot analysis. The proteins were first transferred electrophoretically onto a nitrocellulose membrane in the Western blot transfer apparatus. The nitrocellulose membrane was then incubated with an appropriate probe conjugated to the alkaline phosphatase (AP) enzyme. Addition of AP substrates then resulted in the detection of the bound protein.

11-1. Transfer of proteins to nitrocellulose membrane.

For transfer of proteins from the gel onto a nitrocellulose (NC) membrane, the NC filter and the gel were sandwiched between Whatman 3MM filter paper in the transfer apparatus (64). Six sheets of Whatman 3MM filter paper and a single sheet of Immobilon$^{TM}$-NC nitrocellulose membrane were cut to the exact size of the gel. The NC membrane was gently soaked in ddH$_2$O for a few min, while the Whatman sheets and two porous pads were soaked in transfer buffer. The gel was rinsed briefly in deionized water.

The transfer block was then assembled by successive layering of all of the above materials within the transfer block. The porous pad was placed on the anode plate, followed by three sheets of Whatman paper, NC membrane, gel, three sheets of Whatman paper, another porous pad and finally the cathode plate of the transfer block. Care was taken to ensure that there were no air bubbles between the successive layers in the stacked assembly by squeezing out any air bubbles using a glass rod at each stage of layering. The transfer block was then placed in the transfer cell filled with 3 L of transfer buffer (see Part II-1, 1-4). The cell was either electrophoresed at 250 mA for 3-4 h at RT with sufficient cooling or at 50 mA at 4°C overnight. After the electrophoretic transfer was complete, the NC membrane was rinsed briefly in deionized water and probed with the appropriate probe conjugated to alkaline phosphatase.

11-2. Detection of biotinylated subtilin using streptavidin-alkaline phosphatase conjugate.

This protocol was used to detect both biotinylated subtilin bound to the NC membrane, and also to detect biotinylated subtilin bound to bacterial proteins that had been membrane-immobilized. A 1 L solution of TBST (10 mM Tris-HCl at pH 8, 150 mM NaCl, 0.05% Tween-20) was prepared as described in Part II-1, 1-4. The NC membrane with immobilized biotinylated subtilin was first incubated in 50 ml of blocking buffer (1% BSA in TBST) for 1 h at RT with gentle agitation. The NC membrane was then washed with 2 x 50 ml of TBST for 5 min. The streptavidin-AP conjugate was diluted 1:1,000 in 30 ml of TBST and the NC membrane was incubated with the streptavidin-AP probe solution for 1 h at RT with gentle agitation. The NC membrane was again washed with 2 x 50 ml of TBST for 5 min. The developing solution

46

was then prepared by adding 99 μl of 15 mg/ml of 5-bromo-4-chloro-3'-indolylphosphate (BCIP) and 198 μl of 30 mg/ml of nitro-blue tetrazolium chloride (NBT) to 30 ml of the AP developing buffer (100 mM Tris-HCl at pH 9.5, 100 mM NaCl, 50 mM $MgCl_2$) just before development of the membrane. BCIP and NBT react to form a purple, insoluble precipitate after cleavage of the BCIP phosphate group by AP. The NC membrane was incubated in the developing solution for several min with agitation until color development of the desired intensity was observed. The NC membrane was then rinsed with 2 x 50 ml of $ddH_2O$ for 5 min and dried between sheets of paper towels. The developed NC membrane was then scanned on a computer scanner to obtain a digital image of the developed protein bands.

Part II-12.  Screening of peptide targets of subtilin using Phage Display.

Phage Display was used as a selection technique to identify peptide sequences that interact favorably with subtilin. Two libraries, differing in the length of the random peptide displayed on M13 bacteriophage were screened against subtilin. Both peptide libraries, Ph.D.-12 and Ph.D.-7, were obtained as kits from New England Biolabs. Subtilin was screened against these random peptide 12-mers or 7-mers displayed on phage by an *in vitro* selection process called biopanning. The biopanning method used here involved incubating the biotinylated subtilin target with the phage-displayed peptide library in solution, affinity-capturing the phage-target complex by immobilized streptavidin, washing away the unbound phage, and eluting the bound phage. The eluted phages were then amplified in *E. coli* and subjected to three more rounds of biopanning and amplification to enrich the phage pool for specifically binding sequences. The

47

individual phages were then subjected to DNA sequencing to identify the binding peptide sequences.

12-1. Biopanning procedure.

Subtilin was biotinylated as described in Part II-8. Two RP-HPLC fractions of biotinylated subtilin exhibiting biological activity were lyophilized and resuspended in small measured volumes of 0.05% TFA. For each round of biopanning, 5 nM of biotinylated subtilin was reacted with 10 μl of the 12-mer phage library or the 7-mer phage library containing 4 X $10^{10}$ plaque forming units (pfu) of phage in a final volume of 150 μl of TBST (50 mM Tris-HCl at pH 7.5, 150 mM NaCl, 0.1% Tween-20). The two biotinylated subtilin fractions were complexed with the phage in duplicates for 1 h at RT. Five wells of a 96-well microtiter plate were coated with 100 μg/ml of streptavidin in 0.1 M $NaHCO_3$, pH 8.6 and incubated at 4ºC overnight in a humidified container. The coating solution was poured off and residual solution removed by firmly tapping the plate face down on a clean paper towel. To reduce non-specific binding, 400 μl of the blocking buffer (5 mg/ml of BSA in 0.1 M $NaHCO_3$ at pH 8.6, 0.02% $NaN_3$) was added to the wells and incubated for at least an hour at 4ºC. After discarding the blocking solution, the plate was washed rapidly with 6 x 400 μl of TBST. For each wash, 400 μl of TBST was added to each well, gently swirled, drained, and the plate was inverted and firmly tapped on a clean paper towel. 150 μl of the biotinylated subtilin bound to phage in TBST was added to four of the streptavidin-coated wells and incubated for 1 h at RT. Nonbinding target was discarded by pouring off the solution and washing the wells 10X with TBST. The bound target in two of the wells was eluted with 100 μl of 20 mM DTT in 0.01 M

sodium acetate at pH 5.2 for 30 min, while the bound target in the other two wells was eluted with 100 µl of 0.2 M glycine-HCl at pH 2.2, 1 mg/ml BSA for 10 min. The glycine-HCl eluates were neutralized with 15 µl of 1 M Tris-HCl, pH 9.1. In the control biopanning experiment, streptavidin was used as the target. The blocking solution contained 0.1 µg/µl of streptavidin to complex to any biotin in the BSA. The phage was allowed to react directly with streptavidin bound to the microtiter plate and eluted with 0.1 mM biotin in TBS for 30 min. The control was also subjected to three rounds of biopanning.

12-2.  Phage titering and phage amplification.

A small amount of the eluate was titered while the rest of the eluate was amplified. 5 ml of LB was inoculated with a single colony of *E. coli* ER2537 and incubated with shaking until mid-log phase ($OD_{600}$ ~0.5). 1 µl of the unamplified eluate was titered by incubating 200 µl of the *E. coli* culture at mid-log phase with 10 µl of each dilution ($10^1 – 10^4$) of the eluate in LB for 3 min at RT. The infected cells were mixed with 3 ml of agarose top warmed to 45°C and poured evenly onto a pre-warmed LB/IPTG/Xgal plate. The plate was allowed to cool and then incubated at 37°C overnight. The blue plaques were counted and the number multiplied by the dilution factor to obtain the phage titer in pfu per 10 µl.

The rest of the eluate was amplified in 20 ml of *E. coli* culture in LB at early-log phase for 4.5 hours at 37°C. The culture was centrifuged at 10,000 rpm for 10 min at 4°C. The phage was precipitated from the supernatant in a fresh tube by adding 1/6 volume of PEG/NaCl (20% polyethylene glycol-8000, 2.5 M NaCl) and incubating at 4°C

49

overnight. Precipitated phage was recovered as a pellet by centrifuging the PEG precipitation at 10,000 rpm for 15 min at 4°C. The pellet was then resuspended in 1 ml of TBS. The phage was reprecipitated with 1/6 volume of PEG/NaCl for 1 h on ice. The phage was pelleted by spinning for 10 min at 4°C. The pellet was resuspended in 200 μl of TBS, 0.02% NaN$_3$ to obtain the amplified eluate. 1 μl of the amplified eluate was titered in the dilution range $10^7$–$10^{10}$ on LB/IPTG/Xgal plates and the blue plaques counted to determine the phage titer. This value was used to calculate a volume corresponding to $10^{11}$ pfu to carry out the second round of biopanning. The second round amplified eluate was also titered for the third round of biopanning. The unamplified third round eluate was titered and a number of the resulting plaques were amplified in 1 ml of *E. coli* culture in LB at early-log phase for 4.5 hours at 37°C. The amplified phage was then subjected to DNA purification followed by DNA sequencing to identify the peptide displayed on the phage surface.

12-3.  Purification of sequencing templates.

The plaques obtained from the third round of biopanning were amplified in *E. coli*. 500 μl of the amplified phage was precipitated with 200 μl of PEG/NaCl for 10 min at RT. The pellet obtained after centrifugation at 14,000 rpm for 10 min was suspended in 100 μl of iodide buffer (10 mM Tris-HCl at pH 8, 1 mM EDTA, 4 M NaI) and 250 μl of ethanol was added. A 10 min short incubation at room temperature precipitated single-stranded phage DNA, leaving phage protein in solution. After centrifugation for 10 min, the pellet was washed by suspending the pellet in 500 μl of 70% ethanol, centrifuging for 10 min and discarding the supernatant. The pellet was dried

in the SpeedVac for 30 min to remove any traces of ethanol. The dried pellet was suspended in 10 µl of TE buffer (10 mM Tris-HCl at pH 8, 1 mM EDTA). The purity of the ss-phage DNA was then assessed by running 1 µl of each DNA sample on a 1% agarose gel followed by EtBr visualization on a UV transilluminator.

Part II-13.  Dideoxy sequencing of purified single-stranded phage DNA.

The purified DNA template from Part II-12, 12-3 was subjected to dideoxy sequencing with $^{35}$S to identify the 12-mer and 7-mer peptide sequences that bound to subtilin. Manual dideoxy sequencing of the purified ssDNA was performed using a Sequenase version 2.0 DNA sequencing kit. The sequencing reactions were electrophoresed on a sequencing gel and an autoradiogram of the gel obtained. Sequences were then read from the exposed film.

13-1.  Dideoxy DNA sequencing reaction.

The sequencing reaction comprised of three steps – annealing, labeling and termination. For the annealing reaction, 2 µl of 5X sequenase reaction buffer, 1 µl of –96 gIII sequencing primer diluted 1:1 with ddH$_2$O and 2 µl of ddH$_2$O were added to 5 µl of the ssDNA in a total volume of 10 µl. The -96 gIII sequencing primer used for the annealing reaction was supplied in the Phage Display kit. The annealing mixture was heated at 65°C for 2 min in a beaker of water and allowed to cool slowly to <35°C over 30 min in the beaker of water. The sample was centrifuged for 10 sec and then placed on ice. While the annealing mixture was cooling, four microcentrifuge tubes for each of the samples to be sequenced were set up for the termination reaction by adding 2.5 µl of each

ddNTP termination mix (ddGTP, ddATP, ddTTP, ddCTP) to the appropriately labeled tubes. For the labeling reaction, the dNTP labeling mix (dGTP, dTTP and dCTP) was diluted 1:5 to working concentration with ddH$_2$O, and the sequenase polymerase was diluted 1:8 in ice-cold sequenase enzyme dilution buffer. To 10 μl of the ice-cold annealed DNA mixture, 1 μl of 0.1 M DTT, 2 μl of the diluted labeling mix, 0.5 μl of [α-$^{35}$S]dATP and 2 μl of the diluted sequenase polymerase enzyme were added for a final volume of 15.5 μl. The contents were thoroughly mixed and incubated at RT for 3 min. The termination tubes were pre-warmed to 37°C for 2-3 min during this time. To terminate the reaction, 3.5 μl of the labeling reaction mixture was added to each termination tube (G, A, T, C), mixed well and incubated at 37°C for 5 min. The reactions were stopped by adding 4 μl of stop solution and placing the tubes on ice or at –20°C until being run on a sequencing gel.

13-2.  DNA sequencing gel electrophoresis.

The sequencing gel was comprised of 6% acrylamide/bis, 7 M urea in 0.5X TBE buffer which was prepared by dissolving 25.2 g of urea in 22 ml of ddH$_2$O with low heat, and then adding 3 ml of 10X TBE buffer and 9 ml of 40% acrylamide:bis (19:1). The volume was then adjusted to 60 ml with ddH$_2$O. While the urea was dissolving, the 33 x 42 cm sequencing gel plates were assembled with spacers of 0.4 mm thickness. The sides and bottom of the gel plates were sealed with a rubber gasket. Immediately before pouring the gel, 270 μl of 10% APS and 21 μl of TEMED were added to the gel. The gel was poured into the plate assembly held at an inclination using a 60 ml syringe without a needle. The flat edge of a 68-well sharktooth comb was inserted between the two plates at

the top of the assembly, which was then firmly clamped to ensure a snug fit of the comb. The gel was allowed to polymerize for 1-2 h with the top end of the assembly elevated at ~15° angle during the polymerization. The comb and the gasket were removed after polymerization and the gel plate assembly was clamped into a vertical DNA sequencing electrophoresis apparatus. The upper and lower chambers were filled with a total volume of 2 L of 0.5X TBE buffer (50 mM Tris, 41.5 mM boric acid, 0.5 mM EDTA). The top of the gel was flushed with buffer, and the comb was inserted such that the teeth just touched the top of the gel. The gel was then pre-electrophoresed for 30 min at 1750 – 1800 V. The samples were denatured by heating at 75°C for two min. The sample wells were again flushed with buffer, and the denatured samples were immediately loaded into the wells in 3.5 µl volumes. The four terminated reactions (G, A, T, C) of a single DNA template were loaded in adjacent lanes and the samples electrophoresed at 1750 – 1800 V for 1.5 – 2 h. One of the gel plates was removed and the gel soaked in 5% $CH_3COOH$, 15% $CH_3OH$ for 20 min to remove the urea. A Whatman 3MM paper cut to the exact size of the gel was laid on top of the gel placed in the fixing solution and any air bubbles rolled out with a glass rod. The gel was removed from the solution and blotted dry with paper towels. The gel could then be easily transferred onto the Whatman paper by peeling the gel off from the glass plate. The gel was then covered with saran wrap and dried in a vacuum gel dryer at 80°C for 1.5 h. The dried gel was then subjected to autoradiography.

13-3.  Autoradiography.

The dried sequencing gel mounted on the Whatman paper was placed in a metal cassette between intensifying screens such that the gel faced upwards. In the darkroom, a 35 x 43 cm sheet of unexposed Kodak X-Omat XAR-5 film was placed in the cassette so

that it was in direct contact with the gel. The cassette was closed and the film exposed to the gel for 24 – 48 h at RT. After exposure, the film was removed from the cassette in the darkroom and developed using an automatic film processor. The DNA sequences were then read from the exposed film.

Part II-14.  Sedimentation equilibrium experiments of subtilin and synthetic peptides.

Sedimentation equilibrium technique is useful in characterizing interactions between proteins (39). This technique can be used to obtain the molecular weight and the thermodynamic parameters of associating systems (21). To determine the nature of interaction of subtilin with the 12-mer peptide sequences selected by subtilin from the phage display library, two synthetic peptides, pep16 and pep19 obtained from Research Genetics, Alabama were used for the interaction studies using sedimentation equilibrium.

14-1.  Stability of subtilin at RT for 2 days in different pH buffers.

The maximum solubility of nisin at pH 8 was determined to be 0.25 mg/ml with higher solubility at lower pH (42). So, 25 µg of subtilin was suspended in 100 µl of different buffers of 50 mM sodium citrate at pH 5, 50 mM sodium phosphate at pH 6.5, 50 mM Tris-HCl and 150 mM NaCl at pH 7.5, and 100 mM $NaHCO_3$ at pH 8. Subtilin was incubated at RT for 2 days in the different pH buffers. 10 µl of subtilin in each buffer was electrophoresed on a Tricine-SDS-PAGE gel (see Part II-9, 9-1) and the gel was silver-stained (see Part II-10).

14-2. Equilibrium run of subtilin.

70 μM of subtilin corresponding to an $OD_{280}$ of 0.4 was suspended in 150 μl of TBS (50 mM Tris-HCl at pH 7.5, 150 mM NaCl), the same buffer used in the phage display experiment of subtilin. This buffer was also ideal for sedimentation equilibrium analysis due to the presence of a salt concentration between 100 mM and 200 mM and also because this buffer had a density (1.014 g/ml) close to that of water (1 g/ml) which was preferred (58).

A 2-sector analytical ultracentrifuge cell to hold the sample and reference buffer was assembled together from different components. Two quartz windows were assembled first which was followed by sandwiching the centerpiece cell between the two window assemblies in a cylindrical cell housing (10). 145 μl of the subtilin sample was loaded into the right sector of the centerpiece cell, while 150 μl of TBS buffer to be used as the reference solution was loaded into the left sector. The reference sector was filled slightly more than the sample sector to ensure that the reference meniscus did not obscure the sample meniscus in the absorbance profile. The cell was placed in a four-hole rotor with an equally balanced counterbalance cell in the opposite hole. The Beckman XL-I analytical ultracentrifuge was centrifuged initially at 3k rpm and the $OD_{280}$ of the sample was then scanned. The initial $OD_{280}$ scan of the sample at 3k rpm was performed to check the quality of the sample. The sample was then centrifuged at 42k rpm for 24 h at 20°C. The absorbance as a function of radial position was scanned at 280 nm at the end of the run. The sample was further centrifuged for 3 h at 42k rpm and the $OD_{280}$ of the sample was scanned again. Identical $OD_{280}$ profiles obtained by overlaying the scans of both of

55

the consecutive 42k rpm runs recorded a few hours apart indicated that the sample had reached an equilibrium concentration distribution throughout the cell.

14-3.  Equilibrium run of synthetic peptides pep16 and pep19.

The two peptides, pep16 and pep19 synthesized to test for interaction with subtilin, were centrifuged individually. 70 $\mu$M of pep16 corresponding to an $OD_{280}$ of 0.4 was suspended in 150 $\mu$l of TBS, pH 7.5. 145 $\mu$l of the pep16 sample was loaded into one sector of the centerpiece, while 150 $\mu$l of TBS buffer was loaded into the other sector. The $OD_{280}$ of the sample was initially scanned at 3k rpm. The sample was then centrifuged at 54k rpm for 20 h at 20°C, $OD_{280}$ scanned, then centrifuged again at 54k rpm for 2 h and the $OD_{280}$ scanned again. This process was repeated at 56k rpm for the same sample. Pep19 was also subjected to the same procedure as pep16.

14-4.  Equilibrium run of subtilin with pep16 and pep19.

An equimolar mixture of subtilin and pep16 corresponding to an $OD_{280}$ of 0.3 as determined in the uv-vis spectrophotometer was suspended in 150 $\mu$l of TBS, pH 7.5. The $OD_{280}$ of the sample was initially scanned at 3k rpm. The sample was centrifuged at 45k rpm for 18 h, at 45k rpm again for 1 h, at 50k rpm for 18 h, and at 50k rpm again for 1 h. The $OD_{280}$ and the $OD_{254}$ of the sample were scanned at the end of each run.

Part II-15.  Detection of subtilin protein targets in susceptible bacterial cells using monomeric avidin column.

In order to isolate the biological protein targets of subtilin from susceptible bacterial cells, the natural affinity of biotin for avidin was availed of in this method.

Subtilin was biotinylated, and the biotinylated subtilin was incubated with total bacterial cell protein. This complex protein mixture was incubated on a monomeric avidin column, when biotinylated subtilin bound to bacterial proteins was affinity captured by the immobilized avidin. After washing the avidin column to remove non-specifically bound proteins, the biotinylated subtilin – protein complex was eluted from the column using a biotin-containing buffer followed by a low pH glycine buffer. The proteins thus isolated were analyzed by SDS-PAGE.

15-1.  Incubation of biotinylated subtilin with *B. cereus* and *B. subtilis* 168 cells.

500 µg of subtilin was biotinylated in a 1:1 nanomolar ratio by reacting subtilin with biotin disulfide N-hydroxy succinimide ester as described in Part II-8. Biotinylated subtilin was purified using RP-HPLC (see Part II-6) and halo assay was performed on the HPLC purified fractions to ensure that biotinylated subtilin retained antimicrobial activity.

10 mg of *B. cereus* spores or *B. subtilis 168* spores was heat-shocked for 2 h at 65ºC to break the dormancy of the spores as described in Part II-16, 16-1. The heat-shocked spores were suspended in 1 ml of sterile ddH$_2$O. The spores were streaked onto a medium A plate and incubated overnight at 37°C. 50 ml of medium A solution (see Part II-1, 1-6) in a 250 ml flask was inoculated with a single bacterial colony picked from the plate and incubated at 37°C at 250 rpm until the culture reached an OD$_{600}$ of ~1. The culture was centrifuged at 4,000 rpm for 10 min and the cell pellet suspended in 10 ml of 50 mM Tris-HCl, pH 8. Biotinylated subtilin (500 µg) was then added to the solution and incubated with bacterial cells for 3 h at RT with gentle shaking. The cells were then lysed using a French pressure cell (56). The cell lysate was centrifuged at 4,000 rpm for 10 min

to pellet down the cell debris and the supernatant loaded onto the monomeric avidin column. A 50 ml bacterial cell culture without biotinylated subtilin was used as a control and was subjected to the same procedure. The supernatant from the control cell lysate was loaded onto another monomeric avidin column.

15-2. Elution of bacterial proteins bound to biotinylated subtilin from monomeric avidin column.

Two 2 ml monomeric avidin columns were packed according to the instructions given in the Pierce instruction booklet for the immunopure immobilized monomeric avidin column. Each of the 2 ml columns was washed with 2 x 4 ml of PBS (0.1 M sodium phosphate, 0.15 M NaCl, pH 7.2) first and then with 3 x 2 ml of biotin blocking and elution buffer (2 mM biotin in PBS) to block any non-reversible biotin binding sites on the column. Loosely bound biotin from the reversible biotin-binding sites was removed by washing with 3 x 4 ml regeneration buffer (0.1 M glycine, pH 2.8) and then with 2 x 4 ml of PBS. The cell lysate supernatant containing biotinylated subtilin was added onto one of the columns dropwise, while the control cell lysate supernatant without biotinylated subtilin was loaded onto the other monomeric avidin column. After all of the sample solution had been added, 0.25 ml of PBS was added to wash the sample completely into the column. The sample was allowed to incubate on the column for 1 h at RT. The column was washed with at least 6 x 2 ml of PBS and fractions collected. The absorbance of the fractions was monitored at 280 nm until all unbound protein was washed off the column. The bound, biotinylated protein was eluted from the column with at least 6 x 2 ml of the biotin blocking and elution buffer and the absorbance of the collected fractions monitored at 280 nm. In order to elute bound, biotinylated peptide

completely, the column was washed with at least 6 x 2 ml of regeneration buffer and the OD$_{280}$ monitored. The column was then washed with 5 ml of PBS and stored at 4°C.

The samples eluted from the monomeric avidin column were dialyzed using snakeskin pleated dialysis tubing from Pierce (3.5k MWCO) in 5 mM Tris-HCl, pH 8 overnight at 4°C with 2 changes of buffer. The dialyzed samples were lyophilized. After lyophilization, the samples were suspended in 600 μl of modified 1X gel loading buffer (0.05 M Tris-HCl, pH 6.8, 2% SDS, 10% glycerol). 5% 2-mercaptoethanol and 0.1% bromophenol blue were added to 100 μl of the sample and the sample boiled for 3 min before being loaded onto a 12% SDS-PAGE gel (see Part II-9, 9-2) in duplicate. At the end of electrophoresis, one half of the gel was transferred to a nitrocellulose membrane and the membrane probed with streptavidin-alkaline phosphatase conjugate (see Part II-11, 11-1, 11-2). The other half of the gel was silver-stained as described in Part II-10.

Part II-16. Detection of subtilin targets in *B. cereus* spores.

16-1. Incubation of biotinylated subtilin with spores.

0.01 g of spores was weighed and homogenized in 20 ml of sterile ddH$_2$O. The spores were heat shocked at 65°C for 2 h in a water bath. The spores were then centrifuged at 10,000 rpm for 10 min and the spore pellet suspended in 1 ml of sterile ddH$_2$O.

The heat-shocked *B. cereus* spores (200 μg/ml) were incubated with biotinylated subtilin (20 μg/ml) in 1 ml of 1% tryptone-Pi, pH 7.4 for 3 h in a 37°C water bath. Two control spore samples, one with subtilin, and the other without any subtilin, were also incubated for 3 h. After incubation, the samples were observed by phase-contrast

microscopy to check for inhibition of germination of spores by biotinylated subtilin and by subtilin. Ungerminated spores were phase-bright, while germinated spores whose outgrowth was inhibited appeared phase-dark (42). The uninhibited spores without any biotinylated subtilin or subtilin were observed as elongated vegetative cells.

16-2.  Isolation of bacterial spore targets of subtilin by spore lysis.

The samples from Part II-16, 16-1 were centrifuged at 14,000 rpm for 10 min and the spore pellet suspended in 0.7 ml of spore lysis buffer (0.14 M NaCl, 0.3 M sucrose, 0.1 M Tris-Pi, pH 7.4, 2 mM EDTA and 2 mM PMSF). In order to allow subtilin to react with any intracellular targets, 5 µg/ml of biotinylated subtilin was added to one sample, and 5 µg/ml of subtilin added to the other sample. Each sample was mixed with 0.7 g of glass beads (<0.1 mm diameter) in a capsule. The spores were lysed in a dental amalgamator or wig-L-bug in ten 1 min periods of shaking with 1 min intervals on ice to dissipate the heat produced during shaking. The lysed sample was collected and the glass beads rinsed with 0.7 ml of spore lysis buffer (41). The solutions were pooled and centrifuged at 14,000 rpm for 10 min. The supernatant was concentrated by lyophilization. The samples were placed at 4°C until they were electrophoresed on a 12% Laemmli gel.

2X gel loading buffer (0.05 M Tris-HCl, pH 6.8, 0.1% SDS, 20% glycerol, 0.01% bromophenol blue) was added to each sample. The samples were boiled for 3 min before being electrophoresed on a 12% SDS-PAGE gel. The proteins were transferred onto a nitrocellulose membrane and the membrane probed with streptavidin-alkaline phosphatase conjugate.

Part II-17.  Fluorescein-labeling of nisin.

Highly purified, lyophilized nisin was obtained from Aplin and Barrett (Trowbridge, Wilts UK). A 10 mg/ml stock solution of nisin was prepared by dissolving 1 mg of nisin in 1 ml of 0.05% TFA. Immediately before conjugation of fluorescein to nisin, a 10 μg/μl stock solution of NHS-Fluorescein (NHSF) was prepared by dissolving 1 mg of the reagent in 100 μl of DMF. 7 μl of the NHSF stock corresponding to an equimolar concentration of nisin (149 μM) was added to 50 μl of the nisin stock (0.5 mg) and the volume adjusted to 2 ml with 100 mM $NaHCO_3$, pH 8. This was incubated on ice for 2 hours. A control using nisin without the NHSF reagent was also performed. The reactions involving NHSF were performed in the dark since the reagent is light-sensitive. After 2 h, the unreacted nisin was separated from fluorescein-nisin (F-N) using RP-HPLC as described in Part II-6. The collected F-N fractions were assayed for retention of antimicrobial activity by halo assay (see Part II-5). The fractions exhibiting antimicrobial activity were lyophilized in a SpeedVac and pooled together in a 500 μl volume of 0.05% TFA. This was stored at –20°C. The presence of the fluorescein tag was confirmed by electrophoresing fluorescein-nisin on a mini SDS-PAGE gel (see Part II-9, 9-2), followed by detection of fluorescence using a uv-transilluminator or Storm Imager 860. Presence of F-N was also confirmed by silver staining (see Part II-10).

Part II-18.  Electron microscopy of *B. cereus* spores reacted with nisin.

18-1.  Scanning electron microscopy (SEM) of *B. cereus* spores incubated with fluorescein-nisin.

Heat-shocked *B. cereus* spores (200 μg/ml) were incubated with fluorescein-nisin (20 μg/ml) for 2 h at 37°C in 1% tryptone-Pi growth media, pH 7.4. The spores were

washed in 1 ml of PBS (10 mM phosphate, 150 mM NaCl), pH 7.4 thrice to remove any unbound fluorescein-nisin (F-N) by centrifuging at 14,000 rpm for 10 min. The sample was fixed by incubating in 1 ml of 2% glutaraldehyde (GA) in PBS for 1 h at RT in the dark. The sample could then be kept at 4°C until further processing.

The spores were collected on a nucleopore filter (0.4 μ) held in a plastic Swinney filter holder. The spores were washed free of excess GA with three changes of PBS for 5 min each. The spores were then fixed in 1 ml of 1% osmium tetraoxide in PBS for 1 h, and then washed with three changes of dH$_2$O. The filter was transferred to a flat multi-well dish for dehydration. Care was taken not to allow the sample to air dry during these procedures.

The sample was then dehydrated for 10 min each in 75% ethanol and 95% ethanol followed by dehydration in 100% ethanol thrice. The filter with the sample was then dried in a Denton DCP-1 critical point dryer. The filter was fixed to a carbon tab mounted on a metal stub and the filter edge brushed with colloidal carbon. Next, the sample was placed in a Denton vacuum evaporator for a deposition of a Au-Pd coat of ~15 nm thickness on the specimen. The sample was stored in a desiccator until it was viewed in a Hitachi S4700 scanning electron microscope. Two controls were also performed, one control consisting of nisin incubated with spores, and the other control consisting of only spores without F-N or nisin.

18-2.  SEM of immunogold labeled *B. cereus* spores.

500 μg of nisin was biotinylated by reacting nisin with the biotinylating agent BDNHSE as described in Part II-8. Heat-shocked *B. cereus* spores (300 μg/ml) were incubated with biotinylated nisin (50 μg/ml) for 3 h at RT. The sample was washed thrice

with 1 ml of PBS buffer and then fixed in 1 ml of 1% GA in PBS for 1 h at RT with gentle shaking. The sample was washed thrice with 1 ml of PBS.

Before labeling the sample with streptavidin-gold (SA-Au), the sample was incubated in 1 ml of 0.05 M glycine in PBS for 15 min and then washed with three changes of PBS buffer. The sample was next incubated in 1 ml of PBS buffer with 5% BSA for 30 min followed by three wash steps. SA-Au (15 nm particle size) was added at a 1/20 dilution in 1 ml of PBS and the sample incubated for 2 h. After washing with PBS for 6 x 5 min, the sample was postfixed in 2% GA in 1 ml of PBS for 5 min. The sample was washed in 1 mL of PBS for 3 x 5 min and collected on a nucleopore filter (0.4 µ). The filter was removed to a flat multi-well dish for silver enhancement for 30 min performed using Aurion R-Gent SE-EM initiator, activator and enhancer to increase the average gold cluster or particle size by deposition of metallic silver. The filter was washed thrice with distilled water for 5 min. The sample was then dehydrated, dried and mounted on a metal stub. A thin chromium coating of ~15 nm thickness was deposited on the sample which was then viewed in the Amray 1820D and the Hitachi S4700 scanning electron microscopes. A control consisting of spores incubated without biotinylated nisin was also subjected to the same procedure.

18-3. Transmission electron microscopy (TEM) of *B. cereus* spores reacted with nisin.

Heat-shocked *B. cereus* spores (200 µg/ml) were incubated with biotinylated nisin (30 µg/ml) for 2 h at RT. Two controls were also performed, one consisting of nisin and spores, and the other with only spores. The sample was washed thrice with 1 ml of PBS

buffer and then fixed in 1 ml of 2% GA in 1X PBS for 1 h at RT with shaking. The sample was washed with 3 x 1 ml of PBS to remove excess GA.

The sample was post fixed in 2% osmium tetraoxide in 1 ml of PBS for 60 min and washed for 3 x 10 min with $dH_2O$. The sample was again fixed in 2% aqueous uranyl acetate for 60 min and then centrifuged. Dehydration was performed in 35%, 50%, 75% and 95% ethanol for 10 min each, with centrifugation between each dehydration step. This was followed by dehydration in 100% ethanol for 3 x 10 min, and in propylene oxide for 3 x 10 min.

The sample was then treated with propylene oxide:Spurr's resin mixture (1:1) for 2 h, propylene oxide:Spurr's resin mixture (1:2) for 2 h, propylene oxide:Spurr's resin mixture (1:3) for 2 h and then with 100% Spurr's resin for 2 h. The sample was finally embedded in fresh 100% Spurr's resin and incubated (cured) at 70°C for atleast 8 h. The sample was trimmed using a glass knife on a LKB-Nova ultramicrotome followed by manual trimming using a fresh razor. Thin sections (~ 150nm thickness) of the sample were collected using a freshly prepared glass knife.

Part II-19. Reacting fluorescein-nisin with *B. subtilis* 168 vegetative cells.

10 mg of *B. subtilis 168* spores was heat-shocked for 2 h at 65°C to break the dormancy of the spores as described in Part II-16, 16-1. The heat-shocked spores were suspended in 1 ml of sterile $ddH_2O$. Heat-shocked *B. subtilis* 168 spores were streaked onto a medium A plate and incubated overnight at 37°C. 50 ml of medium A solution in a 250 ml flask was inoculated with a single *B. subtilis* colony picked from the plate and incubated at 37°C at 250 rpm until the culture reached an $OD_{600}$ of ~0.5. The culture was

centrifuged at 4,000 rpm for 10 min and the cell pellet suspended in 10 ml of 10 mM Tris-HCl, pH 8. Nisin was labeled with fluorescein as described in Part II-17. Fluorescein-nisin (500 µg) was then added to the solution alongwith 0.1% glucose and incubated with *B. subtilis* cells overnight with gentle shaking. The cells were completely lysed using a French pressure cell (56). After cell lysis, the cell lysate was concentrated in YM-10 centricon tubes by centrifuging at 5,000 x g for 90 min. 2 cell cultures, one with the addition of 500 µg of nisin and the other without any nisin or F-N were also subjected to the same procedure.

The retentate and the filtrate solutions obtained after the YM-10 concentration were both analyzed by SDS-PAGE. 5X gel loading buffer was added to 75 µl of the sample alongwith 5% 2-ME. The samples were boiled for 3 min and then run on a 12% Laemmli gel. Fluorescent bands were detected on the gel using a Storm 860 Imager. The gel was silver stained as well to detect total protein (see Part II-10).

Part II-20.  Detection of fluorescein-nisin using anti-FITC antibodies.

20-1.  Dot blot using anti-FITC antibodies.

The dot blots were performed to determine the optimum concentrations of the anti-FITC antibodies and the 2° Ab-alkaline phosphatase conjugate required for optimal detection. In the dot blots, four nitrocellulose (NC) membrane strips were wet with distilled water for 1 min. After the NC strips had dried, different amounts of F-N (0.5 µg, 1 µg, 1.5 µg, 2 µg, 3 µg and 5 µg) were spotted. The NC strips were allowed to dry and then blocked with 3% BSA in 50 ml of TBST (10 mM Tris-HCl at pH 8, 150 mM NaCl and 0.05% Tween-20) for 1 h at RT with gentle agitation. Rabbit anti-FITC Ab (1° Ab)

was added as 1:100, 1:250, 1:500 and 1:1000 dilutions in 30 ml of TBST. Each of the four NC strips was incubated in one of these Ab dilutions for 1 h at RT. The strips were washed with 2 x 50 ml of TBST for 5 min, followed by incubation for 1 h with goat anti-rabbit antibody-alkaline phosphatase enzyme conjugate (2º Ab-AP conjugate). The 2º Ab-AP conjugate was added at a dilution of 1:2500 in 30 ml of TBST. The strips were again washed with 2 x 50 ml of TBST for 5 min. 30 ml of the 1-Step$^{TM}$ NBT/BCIP substrate solution was added to each of the four NC strips and the NC strips developed for 2 min. The NC strips were washed with 2 x 50 ml of ddH$_2$O for 5 min and then dried.

20-2.  Immuno blot detection of immobilized fluorescein-nisin.

This protocol was used to detect membrane-immobilized fluorescein-nisin bound to bacterial proteins. In the immuno blot, fluorescein-nisin (F-N) and bacterial proteins bound to F-N were transferred onto a nitrocellulose membrane overnight at 50 mA at 4ºC as described in Part II-10, 10-1. A 1 L solution of TBST (10 mM Tris-HCl at pH 8, 150 mM NaCl and 0.05% Tween-20) was prepared as described in Part II-1, 1-5. The NC membrane with bound F-N was incubated in 50 ml of blocking buffer (3% BSA in TBST) for 1 h at RT with gentle agitation. The NC membrane was then incubated with rabbit anti-FITC Ab as a 1:500 dilution in 30 ml of TBST for 1 h with agitation. The NC membrane was washed with 2 x 50 ml of TBST for 5 min each, and then incubated with the 2º Ab-AP conjugate as a 1:2500 dilution in 30 ml of TBST for 1 h at RT. The NC membrane was again washed with 2 x 50 ml of TBST for 5 min, and the membrane developed in 30 ml of the 1-Step$^{TM}$ NBT/BCIP substrate solution (Pierce) for a few min. The NC membrane was then rinsed with 2 x 50 ml of ddH$_2$O for 5 min, dried and scanned on a computer scanner to obtain a digital image of the developed protein bands.

Part II-21.  Size exclusion chromatography using macrosphere column.

For size exclusion chromatography, an Alltech macrosphere GPC column was used which was of 250 mm length and 4.6 mm internal diameter with 7 µm spherical particles and 100 Å pores. For every sample run on the column, the column was first washed with HPLC-grade water (wash buffer) for 15 min at a flow rate of 0.3 ml/min. The column was equilibrated with the mobile phase buffer, solvent C (0.05 M $KH_2PO_4$, 0.1 M NaCl, pH 6.8) for 30 min at a flow rate of 0.3 ml/min (5). The sample was then loaded onto the column, eluted using the mobile phase buffer and 0.3 ml fractions collected every min for 30 min. The column was then washed with the wash buffer.

To test the SEC column, blue dextran (~2,000 kDa) at 2 different concentrations of 20 µg/150 µl and 40 µg/150 µl was loaded on the SEC column and eluted. Next, ethidium bromide (~394.3 Da) at 10 µg/150 µl and then at 100 µg/150 µl was eluted from the column and fractions collected. 2,4-dinitro phenol (~184.1 Da) was then eluted at a concentration of 100 µg/150 µl.

The lysate of *B. subtilis* 168 cells treated with fluorescein-nisin (F-N) and a negative control cell lysate sample without F-N (from Part II-19) were concentrated using YM-3 centricon tubes. 50 µl of the concentrated control cell lysate sample was centrifuged to remove cell debris. To the supernatant, 100 µl of the mobile phase buffer was added. The sample was eluted from the SEC column and fractions collected every min. The fractions were run on a gel and silver stained. Also, to another 50 µl of control cell lysate, 100 µl of mobile phase and 0.1% SDS were added and the sample boiled for 3

min. This was centrifuged to remove debris and then run on the SEC column. The same procedure was repeated with the F-N + cell lysate samples.

Part II-22.  Affinity chromatography using immobilized protein A-antibody complex.

22-1.  Preparation of the protein A-antibody complex column.

A 2 ml protein A column from an immunopure protein A IgG orientation kit (Pierce) was brought to room temperature. 50 µg – 1 mg of anti-FITC antibody (Ab) from Zymed Laboratories was diluted 1:1 with the antibody binding/wash buffer (50 mM sodium borate, pH 8.2) and added to the column. The gel was suspended by gentle inversion at 4°C overnight to allow binding of the anti-FITC-Ab to the protein A matrix. The gel was then allowed to settle and then washed with 2 x 5 ml of antibody binding/wash buffer. The wash fractions were collected to test for any unbound Ab. The Ab bound to the protein A matrix was then crosslinked by adding 13.2 mg of DMP (dimethyl pimelimidate) dissolved in 2 ml of the DMP crosslinking buffer (0.2 M triethanolamine, pH 8.2) and mixing the gel gently for 1 h at room temperature. The gel was allowed to settle while the remaining solution passed through, taking care not to allow the gel bed to run dry. The gel was then washed with 5 ml of the crosslinking buffer. In order to block any remaining unreacted imidate groups, 2 ml of blocking buffer (0.1 M ethanolamine, pH 8.2) was added and the gel mixed gently for 10 min. The gel was then washed with 5 ml of IgG elution buffer, pH 2.8 to elute any Ab that was not covalently attached to the immobilized protein A. The gel was then washed with 2 x 5 ml antibody binding/wash buffer and stored at 4°C in an aqueous solution containing

0.02% sodium azide. The same procedure was repeated with another 2 ml protein A column so as to use this column for the control cell lysate sample.

22-2. Affinity chromatography of fluorescein-nisin incubated with *B. subtilis* 168 proteins.

The prepared immunoaffinity column was allowed to come to room temperature. After the storage solution had drained, the column was equilibrated with 2 x 5 ml of binding buffer (10 mM Tris buffer, pH 7.5). The lysate of *B. subtilis* 168 cells treated with fluorescein-nisin (F-N + cell lysate sample) was concentrated from 10 ml to 1.5 ml using YM-3 centricon tubes. The sample was centrifuged to remove cell debris. The supernatant was diluted 1:2 with binding buffer. The sample was applied to the column dropwise and incubated on the column for 1 h at room temperature. After 1 h, the sample was allowed to flow through the column and the unbound protein collected. The column was then washed with 6 x 2 ml of binding buffer and fractions collected. The $OD_{280}$ of the wash fractions was determined to check that all non-specifically bound protein was washed off the column. The bound protein was then eluted with at least 6 x 2 ml of 0.1 M glycine-HCl buffer, pH 2.8 and the elution of protein was monitored by measuring $OD_{280}$. The pH of the eluted fractions was raised to neutral by adding 100 µl of 1 M Tris-HCl, pH 9.5 to each of the 2 ml fractions. The same procedure was repeated with the control cell lysate sample on a different 2 ml affinity column. The affinity column was regenerated by washing the column with 4 column volumes (8 ml) of glycine-HCl buffer. The column was stored at neutral pH in water containing 0.02% sodium azide. The fractions were concentrated using YM-3 centricon tubes by centrifuging at 7,500 x g for 1 h. 5X gel loading buffer was added and the samples analyzed by SDS-PAGE. The gel

was examined on a Storm 860 Imager followed by silver staining (see Part II-10). A negative control cell lysate sample without F-N was also subjected to the same procedure.

22-3. Affinity chromatography of fluorescein-nisin.

The same procedure used for affinity chromatography of the F-N + cell lysate sample was followed for F-N. 25 μl of F-N corresponding to 25 μg was diluted with the binding buffer and incubated on the column for 1 h. The column was washed with binding buffer and fractions collected. F-N was eluted with glycine-HCl buffer. The fractions were concentrated in YM-3 tubes and run on a gel.

Part II-23. Classic immunoprecipitation using protein A column.

The Seize Classic (A) Immunoprecipitation Kit from Pierce was used for immunoprecipitation. An immune complex of the anti-FITC Ab and the antigen, the fluorescein-nisin-bacterial protein complex was prepared by incubating 100 μg of the anti-FITC Ab with 100 μl of the antigen in 10 mM Tris-HCl, pH 8 in a total volume of 0.4 ml at 4°C overnight with gentle shaking. 0.4 ml of the immobilized protein A (50% slurry) was added into a spin cup column which was placed inside a microcentrifuge tube. The tube was centrifuged and the buffer discarded. The gel was washed twice by adding 0.4 ml of binding/wash buffer (140 mM NaCl, 8 mM sodium phosphate, 2 mM potassium phosphate, 10 mM KCl, pH 7.4), mixing gently for 2 min and centrifuging the tube. The spin cup was then placed in a new microcentrifuge tube.

The prepared immune complex was added to the spin cup containing equilibrated protein A, mixed by inversion and incubated for 30 min at room temperature with gentle shaking. The tube was then centrifuged and the flow-through containing unbound protein

was collected. The gel was washed 5 times by adding 0.5 ml of wash buffer, mixing by inverting, and by centrifuging the tube. The wash fractions were collected for gel electrophoresis. The bound protein was eluted by adding 6 x 190 µl of elution buffer (glycine-HCl, pH 2.8), mixing by inverting at least 10 times, and then centrifuging. The eluate was neutralized by adding 10 µl of 1 M Tris, pH 9.5 to each fraction. All the collected fractions were analyzed by SDS-PAGE. The gel was regenerated by adding 2 x 0.5 ml of wash buffer, mixing by inverting and then centrifuging the tube. 0.5 ml of wash buffer with 0.02% sodium azide was then added to the spin cup, which was placed in a microcentrifuge tube. The cap of the tube was wrapped with parafilm to prevent the gel from drying and the tube placed at 4ºC. The same procedure was followed with the control cell lysate.

Part II-24.  Small-scale immunoprecipitation using immobilized protein A.

24-1.  Preparation of the protein A-antibody complex column.

Immobilized protein A from a seize X protein A immunoprecipitation kit from Pierce was allowed to come to room temperature. 0.4 ml of protein A (50% slurry) was added into a spin cup column, which was placed inside a microcentrifuge tube. The tube was centrifuged and the buffer discarded. The gel was washed twice by adding 0.4 ml of binding/wash buffer (140 mM NaCl, 8 mM sodium phosphate, 2 mM potassium phosphate, 10 mM KCl, pH 7.4), mixing by inverting with gentle shaking and then centrifuging the tube. The spin cup was then placed in a new microcentrifuge tube. 400 µg of anti-FITC antibody prepared in binding/wash (PBS) buffer was added to the column and allowed to bind overnight at 4°C with shaking. After overnight incubation,

the column was centrifuged and the flow-through saved. The spin cup was placed in another microcentrifuge tube and washed with 3 x 0.5 ml of PBS buffer.

The spin cup was transferred to a new microcentrifuge tube and 0.4 ml of PBS buffer was added to it. 25 μl of the cross-linker disuccinimidyl suberate (DSS) corresponding to 625 μg of DSS in dimethyl formamide was added to the spin cup and gently mixed for 1 h at room temperature. After centrifuging the tube, the antibodies that were not covalently bound to protein A were eluted with 5 x 0.5 ml of elution buffer at pH 2.8. The eluates were saved for analysis. The spin cup was placed in a new microcentrifuge tube and washed with 10 x 0.5 ml of PBS buffer to ensure complete regeneration of the bound antibody. For storage, 0.5 ml of PBS buffer was added alongwith 0.02% sodium azide and the gel stored at 4°C.

24-2.  Affinity chromatography of fluorescein-nisin bound to bacterial proteins.

The gel was first brought to room temperature and then washed with 10 x 0.5 ml of PBS buffer. 10 μg of fluorescein-nisin (F-N) was diluted with binding/wash buffer to a total volume of 200 μl and incubated with the bound antibody with gentle shaking at 4°C overnight. The tube was centrifuged and the flow-through collected. The gel was washed with 4 x 0.5 ml of PBS buffer and the first wash fraction saved. The antigen was eluted under different eluting conditions. Elution at low pH involved adding 190 μl of elution buffer at pH 2.8, inverting the tube several times and then centrifuging the tube. This was repeated 6-10 times and the eluates collected. The eluates were neutralized by the addition of 10 μl of 1 M Tris, pH 9.5. Other elution conditions including high salt (3.5 M $MgCl_2$ in 10 mM phosphate buffer at pH 7) and denaturing conditions (8 M Guanidine-

HCl and 1% SDS) were also used to elute F-N from the column. The eluate fractions were then electrophoresed on a 12% gel. The gel was visualized on a Storm 860 Imager and also by silver staining. The column was regenerated by washing with 10 x 0.5 ml of PBS buffer and stored at 4°C.

A similar method of immunoprecipitation was performed for the F-N + cell lysate sample and also the control cell lysate sample (without F-N) using different amounts of the F-N + cell lysate and the control cell lysate samples (10 μl to 150 μl). These samples were eluted using low pH.

**Results and Discussion**

Part I.  Isolation of stable subtilin from *Bacillus subtilis* LH45.

Subtilin previously isolated from its natural producer *Bacillus subtilis* ATCC 6633 by acetone-butanol procedure was unstable and its biological activity was lost during isolation and storage, with chemical instability observed in less than a day at room temperature (44). Although subtilin and nisin share considerable structural homology, subtilin had been observed to be very unstable compared to nisin, which could be stored for months without any detectable chemical or biological changes (42). Therefore, subtilin isolated from the original producer was stored at –80°C to preserve its biological activity (43). In this work, subtilin was isolated from *Bacillus subtilis* LH45, a modified strain of *B. subtilis* 168 that was engineered to produce subtilin (43).

Part I-1.  Isolation of stable subtilin using hydrophobic interaction column.

Subtilin was isolated from *Bacillus subtilis* LH45 using hydrophobic interaction chromatography (HIC) and purified using RP-HPLC. This process resulted in the isolation of subtilin along with succinylated subtilin which eluted after subtilin in a RP-HPLC run. Succinylated subtilin is produced later in the bacterial growth phase than subtilin, and is 10-20 times less active than subtilin although succinylated subtilin retains antimicrobial activity (7). Isolation of subtilin from LH45 also resulted in isolation of sublancin, a recently discovered type A lantibiotic (57), since *B. subtilis* 168 is a natural producer of sublancin. The elution of the peptides was monitored at 254 nm and fractions corresponding to the peaks were collected every min to isolate sublancin, subtilin and

succinylated subtilin. The biological activity of subtilin in the collected fractions was confirmed by halo assays and the presence of subtilin in the individual fractions detected by MALDI-TOF. The RP-HPLC and mass spectroscopic profiles of subtilin are represented in Fig. 7. The predicted mass of non-succinylated subtilin is 3320 Da which agrees with the mass obtained from mass spectroscopic analysis. Sublancin and succinylated subtilin correspond to 3877 Da and 3419 Da in mass, respectively. The fractions containing non-succinylated subtilin were pooled and the concentration of subtilin determined in a uv-vis spectrophotometer at 254 nm using known concentrations of nisin as a standard.

Subtilin isolated using the hydrophobic interaction column was very stable. The biological activity of subtilin as determined from antimicrobial (halo) assays remained unchanged after four months of storage at -20°C (Fig. 8). Subtilin was also stable when stored at room temperature for 2 days in different pH buffers (see Results, Part III). Isolation of subtilin from the LH45 culture using HIC also resulted in a copious quantity of subtilin compared to that obtained from the 6633 culture using acetone-butanol procedure. 2.5 – 3 mg of subtilin could be isolated from 500 ml of LH45 culture compared to 100 μg of subtilin purified from 500 ml of the 6633 culture (59).

The stability of subtilin isolated from LH45 using HIC was comparable to that of nisin. Studies of type A lantibiotics had been performed mainly using nisin as a model type A lantibiotic and not subtilin, although nisin and subtilin are structurally related in terms of both their chemical structure and their conformation in aqueous solution (7). A possible reason could probably have been the instability of subtilin, which rendered subtilin of little practical value in spite of having a broad spectrum of action (44).
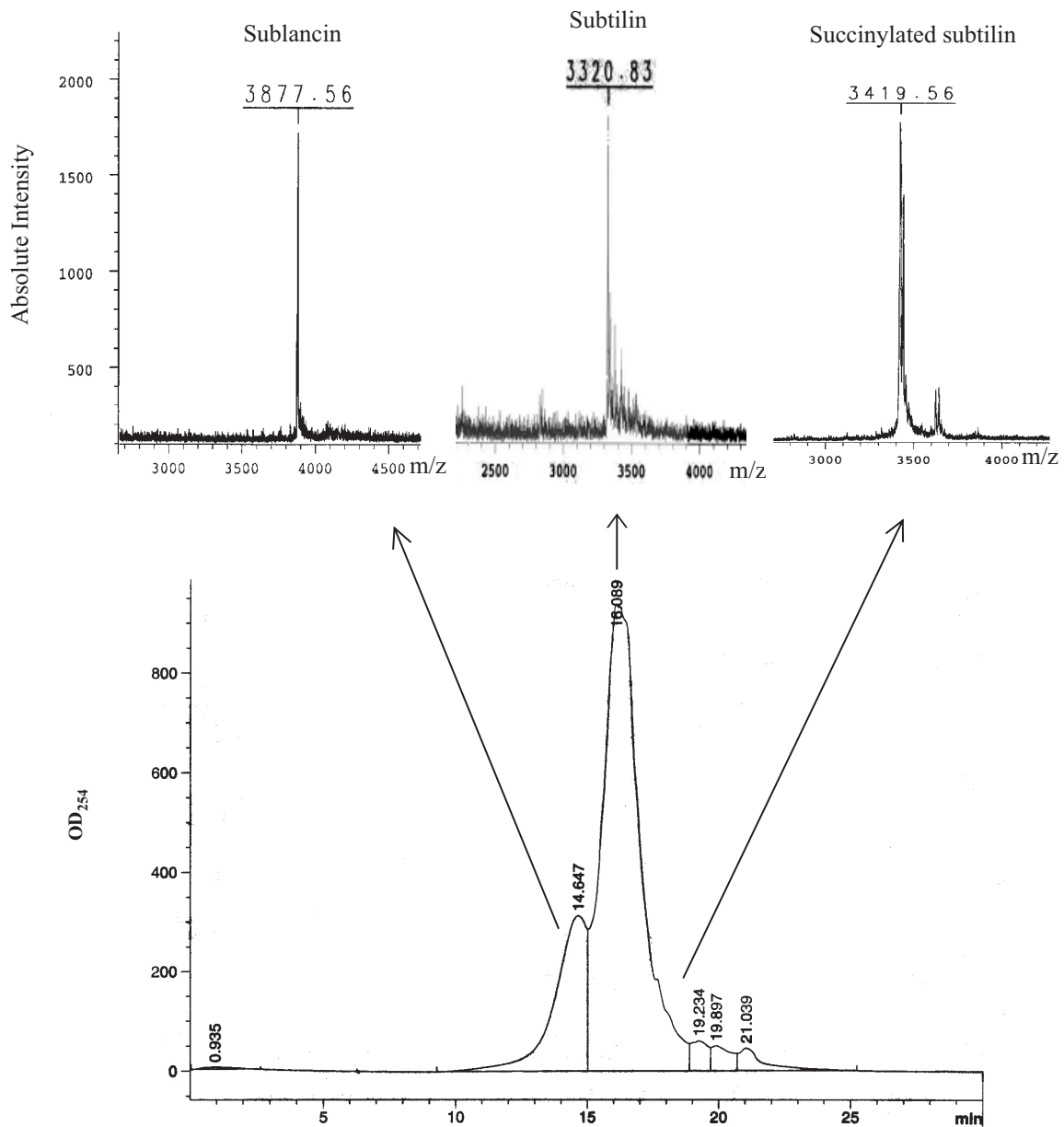
**Figure 7. RP-HPLC and MALDI-TOF profiles of subtilin isolated using HIC.**

Subtilin isolated from *Bacillus subtilis* LH45 using hydrophobic interaction chromatography (HIC) was further purified by reverse phase - HPLC. The RP-HPLC profile is depicted in the bottom figure. Fractions corresponding to the peak were collected every min and analyzed by MALDI-TOF. Mass spectrometric analysis of the fractions detected sublancin, subtilin and succinylated subtilin in different fractions as seen in the figures above.
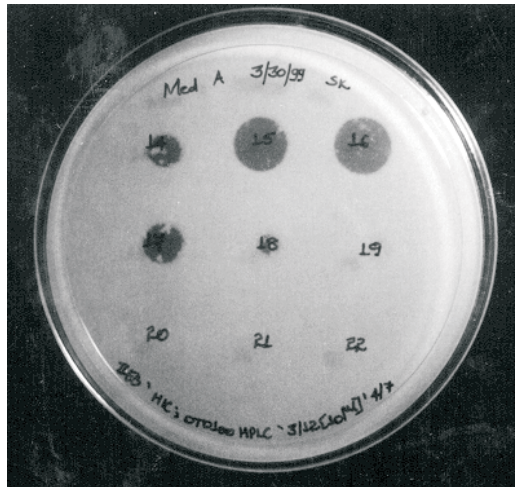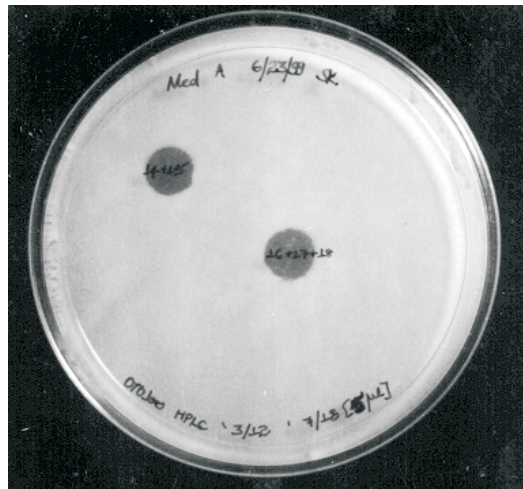
**Figure 8. Antimicrobial (halo) assay of stable subtilin.**

Subtilin isolated using HIC and purified by RP-HPLC was collected as 1.2 ml fractions every min. In panel A, 10 µl of fractions corresponding to elution between 14 - 22 min of the RP-HPLC run was tested for antimicrobial activity against *Bacillus cereus* spores. The fractions 14 - 17 that exhibited antimicrobial activity were stored at -20ºC. 5 µl from fractions 14 and 15, and 5 µl from fractions 16, 17 and 18 were again tested for antimicrobial activity after four months, as seen in panel B. From the zones of inhibition in panels A and B, subtilin appears to be stable after four months of storage at -20ºC with little loss of biological activity.

Isolation of stable subtilin has thereby enabled subtilin to be used as a model to study its specificity and antimicrobial mechanism of action. This has also enabled the generation of rabbit anti-subtilin antibodies against subtilin obtained from Research Genetics, Alabama.

Part I-2.  Isolation of stable subtilin using non-ionic cellulose column.

Nisin was found to bind to cellulose under mildly alkaline conditions and was released from non-ionic cellulose under acidic conditions (78). This work showed that subtilin, a structural analog of nisin, also bound to non-ionic cellulose under alkaline conditions and eluted from cellulose using an organic solvent. It is unusual for a polypeptide to bind to an inert matrix such as non-ionic cellulose. A possible biological significance of the interaction of nisin and subtilin with cellulose was realized due to the structural resemblances between cellulose and the polysaccharides present in the bacterial spore coats and cell membranes, both of which can bind nisin and subtilin. Binding of nisin to the carbohydrate moiety of lipid II present in the cell membrane is proposed to facilitate pore formation of nisin according to the lipid II-mediated nisin pore formation model (see Fig. 6). Since subtilin can be eluted from cellulose by an organic solvent, this suggests that binding of subtilin to cellulose occurs through hydrophobic interactions. This possibility may also reflect the ability of subtilin and nisin to bind to the mucopolysaccharide of the bacterial cell envelope.

The ability of subtilin to bind cellulose under alkaline conditions and to dissociate from cellulose using an organic solvent also provided a method of isolation of subtilin from bacterial culture supernatant. *Bacillus subtilis* LH45 was grown for 27 h to allow for

synthesis and secretion of subtilin into the extracellular medium. The culture was centrifuged to obtain the culture supernatant and the pH of the supernatant adjusted to 8. A column packed with non-ionic cellulose powder supernatant was equilibrated with 7 volumes of 100 mM Tris-HCl, pH 8 (wash buffer). The supernatant was also equilibrated with Tris-HCl (pH 8) to a final concentration of 100 mM and then loaded onto the cellulose column in a manner similar to loading the supernatant onto the hydrophobic interaction column. After washing the column with 7 volumes of wash buffer, peptides bound to cellulose were eluted with 2 volumes of 50% acetonitrile in 0.05% TFA. The column eluate was analyzed for biological activity by halo assay and then purified using RP-HPLC. The $OD_{254}$ RP-HPLC elution profile showed a peak with a retention time of ~16 min which is similar to the retention time of subtilin isolated from HIC and eluted under the same RP-HPLC conditions (Fig. 9). The fractions corresponding to the peak exhibited antimicrobial activity against *B. cereus* spores. MALDI-TOF analysis of RP-HPLC purified sample detected a peak corresponding to the molecular mass of subtilin with an added water molecule (3338 Da).

Subtilin isolated using the cellulose column was stable for atleast a month when stored at 4°C. Since subtilin was the only detectable peptide present in the cellulose column eluate, this indicates that cellulose is highly selective for subtilin. This manner of isolation of stable subtilin from bacterial culture supernatant provides an alternative and inexpensive method to isolate hydrophobic peptides. In addition, since stable subtilin could be easily isolated from LH45 culture supernatant using a cellulose column, this method of isolation of subtilin could be utilized to provide an easy, single step procedure for large-scale preparation of highly purified, stable subtilin from bacterial cultures.
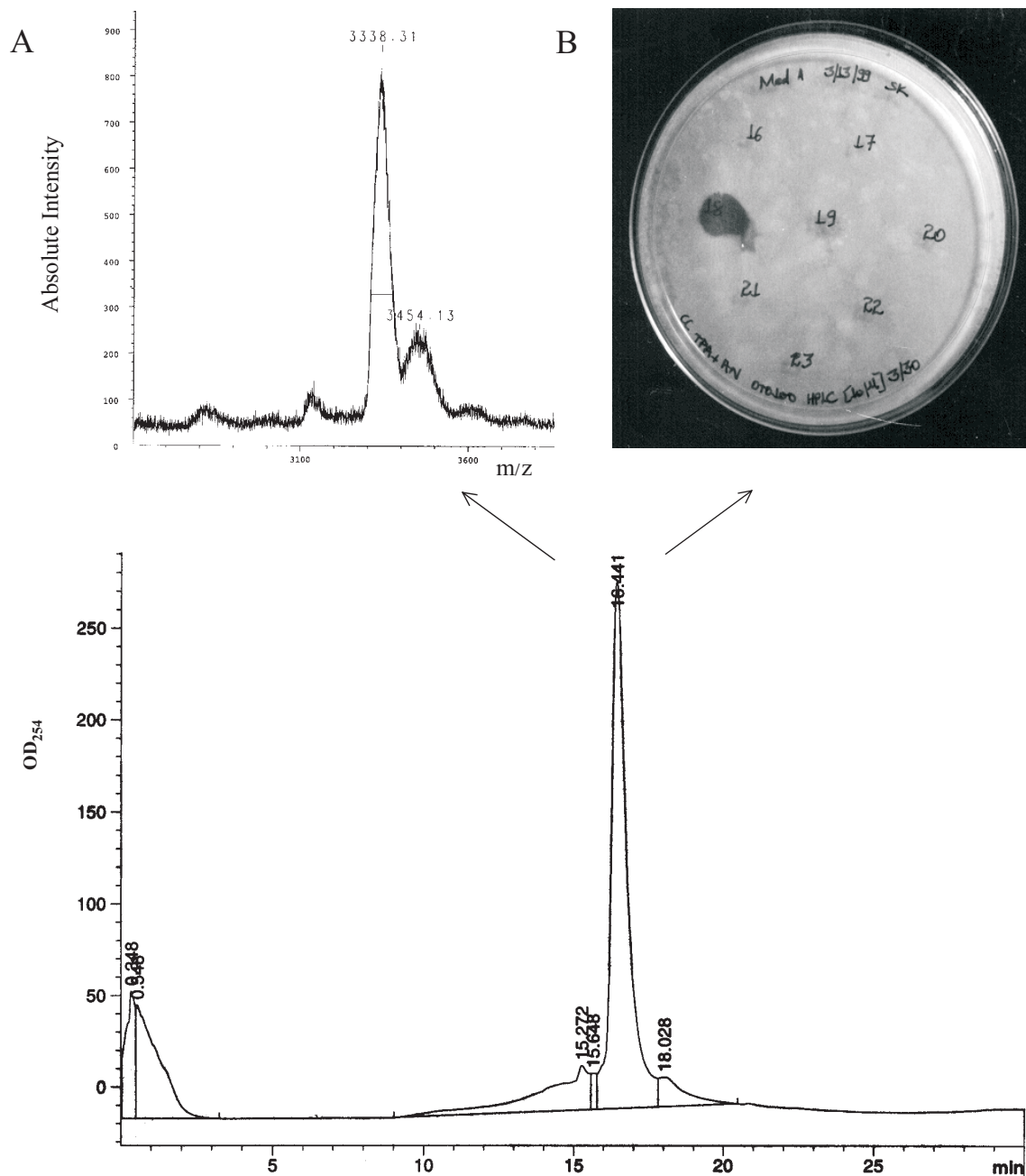
**Figure 9. RP-HPLC, MALDI-TOF and halo assay of subtilin isolated from cellulose column.**

Subtilin isolated from *Bacillus subtilis* LH45 using cellulose column was further purified by reverse phase - HPLC. The RP-HPLC profile is depicted in the bottom figure. Fractions corresponding to the peak were collected every min and analyzed by MALDI-TOF. Mass spectrometric analysis of the fractions detected subtilin as seen in panel A. The mass of 3338 Da is probably due to the addition of a water molecule to subtilin which has a mass of 3320 Da. Fractions were also tested for antimicrobial activity as shown in panel B.

Part II.  Exploring functionality of subtilin using phage display and genomics.

The possibility that specificity of subtilin is conferred by interaction of subtilin with specific bacterial protein targets was explored using phage display, an *in vitro* selection technique that was employed to identify peptide sequences interacting with subtilin. Subtilin was allowed to select for specific peptide structural motifs from random peptide libraries displayed on the surface of M13 bacteriophage to identify potential peptide targets of subtilin. The phage display peptide library is based on a combinatorial library of random peptide sequences fused to the minor coat protein (pIII) of the M13 bacteriophage. The displayed peptides are expressed at the N-terminus of pIII followed by a short spacer (G-G-G-S) and then the wild-type pIII sequence. Thus, the phage display technique has been used to create a linkage between the random peptide sequences displayed on the phage and the DNA encoding that sequence (54). Determination of the DNA sequence of the phage selected by subtilin therefore allowed for the identification of the 12-mer or the 7-mer peptide sequence binding to subtilin. The peptide sequences thus identified were then aligned to identify general peptide motifs. Since subtilin is active against Gram-positive bacteria, these motifs were used in homology searches against all proteins encoded by the genome of the prototypical Gram-positive bacterium *Bacillus subtilis* 168 to identify the bacterial proteins containing these motifs. The bacterial proteins thus identified could form potential targets of subtilin, and identification of these bacterial targets would provide an insight into the specificity and also the antimicrobial mechanism of action of subtilin.

Part II-1. Screening of 12-mer and 7-mer peptide phage display libraries against subtilin.

Screening of 12-mer and 7-mer peptide phage display libraries against subtilin involved the use of affinity capture for biopanning. This was used as an alternative to the simpler biopanning procedure which involves incubating the phage-displayed peptide library directly with the target coated on a plate. The alternate biopanning procedure was chosen as it allowed for incubation of the subtilin target with phages in solution resulting in improved binding, followed by affinity capture of the phage-target complexes by immobilized streptavidin (Fig. 10). In addition, biotinylation of subtilin using biotin disulfide N-hydroxy succinimide ester (BDNHSE) resulted in covalent linkage of subtilin to the biotin moiety through a disulfide linkage. This allowed for elution of the bound phage by reducing the –S-S- linkage between subtilin and biotin, which disrupts both covalent and non-covalent interactions, so that all interactions could be detected. The bound phage was also eluted with low pH to identify peptides interacting non-covalently with subtilin.

1-1.  Biotinylation of subtilin.

The maximum solubility of nisin at pH 8 was determined to be 0.25 mg/ml with higher solubility at lower pH (42). So, 0.5 mg of subtilin was biotinylated by reacting with the biotinylating agent BDNHSE in pH 8 buffer in a total volume of 2 ml. Subtilin was incubated with BDNHSE in a 1:1 nanomolar ratio to ensure that subtilin was biotinylated at only one of its three lysine residues. Biotinylated subtilin was purified using RP-HPLC after incubation on ice for 2 h, and fractions corresponding to biotinylated subtilin were collected every min (Fig. 11). As seen from the halo assay, the RP-HPLC fractions of biotinylated subtilin retained biological activity comparable to that
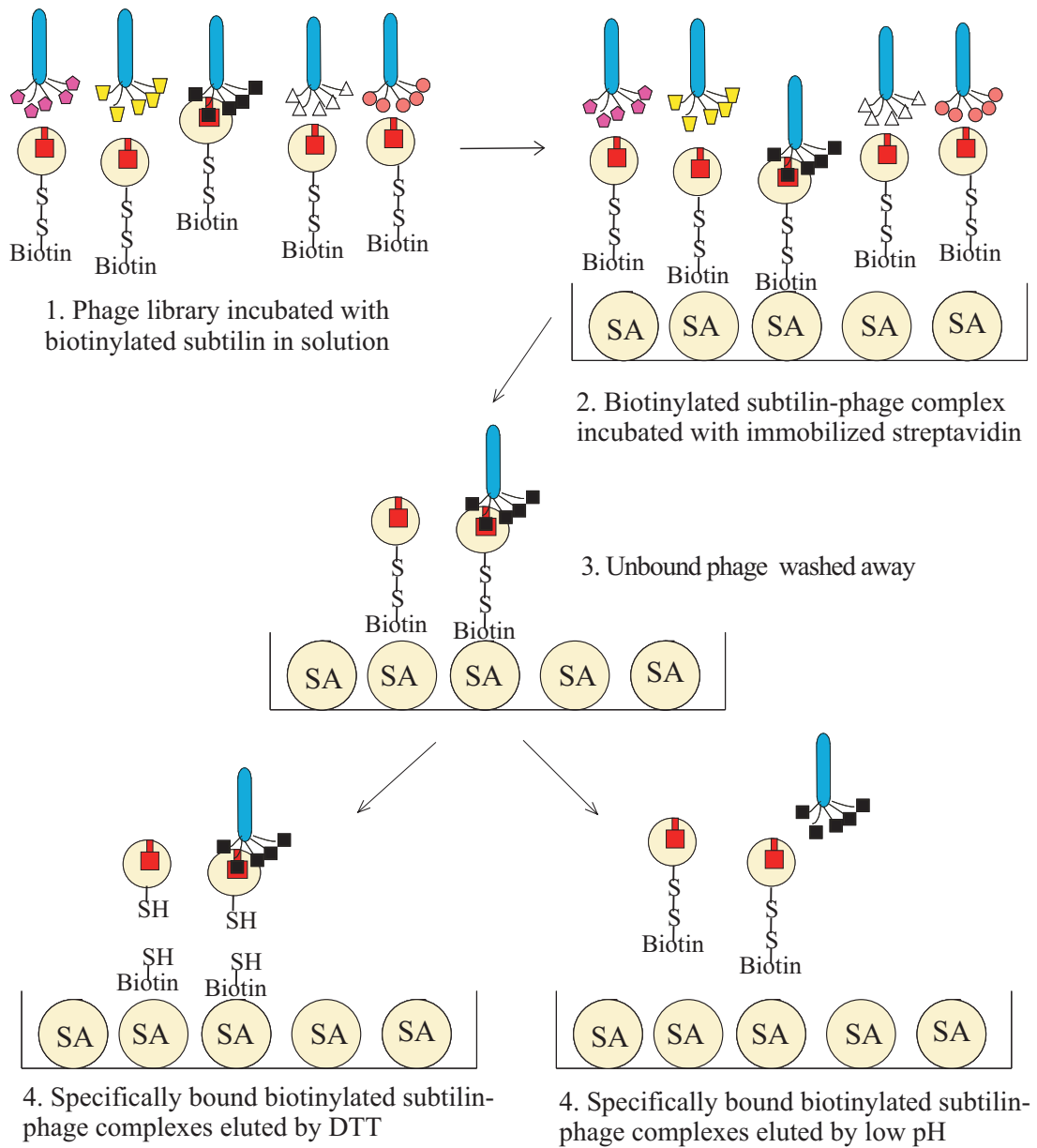
**Figure 10. Schematic representation of modified phage display using affinity biopanning.**

Biotinylated subtilin was incubated with the phage library in solution. The bound biotinylated-subtilin phage complexes were then incubated with streptavidin immobilized in microtiter plate wells to allow capture of the biotinylated-subtilin phage complex by streptavidin. The unbound phages were washed away. Specifically bound phages were eluted either by DTT or by low pH. Elution by DTT disrupts all non-covalent as well as covalent interactions, whereas low pH disrupts all non-covalent interactions. The eluted pool of M13 phages was amplified in *E. coli*. The biopanning process was repeated for two more rounds. After three rounds of biopanning, individual phage clones were sequenced to identify the peptide sequence interacting with subtilin.
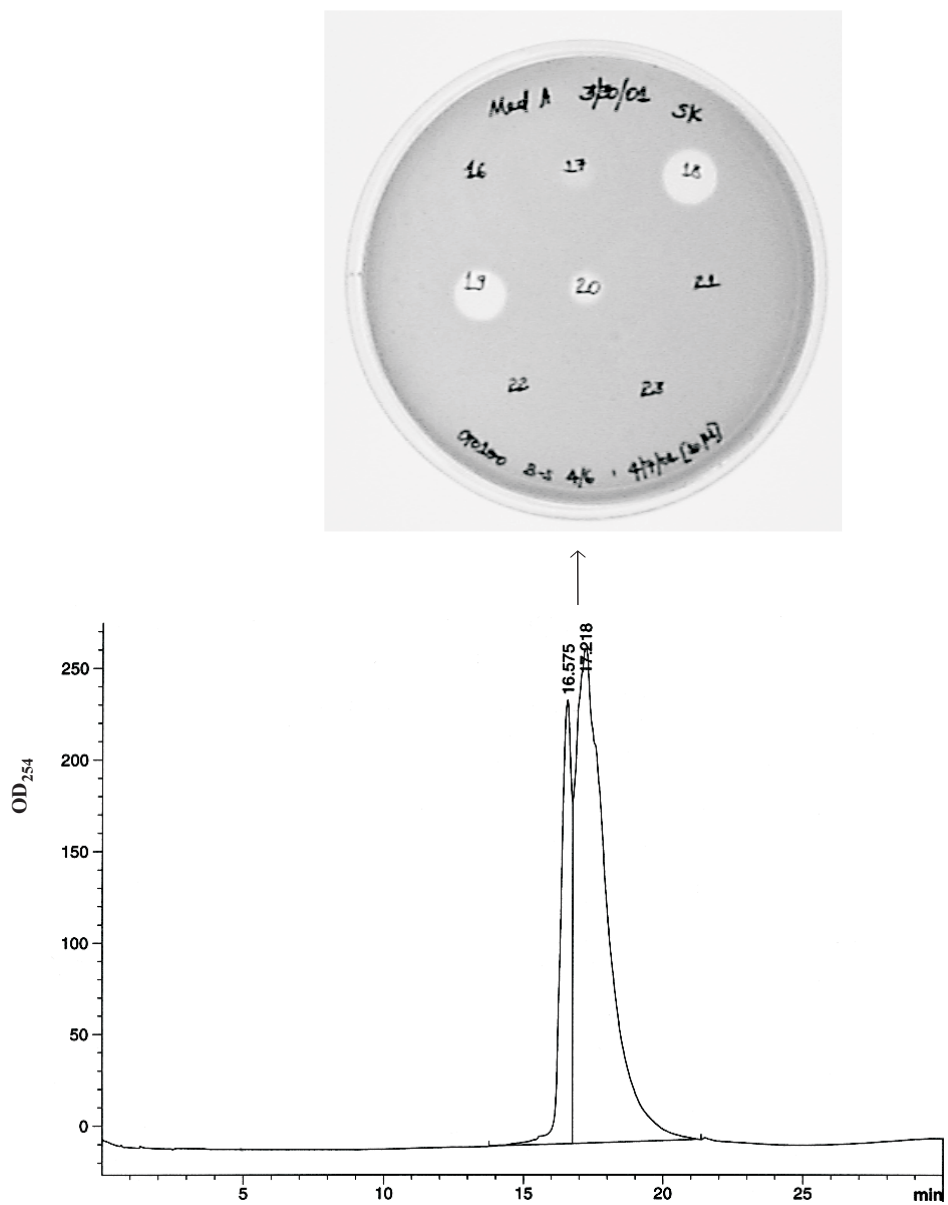
**Figure 11.  RP-HPLC and halo assay of biotinylated subtilin.**

Subtilin was incubated with biotin disulfide N-hydroxy succinimide ester (BDNHSE) in a 1:1 nanomolar ratio for 2 h on ice. Biotinylated subtilin was purified using RP-HPLC. The RP-HPLC profile of biotinylated subtilin is depicted in the bottom figure. Fractions corresponding to the peak were collected every min and tested for antimicrobial activity as shown in the top figure.

of unmodified subtilin. Concentration of biotinylated subtilin in each of the RP-HPLC fractions displaying antimicrobial activity (fractions #18 and #19, see Fig. 11) was determined in an uv-vis spectrophotometer at 254 nm using nisin dilutions to plot the standard curve, since subtilin and nisin each have 3 dehydro residues that absorb at 254 nm.

1-2.  12-mer peptide sequences selected by subtilin.

For each round of biopanning, 5 nM of each of the two RP-HPLC biotinylated subtilin fractions displaying antimicrobial activity (fractions #18 and #19) with $4 \times 10^{10}$ plaque forming units (pfu) of phage from the 12-mer phage library for 1 h. The biotinylated subtilin bound to phage was then incubated in a streptavidin-coated microtiter well for 1 h to allow for binding of the biotinylated subtilin - phage complex to streptavidin. After washing non-bound phage, the bound phage was eluted either by DTT or by low pH (Gly-HCl, pH 2.2). The unamplified eluates were titered to determine the number of phages in each of the four eluates and then amplified. The amplified phage was also titered to calculate the volume of the amplified eluate corresponding to $10^{11}$ pfu to carry out the second and third rounds of biopanning. Each successive round of biopanning resulted in an increase in the phage titer of the unamplified eluate as determined by counting the number of blue plaques. 78 plaques were sequenced from the third round of biopanning, which yielded 14 dodecapeptide sequences selected by subtilin from the phage display screening. Sequences of the 12-mers obtained from DTT elution and Gly-HCl elution are represented in Table 1. As seen in Table 1, 5 of the 14 peptide sequences were selected from more than one experimental condition. However, only one

sequence, WPQMAHKTTLLM, was selected by subtilin in all four experimental
conditions. This sequence also dominated over the other sequences, in that 29 of the 78
phages sequenced contained the WPQMAHKTTLLM sequence. The significance of this
sequence has been discussed in Part II-2, 2-1 of the Results section.

| Fraction # | 12-mer sequences identified from DTT elution | 12-mer sequences identified from Gly-HCl elution |
|---|---|---|
| 18 | WPQMAHKTTLLM (5) | WPQMAHKTTLLM (8) |
| 19 | WPQMAHKTTLLM (14) | WPQMAHKTTLLM (2) |
| 18 | SPSMLTSMWPNT (4) | |
| 19 | SPSMLTSMWPNT (5) | SPSMLTSMWPNT (15) |
| 18 | IQSDDLAAAWDL (1) | IQSDDLAAAWDL (1) |
| 19 | | IQSDDLAAAWDL (3) |
| 18 | NFMESLPRLGMH (1) | |
| 19 | NFMESLPRLGMH (1) | NFMESLPRLGMH (3) |
| 18 | YPASHPMMTNSA (1) | |
| 19 | | YPASHPMMTNSA (4) |
| 18 | | YHNMLKGDIPPG (2) |
| 18 | | SQITMAVIPGDI (1) |
| 18 | | RVILSIKLIWSA (1) |
| 18 | TINISIKLIRSA (1) | |
| 18 | NYHMHWSTPHLP (1) | |
| 19 | FYEDPLGARGEK (1) | |
| 19 | SHIFLLIQWPLH (1) | |
| 19 | SHHIPSYQWPLH (1) | |
| 19 | SHHIPYLYVPLH (1) | |

**Table 1.  Sequences of 12-mer peptides selected by subtilin and eluted by DTT or
Gly-HCl.**  A 12-mer peptide phage library was biopanned against subtilin to identify
potential peptide targets of subtilin. Two RP-HPLC fractions (#18 and # 19) of
biotinylated subtilin were incubated with the phage-displayed peptide library in solution
and then captured onto a streptavidin-coated target. After washing away unbound phage,
the specifically-bound phage was eluted either by DTT or by Gly-HCl. After three such
rounds of biopanning, 78 phages from the third round of biopanning were sequenced to
identify 14 dodecapeptide sequences selected by subtilin from the 12-mer phage library.
The number in parentheses next to the 12-mer sequence denotes the number of
occurrence of each sequence.

The 12-mer sequences selected by subtilin were examined to detect common motifs. The 12-mers exhibited several classes of motifs that were identified based on similarities in amino acid sequence within the 12-mer peptides. The 12-mer sequences that had amino acid sequence motifs in common were aligned according to their motifs as seen in Fig. 12. Analysis of these motifs is discussed in Results, Part II-2.

RVILSIKLIWSA  
  TINISIKLIRSA    }    SIKLI motif

IQSDDLAAAWDL  
FYEDPLGARGEK    }    DXLAAXXD motif

SQITMAVIPGDI  
  YHNMLKGDIPPG    }    IXGDI motif

SHHIPSYQWPLH  
SHHIPYLYVPLH    }    SHHIPXXXXPLH motif

SHHIPSYQWPLH  
 SHIFLLIQWPLH    }    QWPLH motif

WPQMAHKTTLLM $\rightarrow$ KTTLL motif
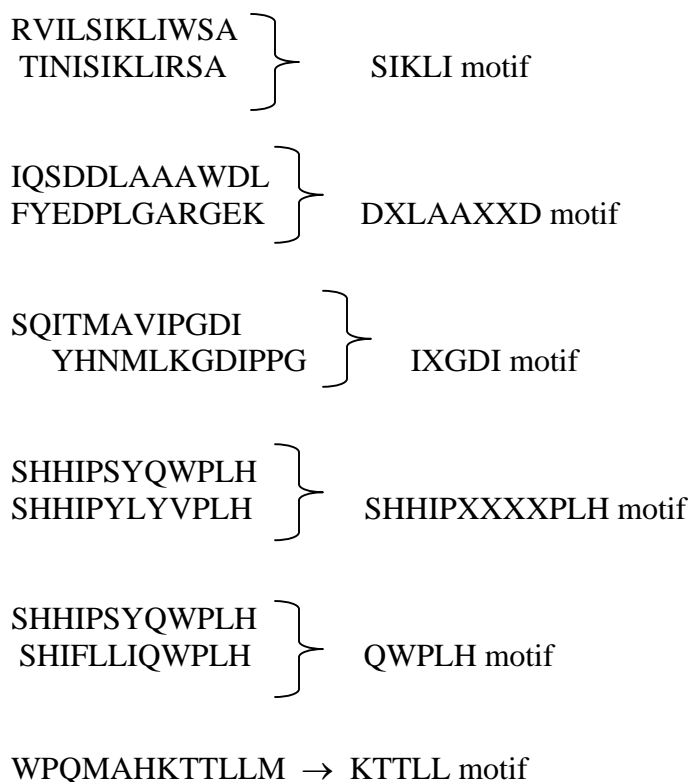
**Fig. 12: Alignment of 12-mer peptide sequences selected by subtilin from phage display screening.** The 12-mer peptide sequences selected by subtilin were identified after the third round of biopanning. Some of the sequences have been aligned based on similarities in the amino acid sequence of the peptides to identify six motifs.

1-3. 7-mer peptide sequences selected by subtilin.

Phage display screening using a 12-mer peptide library was employed to detect potential peptide targets of subtilin. The 12-mer library screening against subtilin identified several 12-mer peptide sequences selected by subtilin. However, the

disadvantage in using a 12-mer phage library is that it contains so many variant 12-mers that it is possible to screen only a small subset (approximately $1.9 \times 10^9$) of the entire population ($20^{12}$ possible sequences) for subtilin binding (80). A 7-mer phage library would theoretically permit screening of all possible random sequences ($1.28 \times 10^9$) for subtilin binding. Therefore, a 7-mer peptide phage library was screened against subtilin with the expectation that the peptides selected by subtilin from the 7-mer library would be identical or similar to those obtained from the 12-mer library screening.

In the 7-mer phage display screening against subtilin, the 7-mers bound to subtilin were also eluted both by DTT and by Gly-HCl, in a manner similar to the procedure used in the 12-mer phage elution. Three rounds of biopanning were performed, and the phages obtained from the third round of biopanning were sequenced. The 7-mer sequences obtained from sequencing 61 phages are represented in Fig. 13. The 7-mer peptide sequences when compared to the 12-mer sequences did not show much similarity to the 12-mer sequences, except for the presence of short HLP and RSA motifs seen in both the 12-mer and the 7-mer sequences. This could have occurred if subtilin requires a peptide surface larger than that of a 7-mer for efficient binding. Analysis of each of the 7-mer sequences involving homology searches against the *B. subtilis* 168 proteome did not result in any proteins being identified when zero mismatch was allowed. However, when the sequence LLDQPPA was used as a query pattern allowing 2 mismatches, the search identified CydC, an ABC transporter and YfmO, a protein with function similar to a multidrug-efflux transporter. YfmO contains the pattern NQKTG**LLSQPKA**VWAVA. CydC is an ABC transporter required for expression of cytochrome bd (ATP-binding protein) with the sequence pattern NRPIL**LLDEPTA**HLDIE.

MATTSPT (2)
PTFQITH (5)
SLPTENM (1)
MAHHLPQ (2)
PPHQEIT (11)
LMHSELT (4)
RNHPEHA (9)
LLDQPPA (9)
YYPLVFS (6)
RNWKPIF (1)
RSASMTI (8)
AWQQTRS (2)
AFITTQT (1)

**Figure 13. Sequences of 7-mer peptides selected by subtilin and eluted by DTT or Gly-HCl.** A 7-mer peptide phage library was biopanned against subtilin to identify potential peptide targets of subtilin. After three rounds of biopanning, 61 phages from the third round of biopanning were sequenced to identify thirteen 7-mer sequences selected by subtilin from the 7-mer phage library. The number in parentheses next to the 7-mer sequence denotes the number of occurrence of each sequence.

Part II-2. Analysis of 12-mer sequences using genomics.

The 12-mer sequences selected by subtilin from the phage display screening were further analyzed using genomics as a tool to decipher their biological relevance to the specificity and the antimicrobial mechanism of action of subtilin. Subtilin exhibits antimicrobial activity against a broad spectrum of Gram-positive bacteria. This indicates that any bacterial protein target of subtilin should be present in all susceptible Gram-positive bacteria. Since the entire genome of the prototypical Gram–positive bacterium *Bacillus subtilis 168* has been sequenced (36), the motifs selected by subtilin from the phage display screening were used in homology searches against all possible translated proteins encoded by the *B. subtilis* 168 genome. These searches were performed using the Search Pattern tool available on the SubtiList World-Wide Web Server at http://genolist.pasteur.fr/SubtiList/.

2-1. Analysis of KTTLL motif.

As seen in Table 1, the WPQMAHKTTLLM sequence was selected by subtilin the most number of times, occurring at a frequency of more than 37% of all selected sequences. In addition, this sequence was selected by subtilin under four different experimental conditions, including elution by DTT and also by Gly-HCl. This indicates that the WPQMAHKTTLLM sequence selected by subtilin is a strong contender for being a bacterial peptide target of subtilin. Analysis of the most commonly occurring sequence WPQMAHKTTLLM showed that it contains a motif KTTLL that is characteristic of ATP binding cassette (ABC) transporters. This KTTLL pattern is conserved among ABC transporters and forms part of the ATP binding cassette domain in the cytoplasmic Walker A region (12). The sequence WPQMAHKTTLLM, when input as a search pattern with zero mismatch against all proteins encoded by the *Bacillus subtilis* 168 genome, resulted in no identifiable *B. subtilis* proteins. However, when the KTTLL motif was used as the query pattern, 13 proteins with zero mismatch to the KTTLL motif were extracted and these are represented in Table 2. The proteins thus identified mainly comprised of ABC transporters, some of which were similar to glutamine, anion transport and iron transport ABC transporters. These ABC transporters are mainly located on the cell membrane and could form potential protein targets of subtilin. In addition, initiation factor IF-2 (InfB) was also identified as a potential subtilin target from these results. Initiation factor IF-2 (~78 kDa in *B. subtilis* 168) is involved in protein synthesis at the initiation stage, and is an initiator tRNA and a GTP binding protein.

| *gene:* Description | Pattern sequence |
| --- | --- |
| *infB*: initiation factor IF-2 | HVDHG**KTTLL**DSIRK |
| *expZ*: ATP-binding transport protein | PNGSG**KTTLL**NIILG |
| *yckI:* unknown; similar to glutamine ABC transporter (ATP-binding protein) | PSGSG**KTTLL**RCLNA |
| *ytlC:* unknown; similar to anion transport ABC transporter (ATP-binding protein) | PSGCG**KTTLL**SIIAG |
| *yvrA:* unknown; similar to iron transport system | PNGSG**KTTLL**HLLTG |
| *yfmM:* unknown; similar to ABC transporter (ATP-binding protein) | ANGIG**KTTLL**KSLLG |
| *yfmR*: unknown; similar to ABC transporter (ATP-binding protein) | PNGIG**KTTLL**NALAG |
| *ytsC:* unknown; similar to ABC transporter (ATP-binding protein) | ASGSG**KTTLL**NVLSS |
| *yvcR:* unknown; similar to ABC transporter (ATP-binding protein) | PSGSG**KTTLL**NLLAT |
| *yciC:* unknown; similar to unknown proteins | YLGAG**KTTLL**NSILQ |
| *smc:* chromosome condensation and segregation SMC protein | RLYKQ**KTTLL**KDEEV |
| *spoIIIAA*: mutants block sporulation after engulfment | PPQTG**KTTLL**RDLAR |
| *yxdL:* unknown; similar to ABC transporter (ATP-binding protein) | PSGSG**KTTLL**NIIST |

**Table 2. *Bacillus subtilis* 168 proteins containing the KTTLL motif**. The KTTLL motif found in the 12-mer WPQMAHKTTLLM sequence selected by subtilin was used as a search pattern against all proteins in the *B. subtilis* 168 genome. This resulted in the identification of 13 proteins with zero mismatch to the KTTLL motif. The first column lists the gene name in italics, followed by a brief description of the protein encoded by the gene. The second column indicates the segments of the *B. subtilis* proteins that contain the KTTLL motif.

Another interesting result was obtained when the KTTLL motif was used as a search pattern by allowing one mismatch for the KTTLL motif. Of several proteins identified, elongation factor Tu (TufA) was of particular interest. Elongation factor Tu is also involved in protein synthesis like the initiation factor IF-2 identified in Table 3. TufA (~43 kDa) is involved in the elongation of the peptide chain during protein synthesis, and is also an aminoacyl tRNA and a GTP binding protein like IF-2. Other proteins identified by allowing one mismatch for the KTTLL motif included penicillin-binding protein DacB and several proteins with functions similar to multidrug resistance proteins as seen in Table 3.

| *gene:* Description | Pattern sequence |
|---|---|
| *tufA*: elongation factor Tu | HVDHG**KTTLT**AAITT |
| *dacB*: penicillin-binding protein 5 | ENVKI**NTTLL**KPKKA |
| *yqjV*: unknown; similar to multidrug resistance protein | DMTEE**KTRLL**VF-NLR |
| *ycnB*: unknown; similar to multidrug resistance protein | FGVFS**LTTLL**GTLVF |
| *yfmO*: unknown; similar to multidrug-efflux transporter | TQVNQ**KTGLL**SQPKA |

**Table 3.** ***Bacillus subtilis* 168 proteins containing the KTTLL motif with one allowed mismatch**. The KTTLL motif found in the 12-mer WPQMAHKTTLLM sequence selected by subtilin was used as a search pattern against all proteins in the *B. subtilis* 168 genome. This resulted in the identification of several proteins when one mismatch for the KTTLL motif was allowed. The first column lists the gene name in italics, followed by a brief description of the protein encoded by the gene. The second column indicates the segments of the *B. subtilis* proteins that contain the KTTLL motif with one mismatch.

2-2. Analysis of other motifs seen in the 12-mer peptide sequences.

The motif **SIKLI** seen in the 12-mers RVIL**SIKLI**WSA and TINI**SIKLI**RSA identified several proteins when one mismatch was allowed, with proteins having functions similar to multidrug resistance proteins being identified. The motif IXGDI seen in Fig. 12 identified another elongation factor FusA with zero mismatch to the motif. FusA or elongation factor G with the pattern sequence YMGD**IMGDI**TSRRG is also involved in protein synthesis. Another motif, DXLAAXXD also identified FusA with the pattern sequence LDAVL**DYLPAPTD**VAAIK when one mismatch was allowed.

The results obtained from the homology searches appear to indicate that subtilin could potentially act as an inhibitor of protein synthesis, either at the initiation stage or at the elongation stage. This would then suggest an alternative mechanism of action of subtilin, in addition to pore formation. Further, the identification of ABC transporters as potential protein targets of subtilin appears to indicate that the ABC transporters within the cell membrane could facilitate binding of subtilin to the cell membrane, which is then followed by insertion of subtilin into the cell membrane leading to pore formation. This would contribute to the specificity of antimicrobial action of subtilin.

Part III. Sedimentation equilibrium analysis of subtilin, pep16 and pep19.

Sedimentation equilibrium experiments are useful in studying a variety of interactions, including the self-association of macromolecules and the binding of heterogeneous macromolecular interactions (58). To determine the nature of interaction of subtilin with the 12-mer sequences selected by subtilin from the phage display screening, two synthetic peptides were obtained from Research Genetics, Alabama. The

sequence of one of the synthetic peptides, pep16, corresponded to the 12-mer peptide sequence with the KTTLL motif that was selected the most number of times by subtilin. The sequence of the other synthetic peptide (pep19) was part of the protein encoded by the gene *yxdL* in *B. subtilis* 168 (see Table 2). This protein also has the KTTLL motif and is thought to have a function similar to an ABC transporter. The sequences of pep16 and pep19 were WPQMAHKTTLLMGGGC-[CONH$_2$] and PSGSGKTTLLNIISTGGGC-[CONH$_2$], respectively. The sequence of the synthetic peptides was designed taking into consideration two factors. The 12-mer phage library had been constructed to include a peptide spacer fused to the pIII coat protein, and therefore, a G-G-G-C spacer was included at the C-terminus of the selected 12-mer sequence to design the synthetic peptide. Also, the C-terminus of the 12-mer displayed on the M13 phage was fused to its pIII coat protein, while the N-terminus was free during biopanning. This ensured that the C-terminus of the 12-mer did not contain a free negatively charged carboxylate during panning. The C-terminal carboxylate of the synthetic peptide was therefore amidated to block the negative charge to ensure that this charge did not interfere with binding of the synthetic peptide to subtilin.

Sedimentation equilibrium experiments were performed to examine the interaction between subtilin and the synthetic peptides, pep16 and pep19. The sedimentation equilibrium experiments were designed to centrifuge the macromolecules at low speeds over a period of 2 days so as to obtain an equilibrium distribution concentration of the macromolecules throughout the centrifuge cell (21). Subtilin isolated previously from *B. subtilis* 6633 by the method of acetone-butanol procedure was unstable at RT with loss of chemical integrity seen in less than a day (44). Also, nisin was

observed to form multimers at high pH (42). If subtilin were also participating in multimer formation, then self-association of subtilin resulting in the formation of aggregates would have led to complications in the analysis of the interactions between subtilin and the synthetic peptide due to the presence of multiple species. In addition, multimer formation of subtilin might affect subtilin binding to pep16 or pep19. Subtilin was therefore tested for stability at RT for 2 days, since the equilibrium runs were of 1-2 days duration. Subtilin was incubated at RT for 2 days in different pH buffers of 5, 6.5, 7.5 and 8 to determine the best pH buffer for the existence of monomeric subtilin. Each sample was then run on a Tricine-SDS-PAGE gel and silver stained. The silver-stained gel showed that subtilin was stable when incubated at RT for 2 days (Fig. 14) with no multimers seen at pH 5, 6.5, 7.5 or at pH 8. The different pH buffers containing subtilin were also desalted by RP-HPLC and analyzed by MALDI-TOF when monomeric subtilin was detected in each buffer.

The amount of subtilin, pep16 and pep19 for the sedimentation equilibrium experiments was chosen such that the amount corresponded to an $OD_{280} < 0.5$ based on the range of the spectrophotometer used in the Beckman XL-I analytical ultracentrifuge. This OD corresponded to micromolar concentrations of subtilin, pep16 and pep19 used in the sedimentation equilibrium experiments. The amount of subtilin and pep16 was calculated using the molar extinction coefficient of Trp (5690 $M^{-1}$ $cm^{-1}$) and Beer's law (20). Pep19 did not have any Trp residue, but since the molecular weight of pep19 (1762 Da) is approximately that of pep16 (1730 Da), the amount of pep19 used was the same as pep16. Subtilin, pep16 and pep19 were centrifuged individually at first in order to detect
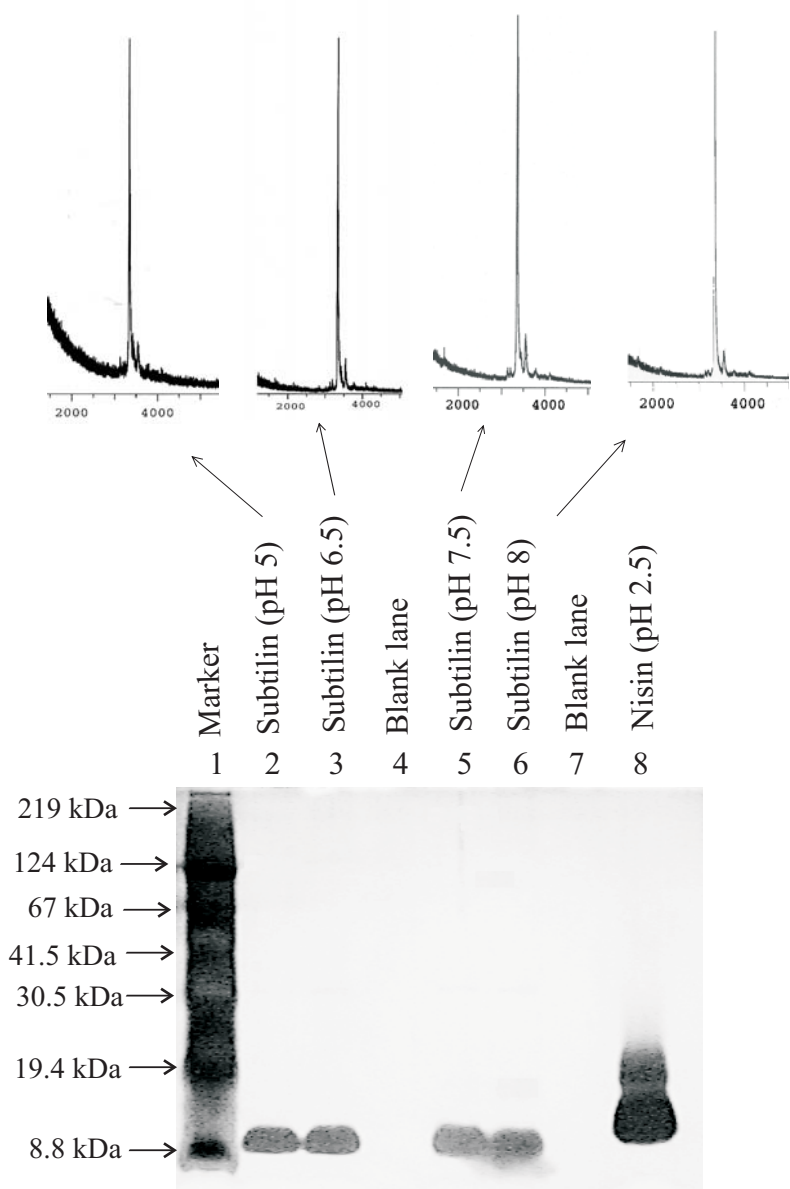
**Figure 14.  Stability of subtilin incubated in different pH buffers for 2d at RT.**

Subtilin was incubated at RT for 2 days in different pH buffers of 5, 6.5, 7.5 and 8 to determine the best pH buffer for the existence of monomeric subtilin. Each sample was then run on a Tricine-SDS-PAGE gel and silver stained. The silver-stained gel showed that subtilin was stable when incubated at RT for 2 days with no multimers seen at pH 5, 6.5, 7.5 or at pH 8 (bottom figure). The different pH buffers containing subtilin were desalted by RP-HPLC and analyzed by MALDI-TOF when monomeric subtilin was detected in each buffer (top four figures).

the formation of aggregates if any of the macromolecules were participating in self-associations. Equimolar amounts of subtilin and pep16 were then centrifuged together to detect the association of subtilin with pep16.

The molecular mass, M, of the macromolecule can be determined from the equation (21)

$$\sigma = M (1 - \bar{v}\rho) \omega^2 / 2RT$$

where σ = reduced molecular mass
     $\bar{v}$ = partial specific volume of the solute
     ρ = density of the solvent
     ω = angular velocity
     R = gas constant
     T = absolute temperature

The partial specific volume of a protein is the ratio between its volume and molecular weight (http://www.basic.nwu.edu/biotools/ProteinCalc.html). The partial specific volume of subtilin, pep16 and pep19 was calculated from a weight average of the partial specific volumes of the component amino acid residues (15). The accurate $\bar{v}$ of subtilin could not be calculated because the $\bar{v}$ of the dehydro residues is not known. Therefore, the partial specific volume of subtilin was calculated to be 0.7198 using estimated values for the dehydro residues, with the partial specific volume of serine and threonine being substituted for dehydroalanine (Dha) and dehydrobutyrine (Dhb), respectively, since Dha and Dhb are formed as a result of the dehydration of Ser and Thr, respectively. The calculated value of 0.7198 for subtilin falls within the 0.70 - 0.75 range of partial specific volumes for proteins, with an average value of 0.73 for most proteins (58).

The reduced molecular mass, σ was determined from the NONLIN least squares analysis values by analyzing the absorbance gradient as one ideal species. The density of

TBS was calculated to be 1.014 g/ml. The molecular weight of subtilin was then computed from the reduced molecular mass (buoyant molecular weight) using estimated values for the partial specific volume of subtilin. The molecular mass of pep19 could not be determined because pep19 precipitated when centrifuged at very high speeds. The molecular masses of subtilin, pep16 and subtilin + pep16 samples as calculated from the equilibrium run data are represented in Table 4.

| Peptide | $\bar{\nu}$ | $\sigma$ | Theoretical molecular mass | Calculated molecular mass (M) |
|---|---|---|---|---|
| subtilin | 0.7198 | 0.79 | 3320 Da | 3663 Da |
| pep16 | 0.7094 | 0.738 | 1730 Da | 2001 Da |
| subtilin + pep16 | 0.7146 | 0.798 | 5050 Da | 3177 Da |

**Table 4: Comparison of theoretical and calculated molecular masses obtained from sedimentation equilibrium experiments.** Interaction between subtilin and the synthetic peptide, pep16 was analyzed by sedimentation equilibrium. Subtilin and pep16 were analyzed individually at first, followed by analyzing an equimolar concentration of subtilin and pep16. The reduced molecular mass, $\sigma$ was determined from a nonlinear least squares analysis and this was used to calculate the molecular mass of subtilin and pep16. The calculated molecular mass of subtilin and pep16 was then compared with the theoretical mass of subtilin and pep16 to determine any interaction between subtilin and pep16.

The data obtained from the individual sedimentation equilibrium runs of subtilin and pep16 indicated that subtilin and pep16 formed monomeric species and did not participate in self-associations, as the resulting absorbance gradient at 280 nm could be fit to a single ideal species. So, for the sedimentation equilibrium run of subtilin with pep16, 1-3 species were expected to be seen depending on the $K_d$ of the association between subtilin and pep16. Tight binding of subtilin to pep16 would result in the formation of a single species of the subtilin-pep16 complex. However, a high $K_d$ would result in three species – free subtilin, free pep16 and the subtilin-pep16 complex. The calculated

molecular mass M of the subtilin and pep16 mixture was less than that expected for a subtilin-pep16 complex. This indicated that subtilin and pep16 were not associating tightly enough to form a single species, since this value of 3177 Da is the average weighted molecular mass of subtilin and pep16.

The observation that the 12-mer peptide sequence selected from the phage library by subtilin bound to the target (subtilin) when presented on the intact phage, but could not bind as a synthetic peptide may be explained if the selected 12-mer sequence required additional elements from adjacent sequence on pIII protein for efficient binding to subtilin (http://www.neb.com/nebecomm/tech_reference/drug_discovery/phdFaq.asp). Also, if the $K_d$ of binding of the synthetic peptide to subtilin is high and possibly in the millimolar range, then the interaction between subtilin and the peptide would not have been detected since micromolar concentrations of subtilin and synthetic peptide were used in the sedimentation equilibrium experiments. The sedimentation results therefore do not conclusively determine that the 12-mer sequence with the KTTLL motif selected by subtilin from the phage library was an artifact, especially in view of the fact that this 12-mer sequence was selected by subtilin in four different experimental conditions of phage display screening (see Table 1).

Part IV.  Isolation of subtilin-binding proteins from susceptible bacterial cells using monomeric avidin column.

Identification of subtilin-binding 12-mer peptide sequences *in vitro* from the phage display screening followed by comparison of the selected 12-mers to the *B. subtilis* 168 proteome resulted in detection of ABC transporters and initiation factor IF-2 as

potential bacterial protein targets of subtilin (see Results, Part II). To confirm that the selected 12-mer with the KTTLL motif in ABC transporters was actually involved in interaction with subtilin and was responsible for its specificity, *in vivo* studies were performed to isolate subtilin-binding proteins from intact bacterial cells. Isolation of bacterial proteins binding to subtilin followed by identification of these subtilin-binding bacterial proteins would then provide an insight into the specificity and antimicrobial mechanism of action of subtilin.

To isolate subtilin-binding bacterial proteins, the same strategy of using biotinylated subtilin as was used in phage display screening to identify subtilin-binding 12-mer peptide sequences was employed. Biotinylated subtilin used in this method provided a means for the isolation of subtilin-binding bacterial proteins from a lysate of susceptible bacterial cells. The advantage of using biotinylated subtilin in this method was that the lysate of bacterial cell proteins incubated with biotinylated subtilin could be further incubated with immobilized monomeric avidin to allow binding of the biotinylated subtilin-bacterial protein complex to avidin, followed by elution of bound proteins by biotin or low pH. The monomeric avidin column provided a support with lower biotin-binding affinity than native tetrameric avidin, and this enabled recovery of biotinylated complexes using biotin or low pH. Biotinylated subtilin was initially incubated with *B. cereus* cells to isolate subtilin-binding bacterial proteins, since *B. cereus* was generally used as the test organism for subtilin activity. However, the availability of the complete genome of *B. subtilis* 168 could facilitate the identification of subtilin-binding bacterial proteins by enabling sequencing of tryptic digests of the isolated protein by tandem mass spectrometry (27) followed by comparison of the peptide

100

sequences thus obtained with protein sequences in the *B. subtilis* 168 protein database using the SEQUEST program (40). Therefore, subtilin was tested for antimicrobial activity against *B. subtilis* 168 spores when subtilin was found to be biologically active against *B. subtilis* 168 spores (Fig. 15). Biotinylated subtilin was then incubated with *B. subtilis* 168 cells to isolate subtilin-binding bacterial proteins.

Part IV-1. Isolation of subtilin-binding proteins from *B. cereus* cells.

Subtilin was biotinylated and purified using RP-HPLC as described in Materials and Methods, Part II-8. Biotinylated subtilin retained antimicrobial activity against both *B. cereus* and *B. subtilis* 168 spores as seen from the halo assays (Fig. 16). 1 or 2 ml monomeric avidin columns were prepared for purification of biotinylated complexes by first blocking the high affinity biotin-binding sites on the avidin columns with a biotin-containing buffer and then eluting loosely bound biotin from the columns with a low pH (Gly-HCl, pH 2.8) solution to reveal the reversible biotin-binding sites. The columns were now ready for purification of biotinylated complexes.

To test the efficacy of the column, 250 µg of biotinylated subtilin was applied to a 1 ml monomeric avidin column as a positive control. After washing with PBS, bound biotinylated subtilin was eluted with a biotin-containing buffer. The column was then regenerated by washing with Gly-HCl buffer. Samples were collected during the PBS wash, and also during the biotin buffer elution and the Gly-HCl wash. The samples were dialyzed and then analyzed by SDS-PAGE and Western blotting. The Western blot showed a ~20 kDa band in the PBS wash and eluted fractions, but no other band was seen (Fig. 17). The same band appeared when some biotinylated subtilin (25 µg) was also run in an adjacent lane, indicating a polymer of biotinylated subtilin.

A
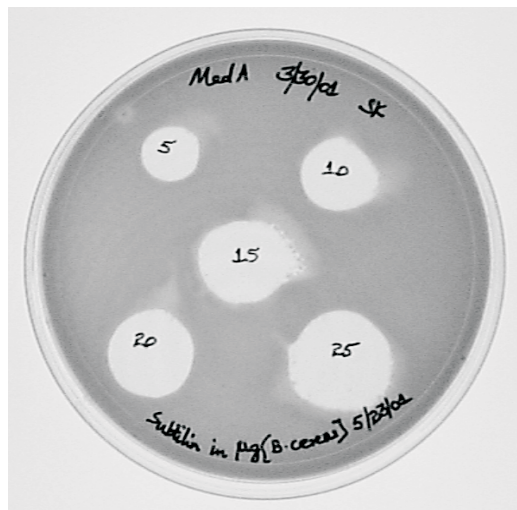


B
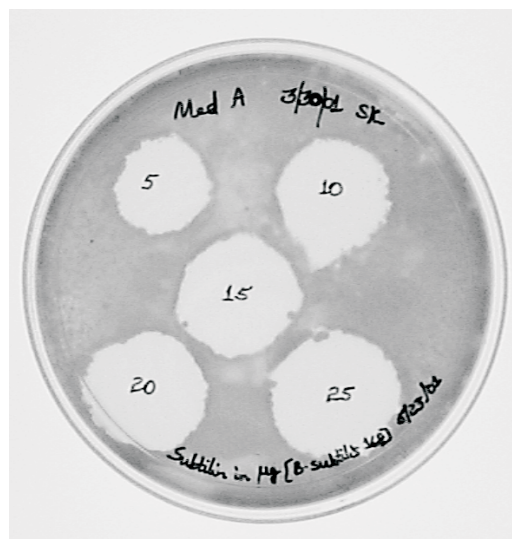
**Figure 15. Antimicrobial assay of subtilin against *B. cereus* and *B. subtilis* 168 spores.**

Different amounts of subtilin varying from 5 µg to 25 µg were tested for antimicrobial activity against *Bacillus cereus* and *Bacillus subtilis* 168 spores by halo assay. In panel A, different amounts of subtilin were spotted on a medium A plate. After allowing the different amounts to dry, the plate was sprayed with *B. cereus* spores and incubated at 37°C overnight. In panel B, different amounts of subtilin were tested for antimicrobial activity against *B. subtilis* 168 spores. From the zones of inhibition seen in panels A and B, subtilin appears to be biologically active against both *B. cereus* and *B. subtilis* 168 spores.
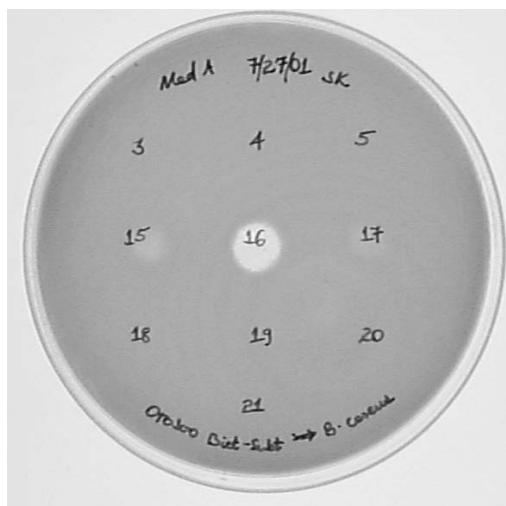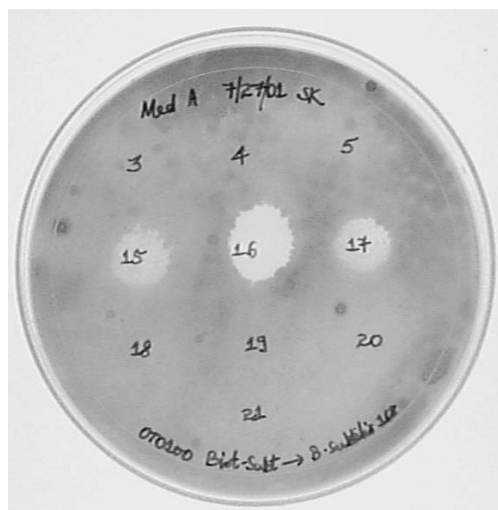
**Figure 16. Halo assay of biotinylated subtilin against *B. cereus* and *B. subtilis* 168 spores.**

Subtilin was biotinylated by reacting with biotin disulfide N-hydroxy succinimide ester and purified using RP-HPLC. RP-HPLC fractions corresponding to biotinylated subtilin were collected every min and tested for antimicrobial activity. In panel A, 10 µl of each RP-HPLC fraction of biotinylated subtilin was tested against *B. cereus* spores whereas in panel B, 10 µl of each RP-HPLC fraction of biotinylated subtilin was tested against *B. subtilis* 168 spores.
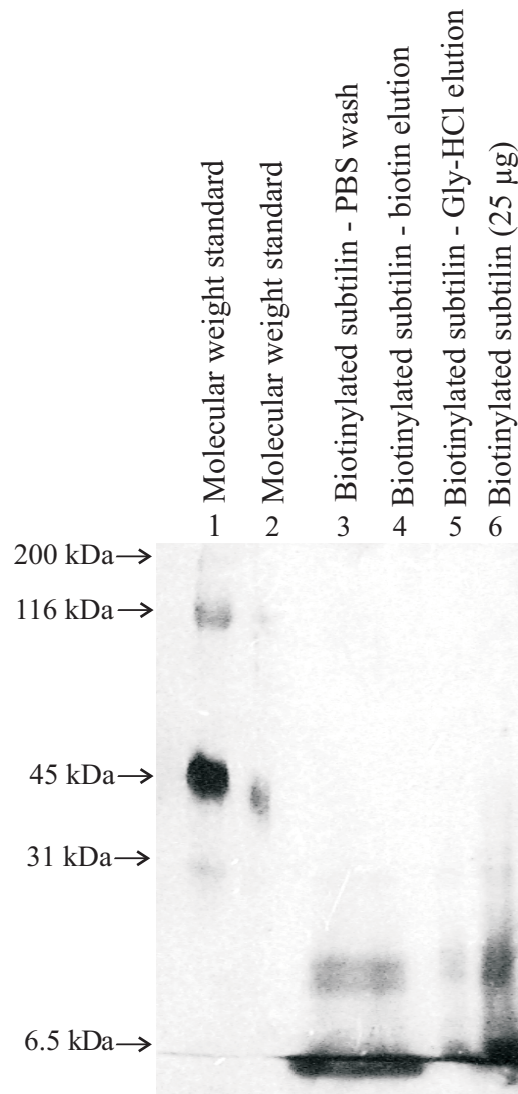
**Figure 17. SDS-PAGE analysis of biotinylated subtilin eluted from monomeric avidin column.**

Biotinylated subtilin was applied to a monomeric avidin column to test for isolation of biotinylated subtilin from the monomeric avidin column. After washing any non-specifically bound protein from the column using PBS, the bound biotinylated subtilin was eluted with biotin followed by a glycine-HCl wash. After dialysis, the PBS wash and elution fractions were analyzed by SDS-PAGE and Western blot. A small amount of biotinylated subtilin was run in lane 6 as a positive control.

To isolate subtilin-binding bacterial proteins, *B. cereus* cells were incubated with 500 μg of biotinylated subtilin for 3 h. The cells appeared to be completely lysed after a 3 h incubation with biotinylated subtilin as seen from loss of solution turbidity. The cells were then passed through a French pressure cell to ensure complete cell lysis. The lysate of bacterial proteins containing biotinylated subtilin-bacterial protein complexes was loaded onto a 2 ml monomeric avidin column for purification. Unbound protein was washed off the column using PBS and wash samples collected. Bound, biotinylated proteins were eluted using a biotin-containing buffer, and proteins eluting off the column were collected. The column was then washed with Gly-HCl buffer to regenerate the column. Samples from Gly-HCl elution were also collected for further analysis. After dialysis, the PBS wash samples, biotin-eluted samples and Gly-HCl eluted samples were analyzed by SDS-PAGE in duplicates and detected both by silver staining and also by Western blotting. A bacterial cell sample without biotinylated subtilin was also subjected to the same procedure as a negative control.

As seen in Fig. 18, more bands were visible in the silver-stained gel than on the Western blot, indicating that many *B. cereus* proteins interact non-covalently with subtilin while subtilin bound covalently only to some specific proteins. Also, more proteins were eluted by Gly-HCl buffer than by biotin elution buffer indicating that the monomeric avidin column was binding biotinylated complexes tighter than those that could be eluted off the column using the biotin elution buffer. A few bands were also seen in the wash fraction of the negative control sample in the Western blot. A band of ~99 kDa size appeared in both the wash fraction of the negative control and also the Gly-HCl eluted fraction of the experimental sample (biotinylated subtilin-bacterial protein
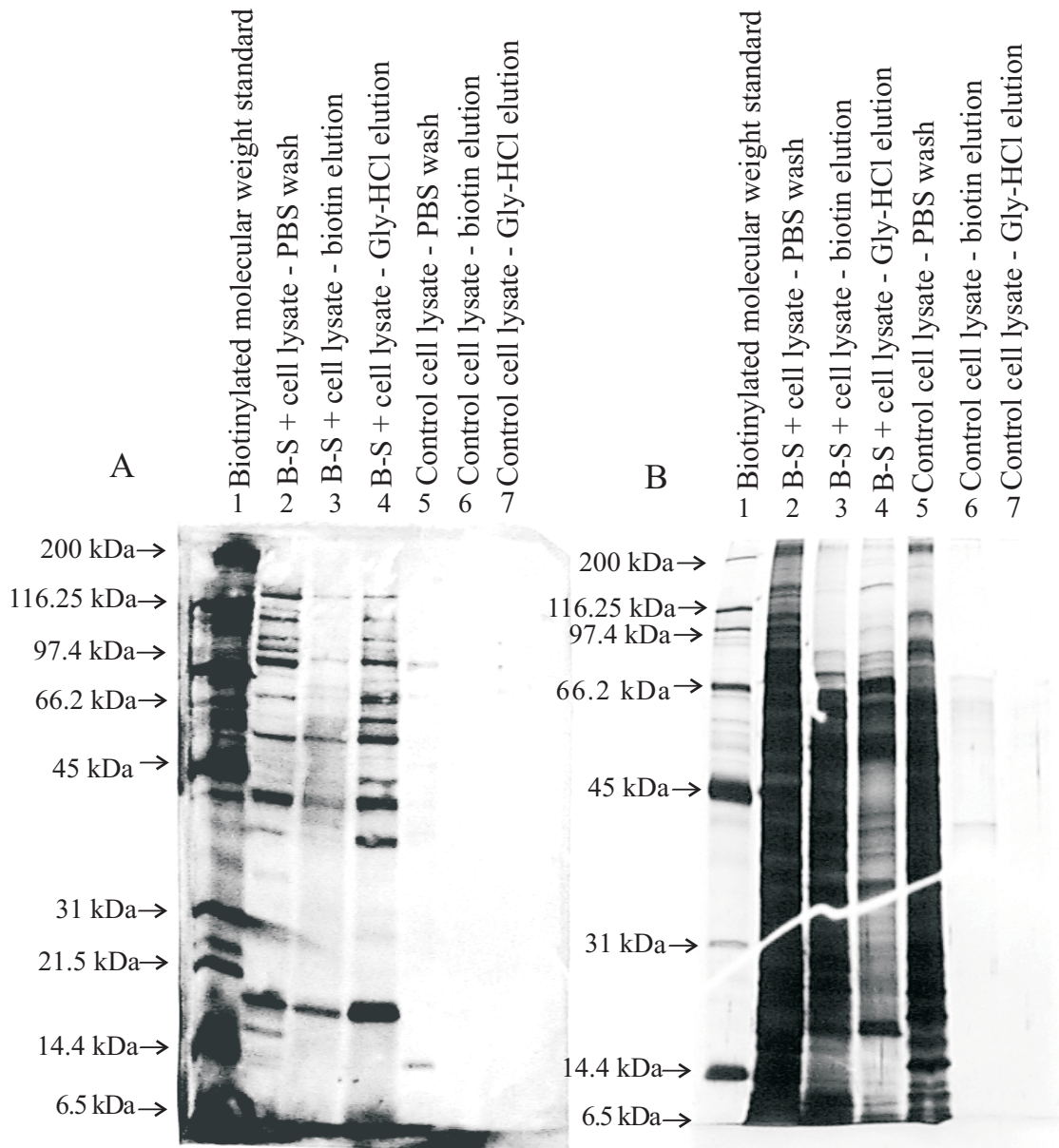
**Figure 18. Isolation of subtilin-binding bacterial proteins from *B. cereus* cells using monomeric avidin column.**

*B. cereus* cells were incubated with biotinylated subtilin (B-S) and the cells lysed after incubation. The B-S + bacterial cell lysate was applied to a monomeric avidin column to isolate subtilin-binding bacterial proteins. Non-specifically bound protein was washed off the column with a PBS wash. The bound protein was eluted first with biotin followed by glycine-HCl elution. A bacterial cell sample without any biotinylated subtilin used as a negative control was also subjected to the same procedure. After dialysis, the PBS wash and elution fractions were analyzed by SDS-PAGE. Bacterial proteins covalently attached to subtilin are seen in the Western blot of the SDS-PAGE gel in panel A. The silver stained gel in panel B shows all noncovalent and covalent interactions of the bacterial proteins with subtilin.

sample), while a band of ~12 kDa appeared only in the wash fraction of the negative control. The presence of bands in the wash fraction of the negative control in the Western blot suggests that some naturally occurring biotin-containing proteins/peptides present in bacterial cells loosely bound to the monomeric avidin column (26), and were washed off by PBS. No proteins from the negative control sample were eluted from the monomeric avidin column either by biotin buffer or Gly-HCl buffer, as seen in the Western blot.

The Gly-HCl eluted fraction of the experimental sample showed bands of ~130 kDa, ~115 kDa, ~108 kDa, ~78 kDa, ~60 kDa, ~50 kDa, ~45 kDa, ~43 kDa and ~40 kDa in the Western blot. The ~78 kDa and the ~43 kDa proteins are of particular interest, since the phage display results identified initiation factor IF-2 (~78 kDa) and elongation factor Tu (~43 kDa) as possible bacterial protein targets of subtilin (see Results, Part II-2). Further, the bands seen in the Western blot represent bacterial proteins bound covalently to biotinylated subtilin, since the biotinylated subtilin-bacterial protein complexes eluted from the monomeric avidin column were probed using a streptavidin-alkaline phosphatase conjugate in the Western blot. This detection method therefore detected only those bacterial proteins that were covalently attached to biotinylated subtilin. Covalent attachment of subtilin to bacterial proteins indicates that the electrophilic dehydro residues of subtilin could be interacting with specific nucleophilic groups in bacterial protein targets. The significance of covalent attachment of subtilin to bacterial protein targets and the possible mechanism of covalent attachment is discussed further in the Discussion chapter.

Part IV-2.  Isolation of subtilin-binding proteins from *B. subtilis* 168 cells.

To identify bacterial proteins interacting with subtilin, *B. subtilis* 168 cells were also subjected to the same protocol of incubation with biotinylated subtilin as the *B. cereus* cells. After incubation and cell lysis, the *B. subtilis* 168 cell lysate with biotinylated subtilin was affinity purified using a monomeric avidin column to isolate subtilin-binding bacterial proteins. The samples eluted from the column were analyzed by SDS-PAGE and visualized by silver stain and Western blot. As seen with the *B. cereus* cellular proteins, more *B. subtilis* 168 proteins were visible in the silver-stained gel than in the Western blot (Fig. 19), further confirming that subtilin was interacting covalently with only some specific bacterial proteins. Some of the higher molecular weight bands (~130 kDa, ~110 kDa, etc.) were seen in both the *B. subtilis* and the *B. cereus* samples eluted by glycine-HCl buffer, suggesting that these proteins could be evolutionarily conserved in both species. The advantage of performing these experiments with *B. subtilis* 168 cells is that bacterial proteins isolated using the monomeric avidin column could now be identified by comparing these proteins with all proteins encoded by the *B. subtilis* 168 genome.

Part V.  Isolation of bacterial protein targets of nisin from *B. subtilis* 168 cells.

The monomeric avidin column used in the purification of subtilin-binding proteins was successful in isolating specific bacterial proteins binding covalently to subtilin. However, this method of isolation also resulted in the isolation of a large number of bacterial proteins interacting noncovalently with subtilin, as seen in Fig. 18. Attempts to identify any bacterial protein covalently attached to subtilin by in-gel tryptic digestion

108
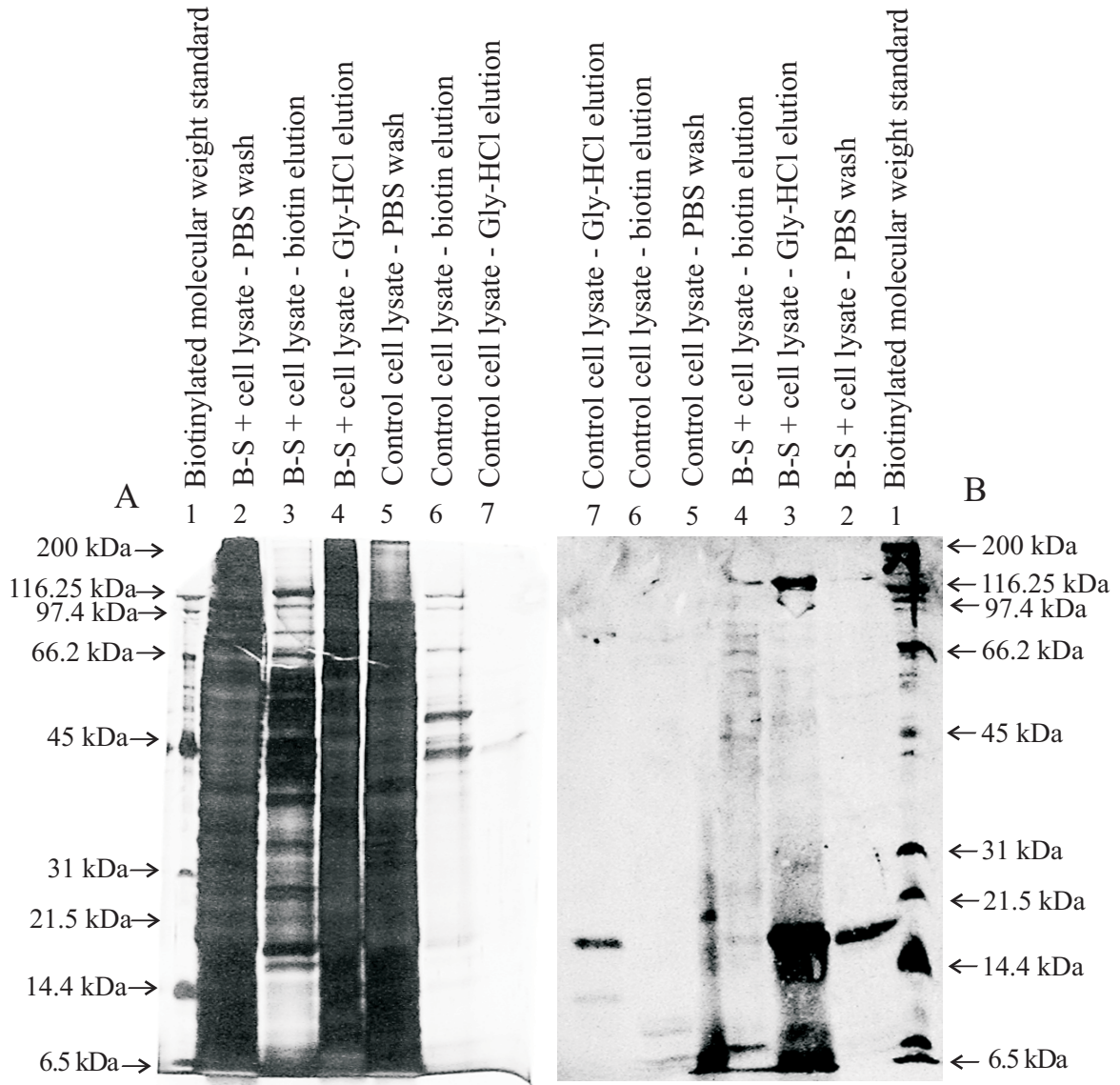
**Figure 19. Isolation of subtilin-binding bacterial proteins from *B. subtilis* 168 cells using monomeric avidin column.**

*B. subtilis* 168 cells were incubated with biotinylated subtilin (B-S) and the cells lysed after incubation. The B-S + bacterial cell lysate was applied to a monomeric avidin column to isolate subtilin-binding bacterial proteins. Non-specifically bound protein was washed off the column with a PBS wash. The bound protein was eluted first with biotin followed by glycine-HCl elution. A bacterial cell sample without any biotinylated subtilin used as a negative control was also subjected to the same procedure. After dialysis, the PBS wash and elution fractions were analyzed by SDS-PAGE. The silver stained gel shown in panel A depicts all noncovalent and covalent interactions of the bacterial proteins with subtilin. The Western blot shown in panel B depicts bacterial proteins attached covalently to subtilin.

of the protein band excised from the gel might have resulted in problems with contamination from other closely migrating, noncovalently interacting bacterial proteins. In addition, several similar bands were seen in both the wash fraction, and the fractions eluted by biotin buffer and Gly-HCl buffer in Fig. 18, suggesting the possibility that the capacity of a 2 ml monomeric avidin column to bind biotinylated subtilin was less than that of 500 µg of biotinylated subtilin that was incubated with the bacterial cells. The capacity of 1 ml of monomeric avidin gel to bind biotinylated protein is theoretically 1.2 mg (http://www.piercenet.com/files/0340as4.pdf). Since the monomeric avidin column had been originally used to isolate biotin-containing bacterial enzymes (26), it is possible that some of the proteins eluted by biotin buffer and Gly-HCl buffer were biotin-containing proteins, thereby resulting in the isolation of unexpectedly large number of proteins as seen in the silver stained gel (Fig. 18).

To overcome these problems, a more direct method of isolation of bacterial protein targets was employed. This method involved labeling nisin with a fluorescent tag so that any bacterial proteins covalently attached to nisin could be directly detected on account of the fluorescent tag on nisin. Bacterial proteins interacting with nisin could then be isolated using affinity chromatography. Therefore, nisin was labeled with fluorescein by reacting with N-hydroxysuccinimide-fluorescein (NHSF). After testing fluorescein-nisin (F-N) for antimicrobial activity, F-N was incubated with *Bacillus subtilis* 168 cells. Nisin-binding bacterial proteins were then isolated by applying the bacterial cell lysate containing F-N to an anti-FITC column and eluting the bound proteins with low pH.

Part V-1.  Fluorescein-labeling of nisin.

Since the maximum solubility of nisin at pH 8 was determined to be 0.25 mg/ml (42), 0.5 mg of nisin was reacted with N-hydroxysuccinimide-fluorescein (NHSF) at pH 8 in a total volume of 2 ml. Similar to the biotinylation reaction of subtilin (see Part II-1, 1-1), nisin was reacted with the fluorescent reagent, NHSF in a 1:1 equimolar (nanomolar) ratio to ensure that nisin would be fluorescently labeled at only one of its three lysine residues. After a 2 h incubation on ice, fluorescein-nisin (F-N) was purified using RP-HPLC and fractions collected every min. Halo assay of RP-HPLC fractions of F-N showed that F-N retained antimicrobial activity, as seen in Fig. 20.

In order to determine the mimimum amount of F-N that could be visualized by fluorescence, and also to test the stability of the fluorescein label on nisin with regard to whether the fluorescence would be quenched on a SDS-PAGE gel, varying amounts of F-N ranging from 1 µg to 15 µg were run on a mini SDS-PAGE gel and visualized on a uv transilluminator and also by silver staining the gel (Fig. 21). All amounts of F-N were visible on the gel, indicating that the fluorescein label was stable and that upto 1 µg of F-N could be detected on the UV transilluminator. The fluorescence imager, Storm 860 Imager later used to detect fluorescence was capable of detecting upto 0.1 µg of F-N.

Part V-2.  Reacting fluorescein-nisin with *B. subtilis* 168 cells.

500 µg of F-N was initially incubated with *B. cereus* cells at an $OD_{600}$ of 1 for 3 h to detect nisin-binding bacterial proteins since *B. cereus* is generally used as the test organism for the antimicrobial activity of nisin. *B. cereus* cells were also incubated with 500 µg of nisin for 3 h to compare the antimicrobial activity of F-N against *B. cereus*
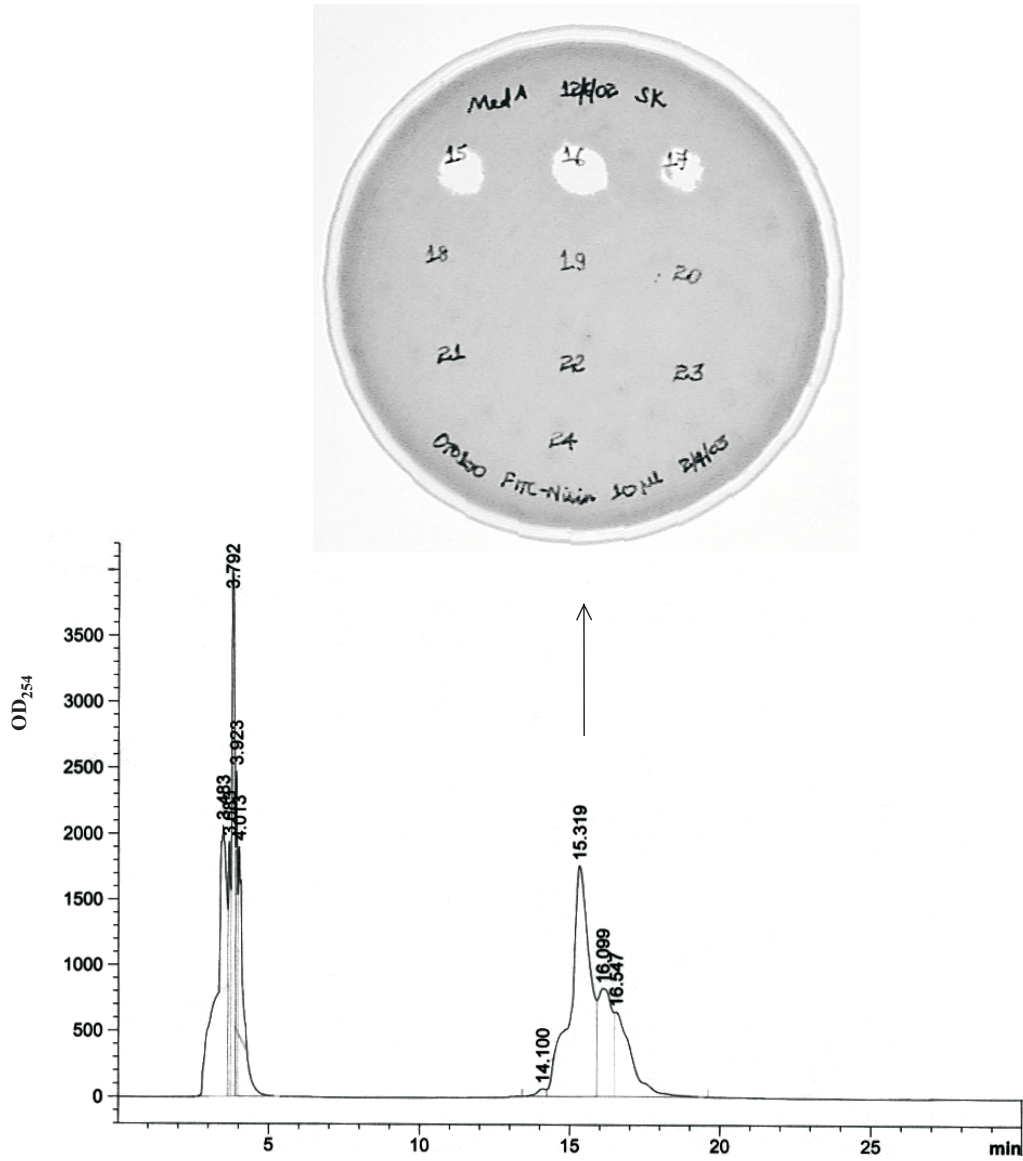
**Figure 20.  RP-HPLC and halo assay of fluorescein-nisin.**

Nisin was incubated with N-hydroxysuccinimide-fluorescein (NHSF) in a 1:1 nanomolar ratio for 2 h on ice. Fluorescein-nisin was purified using RP-HPLC. The RP-HPLC profile of fluorescein-nisin is depicted in the bottom figure. Fractions corresponding to the peak were collected every min and tested for antimicrobial activity as shown in the top figure.
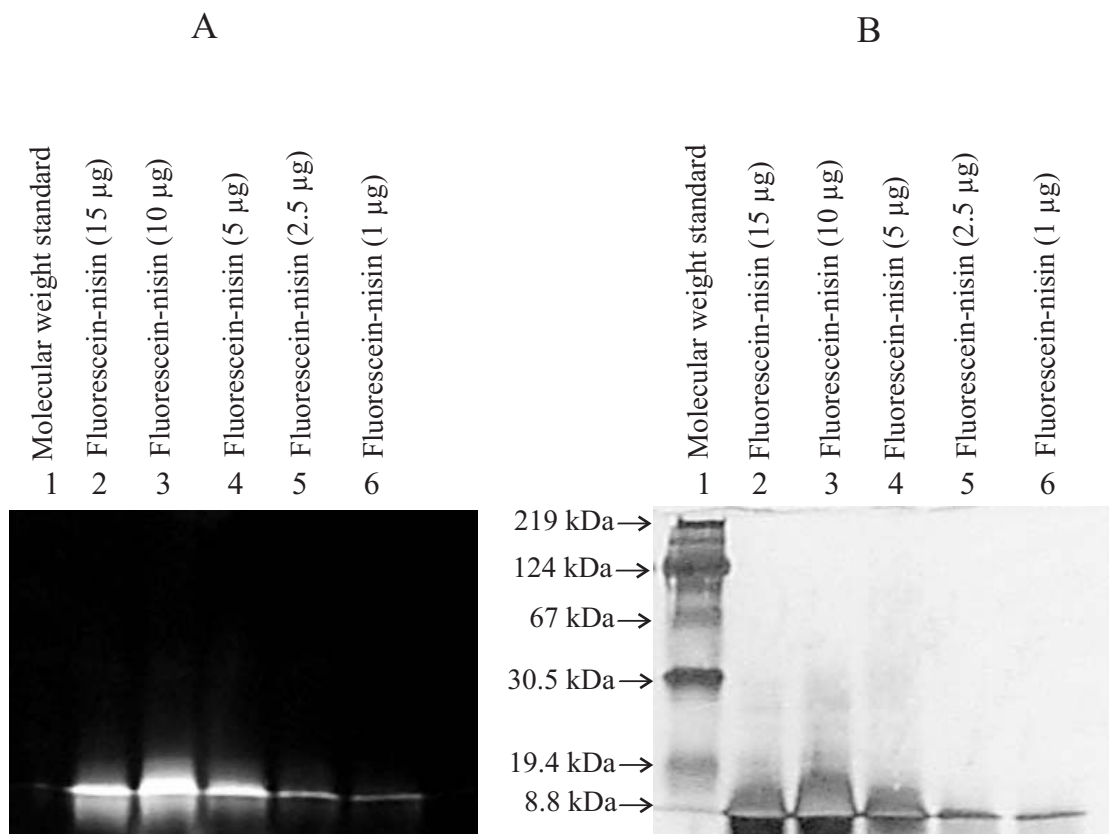
**Figure 21. SDS-PAGE analysis of fluorescein-nisin.**

RP-HPLC purified fractions of fluorescein-nisin (F-N) exhibiting antimicrobial activity were pooled together. Various concentration of F-N ranging from 1 µg to 15 µg were run on a mini SDS-PAGE gel. The gel was visualized on a uv transilluminator to detect fluorescent-nisin (panel A) when all concentrations of F-N could be detected (1 - 15 µg). The gel was also silver stained as seen in panel B.

cells with nisin. When *B. cereus* cells had been treated in a similar manner with biotinylated subtilin to isolate subtilin-binding bacterial proteins, the cells had shown evidence of cell lysis within 3 h as seen by loss of solution turbidity compared to control cells without biotinylated subtilin. However, the cells treated with F-N and nisin did not show any evidence of cell lysis after 3 h. Therefore, several changes were made, including incubating F-N with *B. cereus* cells at an $OD_{600}$ of 0.5 (instead of 1), adding 0.1% glucose to encourage cells to actively metabolize while treating with F-N, and incubating *B. cereus* cells with F-N and nisin overnight. These modifications then resulted in complete cell lysis, suggesting that subtilin is more effective at inhibiting *B. cereus* cells than nisin. The implications of these observations are discussed in the Discussion chapter.

Since the complete genome of *B. subtilis* 168 has been sequenced, fluorescein-nisin was then incubated with *B. subtilis* 168 cells to isolate and identify nisin-binding *B. subtilis* 168 proteins. Overnight incubation of F-N with *B. subtilis* 168 cells resulted in cell lysis, while the *B. subtilis* 168 cells incubated overnight without any F-N as a negative control showed no cell lysis. The cells in both samples were then completely lysed using a French pressure cell (56). The cell lysates were concentrated using YM-10 centricon centrifugal filter devices, which also decreased the amount of free, unbound F-N in the sample containing F-N. Since the YM-10 device has a nominal molecular weight cutoff of 10 kDa, some of the unbound F-N (3.8 kDa) passed through into the filtrate. The samples were boiled for 3 min and then analyzed on a SDS-PAGE gel. Fluorescent bands in the gel were detected using a Storm 860 Imager. Several high molecular weight fluorescent bands were detected in the cell lysate sample containing F-N, while no

fluorescent bands were seen in the control cell lysate sample, as expected (Fig. 22). Detection of high molecular weight fluorescent bands in the cell lysate sample containing F-N indicated that nisin was binding covalently to *B. subtilis* 168 proteins. Covalent attachment of nisin and subtilin to their bacterial protein targets indicates that the electrophilic dehydro residues of nisin and subtilin could be interacting with specific nucleophilic groups in their bacterial protein targets. This result confirmed that the type A lantibiotics nisin and subtilin are both capable of participating in covalent interactions with their bacterial protein targets.

Silver staining of the gel resulted in detection of numerous bands that represent the complex mixture of total cellular protein (Fig. 22). Of the bacterial proteins interacting both covalently and noncovalently with nisin, bacterial proteins covalently attached to nisin were of greater interest. Identification of these covalently attached proteins would probably decipher the role of the dehydro residues of nisin in covalent binding with its target proteins. To isolate these covalent bands, an immunoaffinity column with anti-FITC antibodies could be used. However, the presence of free, unbound F-N in the cell lysate + F-N sample might result in swamping of the antibody binding sites leading to inefficient elution of the required proteins. Therefore, size exclusion chromatography (SEC) was employed to eliminate free unbound, F-N from the cell lysate + F-N sample before isolating the covalently bound bacterial targets of nisin using affinity chromatography. The SEC column used had a pore size of 100 Å with an exclusion limit of 350 kDa and an inclusion limit of 2.5 kDa. However, this column was not very useful in separating the complex mixture of total bacterial protein (data not shown). For samples with a range of molecular weights such as the complex bacterial
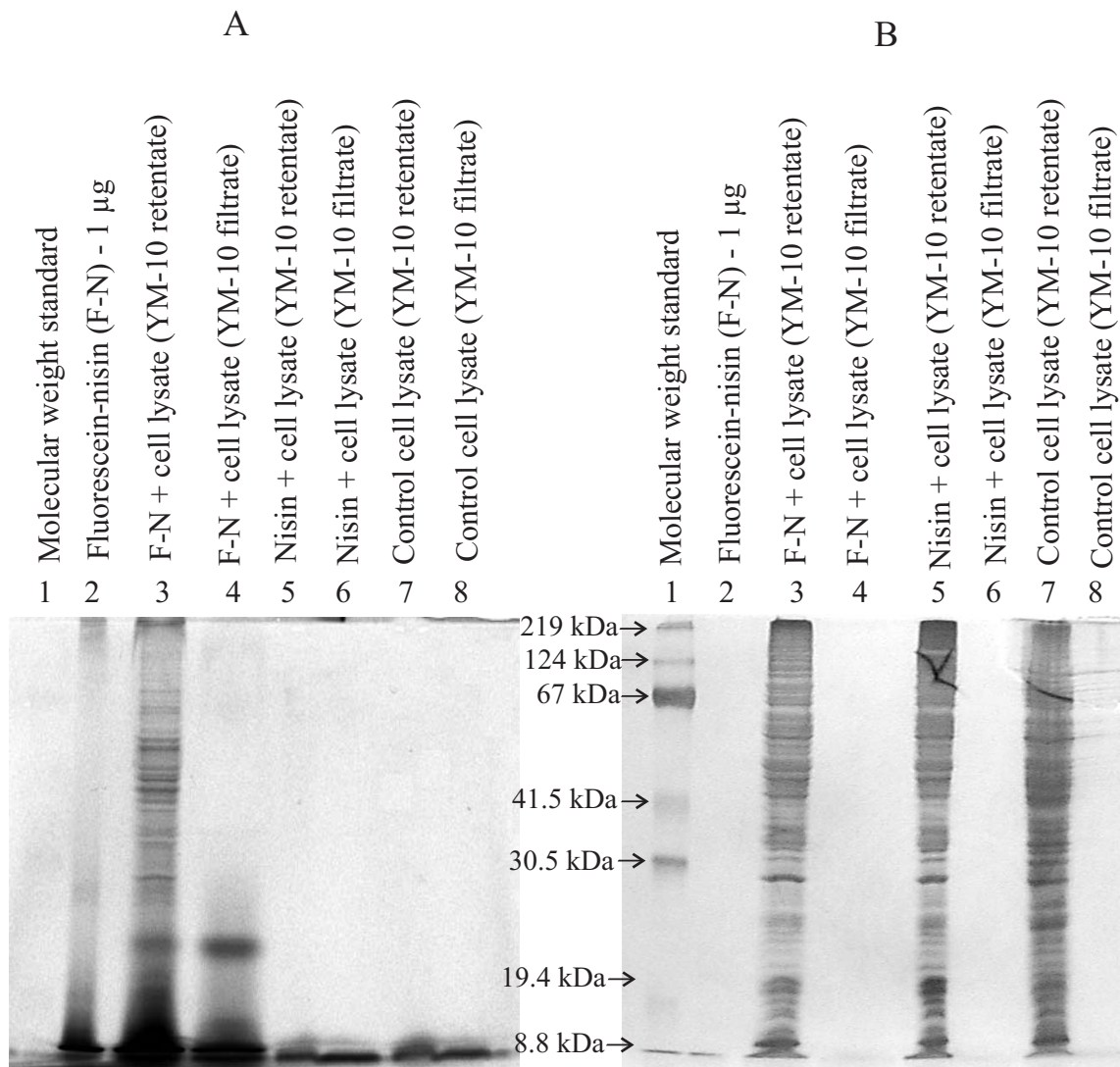
**Figure 22. SDS-PAGE analysis of *B. subtilis* 168 cells treated with fluorescein-nisin.**

*B. subtilis* 168 cells were incubated overnight with fluorescein-nisin (F-N) and nisin and the cells lysed after incubation. The cell lysate was concentrated using YM-10 centricon tubes. The retentate and filtrate samples obtained from YM-10 concentration were boiled for 3 min and then run on a SDS-PAGE gel. Fluorescent bands were detected on the gel using a Storm Imager (panel A). High molecular weight fluorescent bands represent bacterial proteins covalently attached to F-N. Control cell lysate sample without any F-N or nisin was used as a negative control. The gel was then silver stained to detect all proteins (panel B).

protein mixture, two or more columns with different pore sizes joined in series are recommended.

Part V-3.  Affinity chromatography using anti-FITC antibodies.

Since SEC could not be successfully employed in separating excess unbound F-N from the F-N bound to the bacterial proteins, the protocol for incubation of F-N with bacterial cells was modified. *Bacillus subtilis* 168 cells were first incubated with 500 μg of nisin and 0.1% of glucose for 1 h and then centrifuged before cell lysis was seen. This ensured that excess unbound nisin was removed. The cell pellet was resuspended in 10 ml of 10 mM Tris-HCl, pH 8 with 0.1% glucose and incubated for 4 h when there was a slight decrease in solution turbidity indicating cell lysis. Incubation was continued overnight when complete cell lysis was observed. The same procedure was then followed for incubation of F-N with *B. subtilis* 168 cells except that cells were incubated for 90 min before being centrifuged to remove excess unbound F-N, since F-N appears to be slightly less biologically active than nisin as observed from the halo assay.

After French pressure cell lysis, the 10 ml samples were concentrated using YM-3 tubes to ~2 ml. The samples were analyzed by SDS-PAGE, and visualized using the Storm Imager and also by silver staining (Fig. 23). Although this procedural modification did not entirely remove all of the free, unbound F-N, Fig. 23 shows a huge decrease in the amount of free, unbound F-N as compared to Fig. 22. The sample was then loaded onto an anti-FITC antibody column to isolate bacterial proteins bound to F-N.

A

B

Molecular weight standard
Fluorescein-nisin - 1 µg
F-N + cell lysate (YM-3 retentate)
F-N + cell lysate (YM-3 retentate)
F-N + cell lysate (YM-3 filtrate)
Control cell lysate (YM-3 retentate)
Control cell lysate (YM-3 retentate)
Control cell lysate (YM-3 filtrate)

1   2   3   4   5   6   7   8

219 kDa→
124 kDa→
67 kDa→
41.5 kDa →
30.5 kDa→
8.8 kDa→
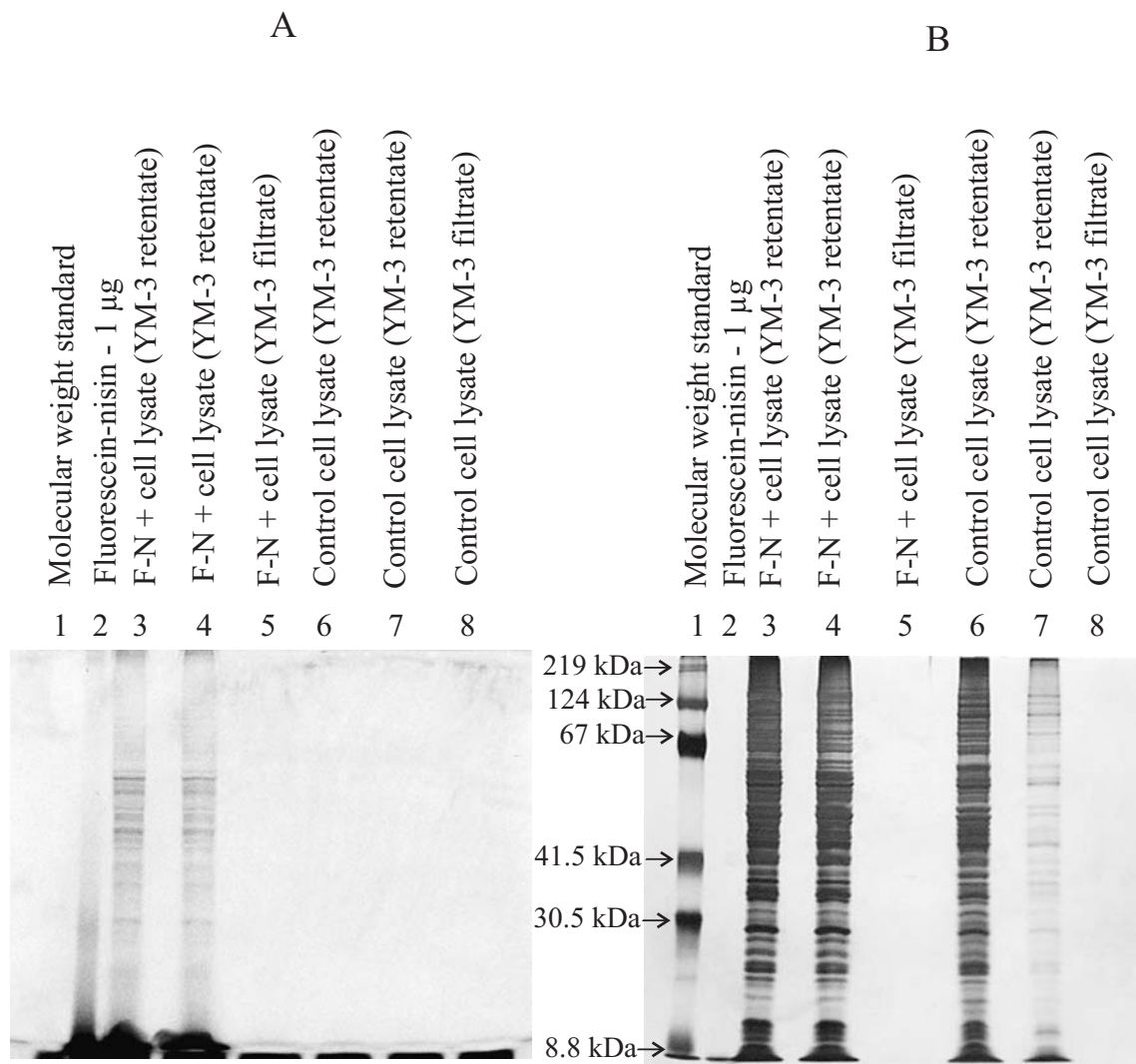
**Figure 23.  SDS-PAGE analysis of bacterial proteins bound to fluorescein-nisin.**

*B. subtilis* 168 cells were incubated with fluorescein-nisin (F-N). The cells were centrifuged to remove free, unbound F-N after 1 hour and incubation continued overnight. The cell lysate was concentrated using YM-3 centricon tubes. The retentate and filtrate samples obtained from the YM-3 concentration were run on a gel and the gel visualized using a Storm Imager (panel A). Some of the retentate samples were centrifuged to remove cell debris before loading on the gel (lanes 4 and 7). Control cell sample without any F-N was used as a negative control. The gel was silver stained as well (panel B).

3-1.  Immuno blot using anti-FITC antibodies.

To check the efficacy of the anti-FITC Ab, a dot blot was first performed to determine the effective concentrations of the anti-FITC Ab and fluorescein-nisin. All dilutions of the anti-FITC Ab used (1:100, 1:250, 1:500 and 1:1000) worked well in detecting all concentrations of F-N used (0.5, 1, 1.5, 2, 3 and 5 µg). This indicated that the anti-FITC Ab was functional in binding to F-N. This was further tested by an immuno blot using a 1:500 dilution of the anti-FITC Ab. F-N + cell lysate samples obtained after incubating F-N with *B. subtilis* 168 cells were run on a gel along with a negative control (bacterial cell lysate without any F-N), transferred onto a nitrocellulose membrane and probed with anti-FITC Ab followed by the 2º Ab-alkaline phosphatase conjugate. The F-N + cell lysate samples showed several bands while the control lanes had none as seen from the immuno blot. The bands seen on the Western blot represent bacterial proteins covalently attached to F-N. The gel was silver stained as well when all proteins were detected (Fig. 24).

3-2.  Affinity chromatography using immobilized protein A-antibody complex.

The lysate of *B. subtilis* 168 cells treated with F-N (F-N + cell lysate) was applied to two different columns, one with 50 µg of anti-FITC Ab covalently linked to a 2 ml of protein A, and another with 1 mg of anti-FITC Ab covalently linked to 2 ml of immobilized protein A. Several fractions were collected from the immunoaffinity columns, including flow-throughs, wash and elution fractions. The fractions were analyzed by SDS-PAGE and visualized using a Storm Imager. No fluorescent bands were seen in any of the elution fractions, although some fluorescent bands were noticed in the
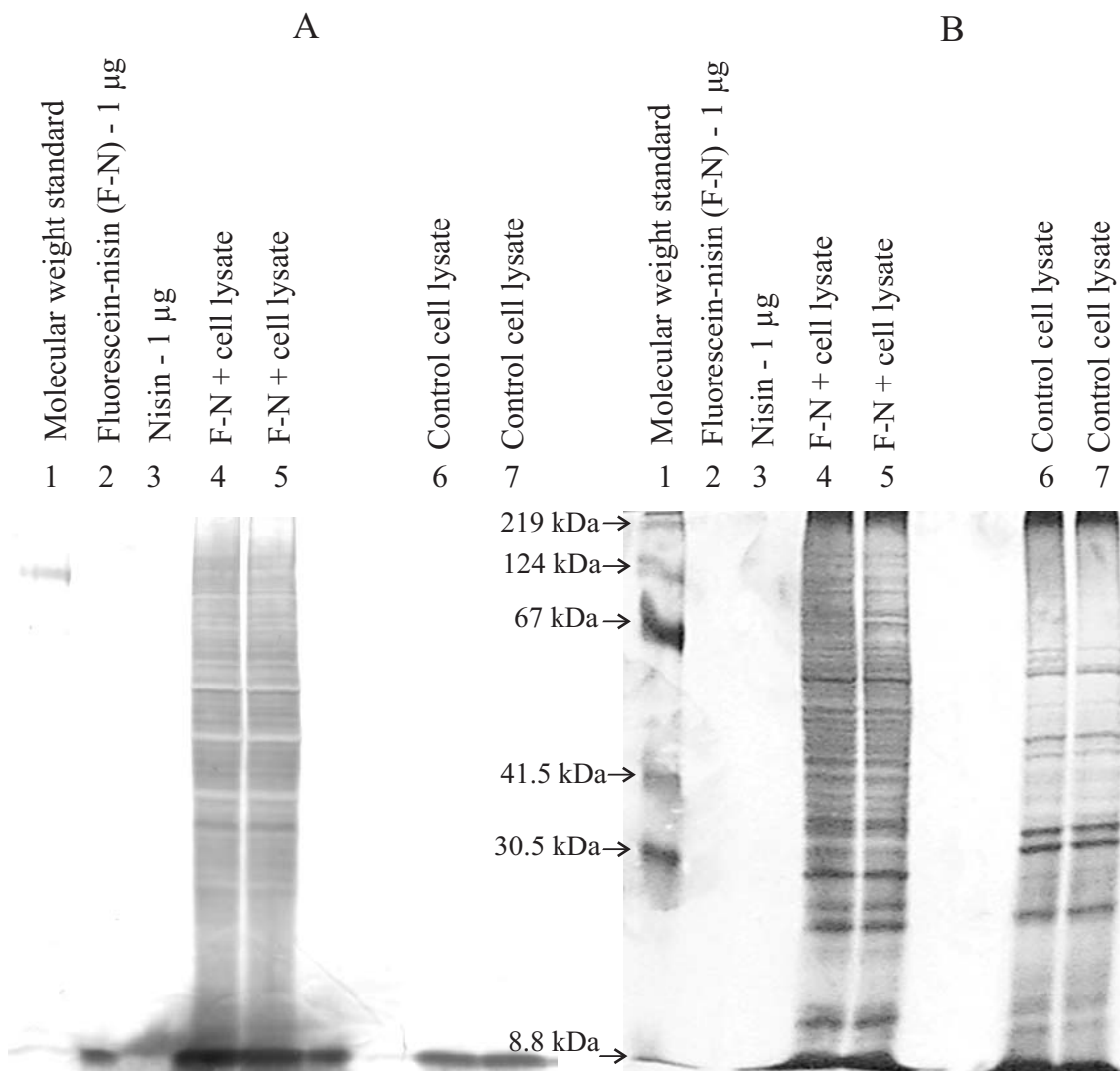
**Figure 24. Detection of bacterial proteins covalently attached to fluorescein-nisin by immunoblotting.**

*B. subtilis* 168 cells were incubated with fluorescein-nisin (F-N). The cells were centrifuged to remove free, unbound F-N after 1 hour and incubation continued overnight. A control cell sample without any F-N was used as a negative control. After incubation and cell lysis, the cell lysates were run on a gel. Some of the cell lysates were centrifuged to remove cell debris before loading on the gel (lanes 5 and 7). The gel was immunoblotted using anti-FITC antibodies to detect bacterial proteins covalently attached to F-N (panel A). The gel was silver stained as well (panel B).

120

wash lanes (data not shown). Similar results were seen with the silver stained gel, indicating that the amount of the F-N + cell lysate sample applied to the column was too large for efficient binding to either of the two columns with 50 μg and 1 mg of anti-FITC Ab. In order to test the efficiency of the immunoaffinity column, 25 μg of F-N was incubated on the immunoaffinity column containing 1 mg of bound anti-FITC Ab and eluted. The wash and elution fractions were run on a gel. No fluorescent band corresponding to F-N was seen in either the wash or the elution fractions (data not shown). As seen in Fig. 24, the immuno blot showed that the anti-FITC Ab was functional in binding to the F-N + bacterial protein. So, a probable reason for the absence of F-N + bacterial protein in the fractions obtained from the immunoaffinity procedure is that insufficient amount of anti-FITC Ab was crosslinked to the protein A column. The binding capacity of the 2 ml protein A column from Pierce is 10 mg/ml for rabbit IgG, and a loading of about 50% of the total protein A binding capacity for the Ab was recommended. However, in the above immunoaffinity experiments, a maximum concentration of 1 mg/ml (10%) of the rabbit anti-FITC Ab was used. Therefore, purification of the F-N bound protein was attempted on a much smaller scale by classic immunoprecipitation using the Sieze Classic (A) Immunoprecipitation kit from Pierce.

3-3. Classic immunoprecipitation using protein A column.

In this method, the anti-FITC antibody was incubated with the antigen, fluorescein-nisin-bacterial protein complex in solution. The immune complex was then applied to immobilized protein A, washed to remove unbound protein and then eluted by low pH. All the wash fractions and the elution fractions from the immunoprecipitation of the F-N + cell lysate sample were run on 2 identical gels. One of the gels was probed by

121

immunoblotting while the other gel was silver stained. 2 bands corresponding to ~50 kDa and ~25 kDa were seen in the first elution fraction in the silver stained gel (data not shown). The immunoblot showed a major band corresponding to ~50 kDa in addition to a few faint bands. The ~50 kDa and the ~25 kDa bands in the silver stained gel probably correspond to the heavy and light chains of the anti-FITC Ab. No other bands corresponding to fluorescein-nisin-bacterial protein complex were visible.

3-4. Small scale immunoprecipitation using immobilized protein A.

To avoid contamination of anti-FITC Ab in the antigen eluate, the Seize X Protein A Immunoprecipitation kit from Pierce was used. 400 μg of anti-FITC antibody was incubated overnight with 0.4 ml of immobilized protein A in a spin cup column placed inside a microcentrifuge tube. After overnight incubation, the bound Ab was cross-linked to immobilized protein A. Anti-FITC Ab not covalently linked to protein A was eluted by low pH several times and the elution fractions collected. To verify that sufficient anti-FITC antibody was cross-linked to the immobilized protein A, the elution fractions were run on a gel. Most of the antibody appeared to be cross-linked to protein A, since the fractions collected after incubation and cross-linking had little to no amount of antibody, as seen from the silver stained gel (Fig. 25).

To test the efficacy of the prepared immunoaffinity column, 10 μg of fluorescein-nisin (F-N) was applied to the immunoaffinity column, eluted by Gly-HCl (pH 2.8) in 6 fractions, and the collected samples analyzed by SDS-PAGE. As seen in the silver stained gel in Fig. 26, F-N eluted off the column in elution fractions # 3-6, although F-N was expected to be eluted in the first three fractions. To check whether F-N was eluting off in fractions later than elution fraction # 6, F-N was again incubated and eluted by
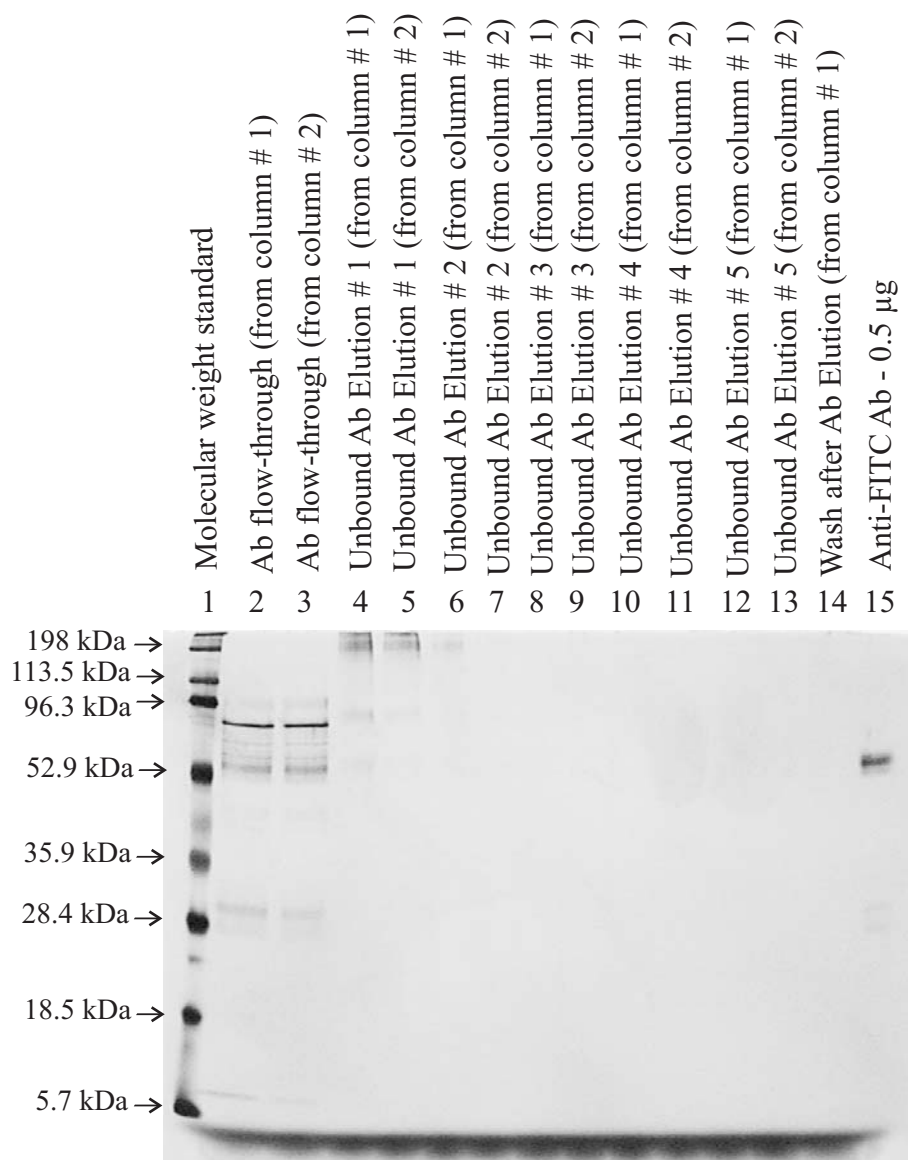
**Figure 25. Analysis of cross-linking of anti-FITC Ab to immobilized protein A.**

400 µg of anti-FITC antibody was incubated overnight with 0.4 ml of protein A gel in a spin cup column placed inside a microcentrifuge tube. Two such columns were prepared. After overnight incubation, the column was centrifuged to collect the unbound Ab flow-through. The gel was washed and the bound Ab cross-linked to protein A. The Ab not covalently linked to protein A was eluted by low pH several times. The elutions were collected after centrifuging the column and analyzed by SDS-PAGE. Most of the anti-FITC Ab appeared to be cross-linked to protein A, since no Ab was eluted by low pH from either of the two columns, as seen from the silver stained gel.
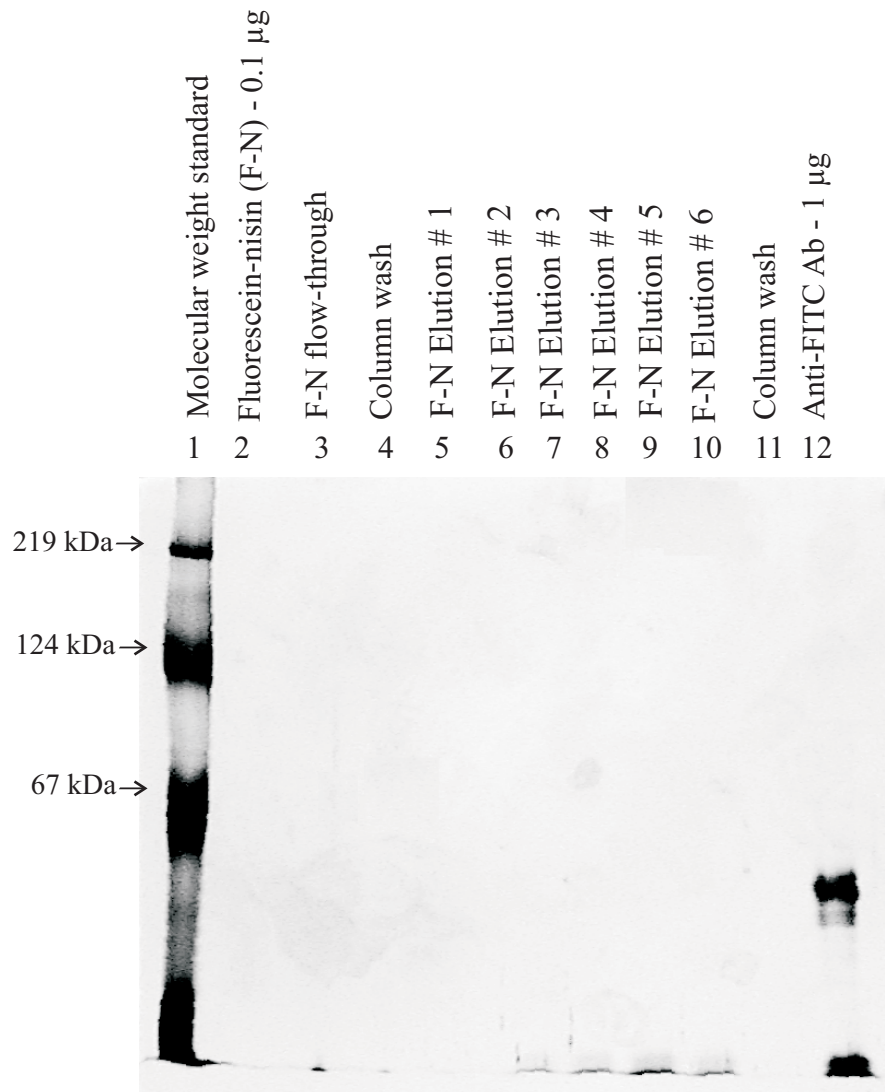
**Figure 26. SDS-PAGE analysis of fluorescein-nisin eluted by low pH from immunoaffinity column.**

10 μg of fluorescein-nisin (F-N) was incubated with anti-FITC Ab cross-linked to protein A in a spin cup column placed inside a microcentrifuge tube. After incubation, the column was centrifuged to collect the unbound F-N flow-through. The gel was washed and the bound F-N was eluted by Gly-HCl (pH 2.8) several times. The elutions were collected and analyzed by SDS-PAGE. As seen from the silver stained gel, F-N was eluted by low pH in elution fractions # 3 - # 6.

low pH ten times. When the elution fractions were analyzed on a gel, F-N was seen to be eluting in fractions as late as # 9 and # 10. F-N therefore appeared to be leaching slowly from the column rather than being eluted off the column in a few fractions.

Since the fluorescein-nisin sample appeared to be leaching from the column rather than eluting, different elution conditions were applied to optimize the elution of F-N from the column. F-N was eluted using high salt instead of low pH. 200 μl of 3.5 M magnesium chloride in 10 mM phosphate buffer, pH 7.0 was added to the F-N sample bound to immobilized anti-FITC Ab, incubated for 5 min with shaking and the eluate collected after centrifugation. This was repeated another 9 times to collect 10 fractions. The high salt in the eluates was removed by desalting using microcon YM-3 tubes and the desalted samples run on a gel. No band corresponding to F-N was seen in any of the eluates, as seen in the silver stained gel in Fig. 27. Therefore, to thoroughly disrupt the antigen-antibody binding interaction, denaturing conditions using Guanidine-HCl (Gu-HCl) and SDS were used to elute the antigen. F-N was incubated with bound antibody at 4°C overnight. F-N was first eluted with 8 M Gu-HCl in 0.1 M phosphate buffer, pH 7. The sample was incubated with 5 x 200 μl of 8 M Gu-HCl for 5 min each and then centrifuged to collect the eluate. To determine whether 8 M Gu-HCl had eluted the F-N sample completely from the column, the same sample was further eluted with 5 x 200 μl of 1% SDS by inverting the column gently 20 times and then centrifuging. The fractions eluted with 8 M Gu-HCl were desalted using microcon YM-3 tubes and all fractions run on a gel. No silver stained bands corresponding to F-N were seen in any of the fractions eluted using 8 M Gu-HCl (Fig. 27). However, a band corresponding to F-N was seen in one of the fractions eluted using 1% SDS (elution fraction #3).
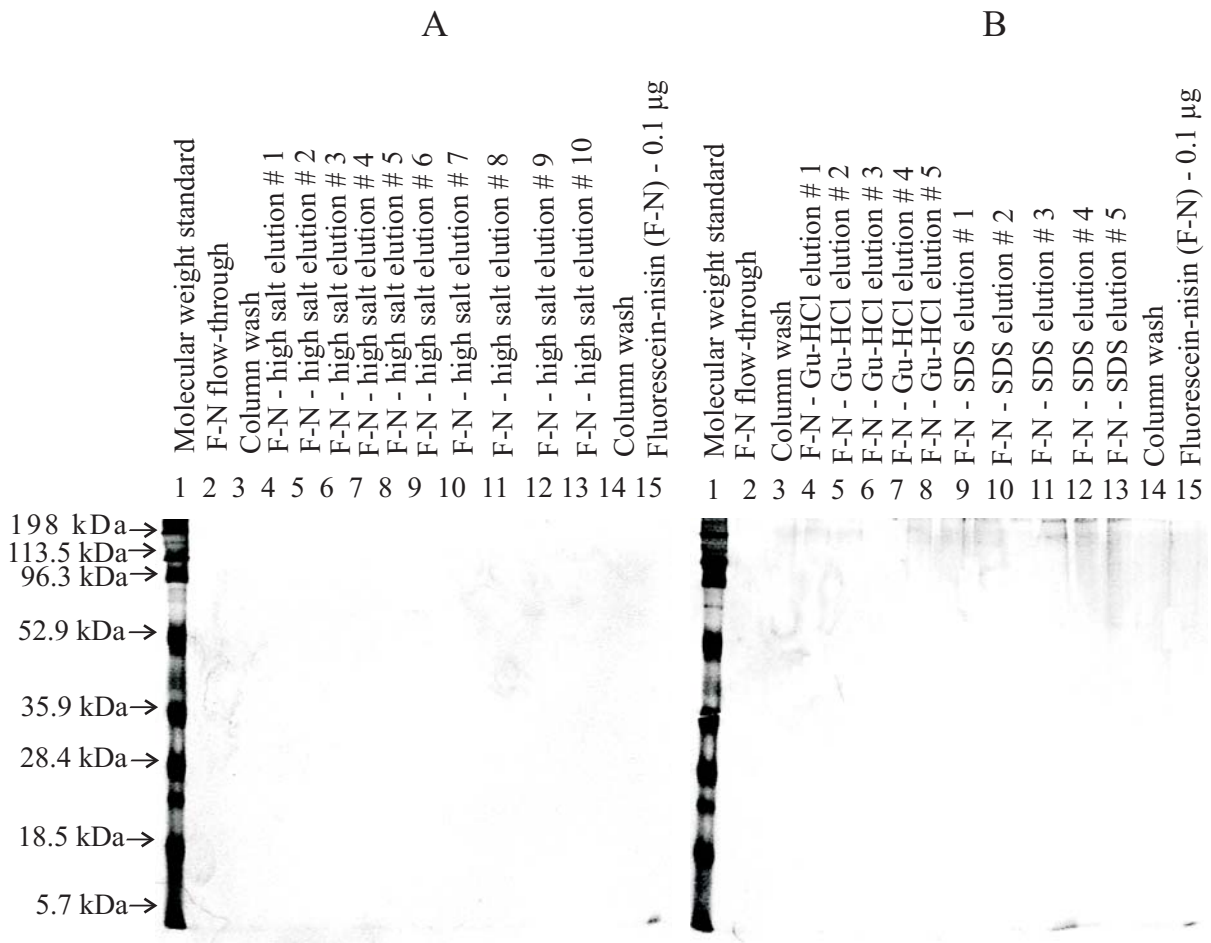
**Figure 27. SDS-PAGE analysis of fluorescein-nisin eluted by high salt, Guanidine-HCl and SDS from immunoaffinity column.**

10 µg of fluorescein-nisin (F-N) was incubated with anti-FITC Ab cross-linked to protein A in a spin cup column placed inside a microcentrifuge tube. After incubation, the column was centrifuged to collect the unbound F-N flow-through. The gel was washed and the bound F-N was eluted by high salt (3.5 M magnesium chloride) several times. The elutions were collected and analyzed by SDS-PAGE. As seen from the silver stained gel in panel A, F-N was not eluted by high salt. 10 µg of F-N was again incubated with immobilized anti-FITC Ab and eluted with 8 M Guanidine-HCl (Gu-HCl) and 1% SDS. As seen from the silver stained gel in panel B, F-N was eluted by SDS (SDS elution # 3) but not by Gu-HCl.

Although SDS could elute F-N from immobilized anti-FITC Ab, the total amount of F-N eluted was less than the amount of F-N loaded onto the column. Low pH appeared to elute F-N better than the other eluting agents. Therefore, the *B. subtilis* 168 cell lysate with bacterial proteins bound to F-N was applied to the immunoaffinity column and eluted with low pH to isolate nisin-binding bacterial proteins. Different amounts of F-N + cell lysate sample were applied to the anti-FITC column and the bound proteins eluted with low pH. Elution of a 10 µl of F-N + cell lysate sample amount applied to the column resulted in the successful isolation of a ~70 kDa protein (Fig. 28). This protein band was not seen in the eluates of the control cell lysate sample (Fig. 29). Several more attempts to isolate more of the ~70 kDa protein from the F-N + cell lysate using anti-FITC column were not very successful. Isolation of a larger amount of the ~70 kDa protein would have enabled the identification of this *B. subtilis* 168 protein by tryptic digestion followed by sequencing of the tryptic peptides and comparison of the peptide sequences with the *B. subtilis* 168 proteome. This would have probably provided an insight into the specificity and also the antimicrobial mechanism of action of nisin.

Part VI.  Detection of bacterial spore targets of subtilin and nisin in *B. cereus* spores.

Detection of covalent attachment of subtilin and nisin to bacterial proteins from vegetative bacterial cells led to experiments performed to detect, isolate and identify covalently bound subtilin and nisin targets from *B. cereus* spores. Morris *et al.* had shown that specific *B. cereus* spore membrane components of 13 kDa, 28 kDa and 29 kDa molecular weights that were covalently modified at their sulfhydryl groups caused inhibition of spore outgrowth. Nisin was shown to act as an inactivator of membrane sulfhydryl groups of germinated *B. cereus* spores toward sulfhydryl agents (51),
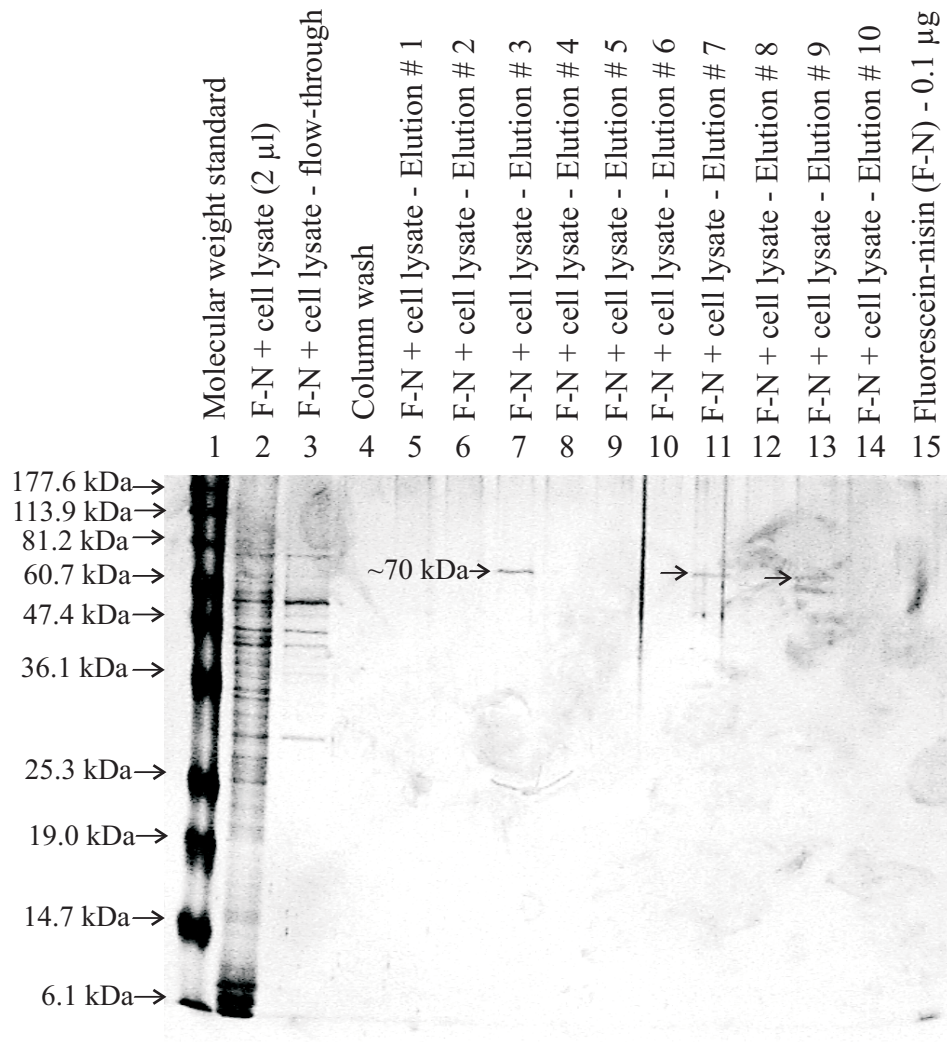
**Figure 28.  Isolation of *B. subtilis* 168 proteins bound to nisin using affinity chromatography.**

10 µl of *B. subtilis* 168 cell lysate with bacterial proteins bound to fluorescein-nisin (F-N) was incubated with anti-FITC Ab cross-linked to protein A in a spin cup column placed inside a microcentrifuge tube. After incubation, the column was centrifuged to collect the unbound F-N + cell lysate flow-through. The gel was washed and bacterial proteins bound to F-N were eluted by Gly-HCl (pH 2.8) several times. The elutions were collected and analyzed by SDS-PAGE. As seen from the silver stained gel, a ~70 kDa bacterial protein was eluted by low pH in elution fractions # 3, # 7 and # 9.

128
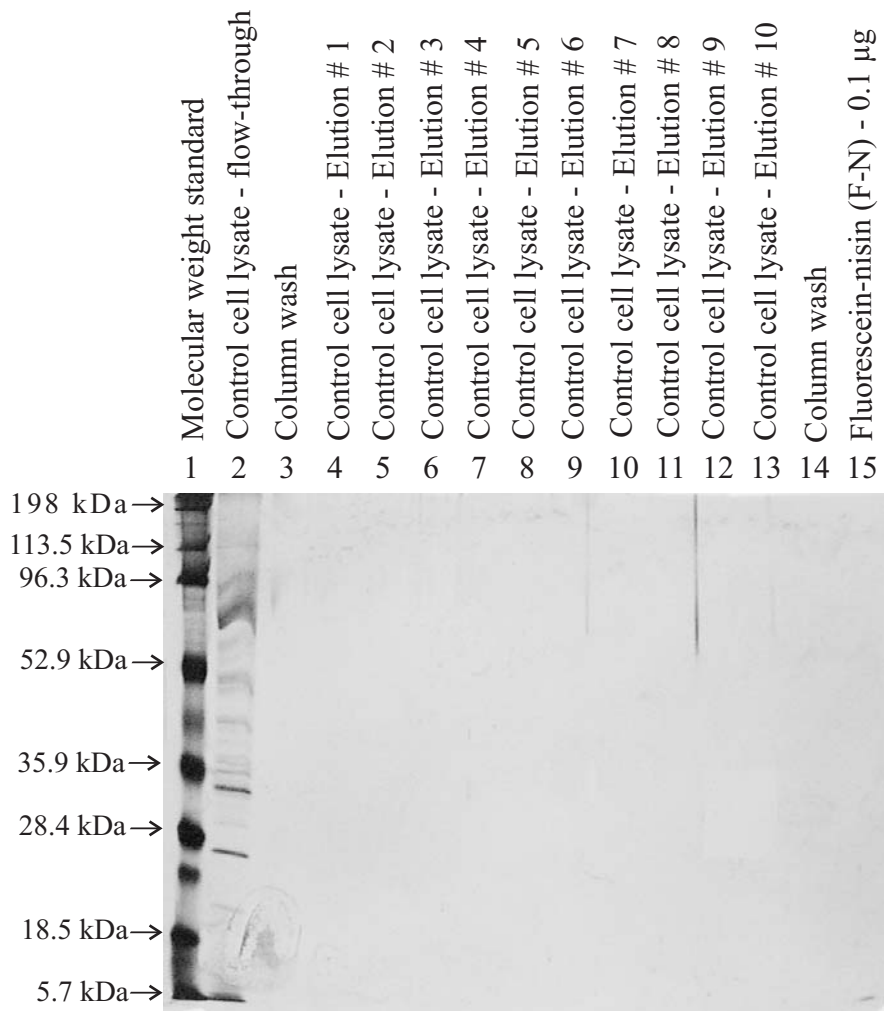
**Figure 29. SDS-PAGE analysis of *B. subtilis* 168 proteins eluted from anti-FITC column.**

*B. subtilis* 168 cell lysate without fluorescein-nisin (F-N) was used as a negative control for *B. subtilis* 168 cell lysate incubated with F-N. 15 μl of the control cell lysate was incubated with anti-FITC Ab cross-linked to protein A in a spin cup column placed inside a microcentrifuge tube. After incubation, the column was centrifuged to collect unbound proteins as the cell lysate flow-through. The gel was washed and any bound bacterial proteins were eluted by Gly-HCl (pH 2.8) several times. The elutions were collected and analyzed by SDS-PAGE. As seen from the silver stained gel, no bacterial proteins were eluted from the anti-FITC column, as expected.

suggesting that these membrane sulfhydryl groups are the natural targets of nisin. To visualize the targets of nisin in bacterial spores, electron microscopy experiments were performed on *B. cereus* spores treated with nisin (81). The targets of nisin action in bacterial spores could then be isolated by disrupting the spores incubated with nisin and subjecting the spore lysate to SDS-PAGE analysis.

Scanning electron microscopy of *B. cereus* spores treated with fluorescein-nisin and immunogold labeled nisin showed the presence of nisin targets in *B. cereus* spores. Heat-shocked *B. cereus* spores were incubated with fluorescein-nisin (F-N) for 2 h in a water bath at 37°C in 1% tryptone-Pi growth media, pH 7.4. After the 2 h incubation, the spores were observed by phase-contrast microscopy to detect spores inhibited at different stages of germination and outgrowth. A control spore sample without any F-N was also incubated in growth media for 2 h. The control sample when observed by phase-contrast microscopy showed the presence of uninhibited, elongated vegetative cells. The untreated spores and the spores treated with F-N were then prepared for scanning electron microscopy as described in Materials and Methods, Part II-18. Fig. 30 shows the scanning electron micrographs of untreated spores and spores with fluorescein-nisin bound to the spore surface. Fluorescein-nisin bound to spores was detected due to extra deposition of Au-Pd metal coating on F-N resulting in clusters. Untreated spores appeared as elongated cells due to lack of inhibition of spore outgrowth.

Nisin bound to the targets on the spore surface was then visualized by immunogold labeling. Heat-shocked *B. cereus* spores were incubated with biotinylated nisin for 3 h at room temperature. Untreated spores without biotinylated nisin were also incubated for 3 h. The samples were labeled with streptavidin-gold and collected on a
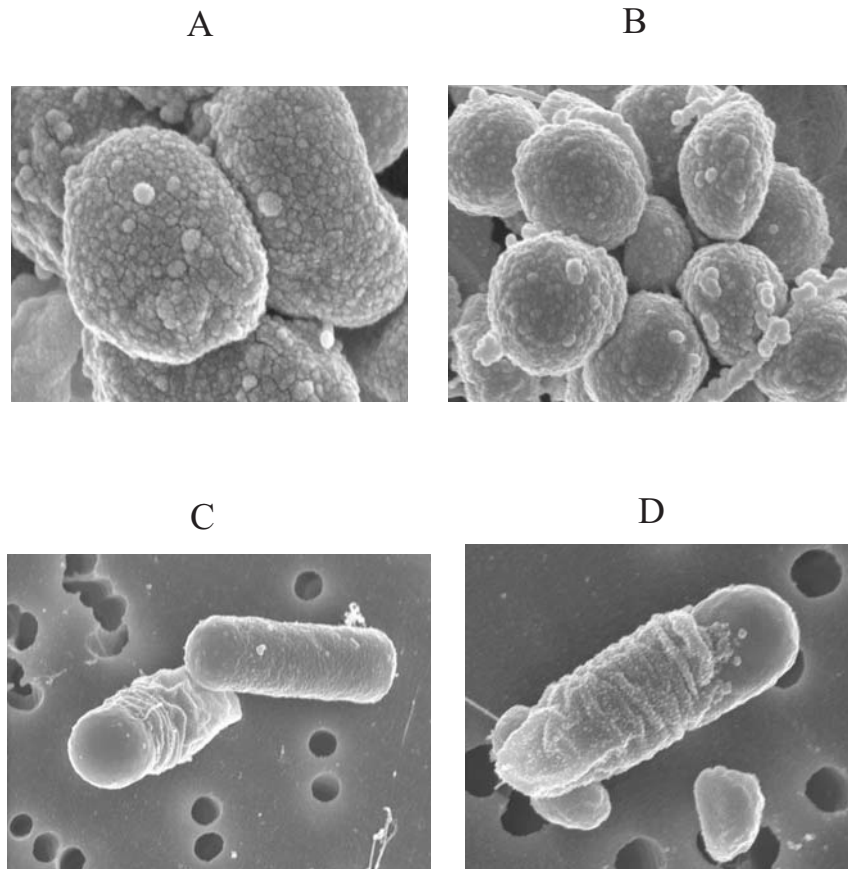
**Figure 30. SEM of *B. cereus* spores treated with fluorescein-nisin.**

*B. cereus* spores were incubated with fluorescein-nisin in growth media. The sample was collected on a nucleopore filter, fixed on the filter, dehyrated and then dried. A thin Au-Pd coating was done and the sample was viewed in a scanning electron microscope (SEM). Spores with bound fluorescein-nisin showed extra deposition of coating seen as clusters in panels A and B. SEM pictures of control spores without fluorescein-nisin are seen in panels C and D. The untreated spores appear as elongated cells due to lack of inhibition of spore outgrowth by fluorescein-nisin.

filter (3). After silver enhancement, the samples were dehydrated, dried and coated with a thin layer of chromium. Scanning electron micrographs of the spore sample treated with biotinylated nisin showed that the spores were immunogold labeled in discrete locations, indicating that nisin was binding to specific targets on the spore surface (Fig. 31). Untreated spores were not labeled with immunogold, as expected.

The scanning electron micrographs detected nisin binding sites on the spore surface. To ascertain whether nisin bound to intracellular spore targets in addition to surface targets, transmission electron microscopy (TEM) of *B. cereus* spores treated with nisin was performed. *Bacillus cereus* spores were incubated with biotinylated nisin for 2 h. A control spore sample without biotinylated nisin was also incubated for 2 h. The samples were fixed in various reagents as described in Materials and Methods, Part II-18. The samples were dehydrated and finally embedded in resin. The samples embedded in resin were sectioned using a glass knife. Upto ~150 nm thin sections of samples were obtained. For TEM, ~60 nm thin sections were required which would then be stained with 2% uranyl acetate followed by 0.1% lead citrate before viewing in a Zeiss EM10CA transmission electron microscope.

SEM of spores treated with nisin helped visualize the spore targets of nisin. To isolate the bacterial spore targets, heat-shocked *B. cereus* spores were treated with subtilin labeled with an affinity tag such as biotin. After incubation with biotinylated subtilin, the spores were observed by phase-contrast microscopy to check for inhibition of spore outgrowth. The spores were observed to be phase-dark, indicating inhibition of spore outgrowth by biotinylated subtilin. The spores were then lysed using glass beads as described in Materials and Methods, Part II-16. The lysed sample was analyzed by

A          B

C          D
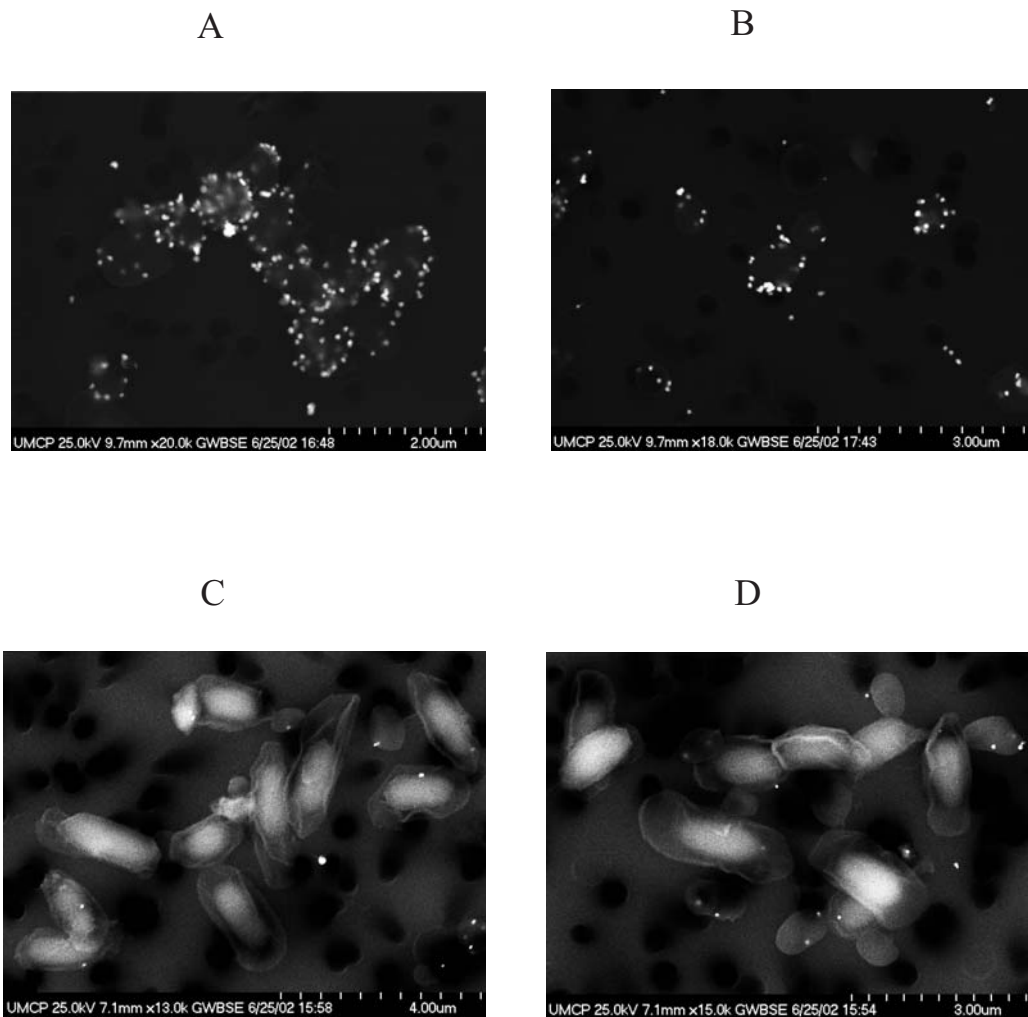
**Figure 31.  SEM of *B. cereus* spores reacted with biotinylated nisin and labeled with streptavidin-gold.**

*B. cereus* spores were incubated with biotinylated nisin. The sample was labeled with streptavidin-gold and collected on a nucleopore filter. A thin chromium coating was done and the sample was viewed in a scanning electron microscope (SEM). Nisin targets in bacterial spores were labeled with immunogold as seen in panels A and B. SEM pictures of control spores incubated without biotinylated nisin and treated with streptavidin-gold are seen in panels C and D. Immunogold labeling was not seen in the control spore sample.

SDS-PAGE and Western blot. Detection of discernible bands on the Western blot was difficult, probably because of the low concentrations of biotinylated subtilin and spores used. Also, it is possible that complete disruption of spores did not occur.

## Summary and Conclusions

Lantibiotics are antimicrobial peptides that contain unusual dehydro and lanthionine residues as a result of posttranslational modifications. These unusual residues enhance the physical, chemical and biological properties of lantibiotics. Lanthionine rings confer extreme thermal stability on lantibiotics. Dehydro residues are electrophilic which make them capable of reacting with a nucleophilic group. Study of the reactivity and specificity of the electrophilic dehydro residues toward different nucleophilic groups can be utilized to explore the range of biological targets that lantibiotics are effective against. This study could also open a new window into understanding the mechanism of the antimicrobial effect of lantibiotics. This knowledge could help in designing analogs that exhibit enhanced antimicrobial properties in addition to acting on a wider spectrum of targets.

Subtilin and nisin are type A lantibiotics that exhibit bactericidal effects against Gram-positive bacterial cells in addition to inhibiting bacterial spore outgrowth by different mechanisms (45). Previous studies on the mechanism of the antimicrobial action of lantibiotics have indicated that they act by forming pores in the cell membrane of susceptible Gram-positive bacteria. Formation of pores was proposed as being facilitated by the binding of nisin to lipid II, a cell membrane component that acts as a precursor to peptidoglycan (4). The explanation that nisin causes pore formation in sensitive Gram-positive bacteria by interacting with a peptidoglycan precursor does not satisfactorily explain its specificity, as peptidoglycan is a component of the bacterial cell wall of both Gram-positive and Gram-negative bacteria. In addition, nisin experiments performed

with artificial liposomes showed that nisin was unable to permeabilize liposomes composed of the anionic phosphatidylglycerol whereas nisin was capable of permeabilizing proteoliposomes prepared from phosphatidylglycerol and beef heart cytochrome *c* oxidase (14). Since protein-protein interactions are highly specific, this work examined the possibility that the specificity of lantibiotics subtilin and nisin is due to their binding to specific protein targets in the bacterial cell membrane, similar to the mechanism of penicillin interacting with the penicillin binding protein in the cell membrane of susceptible bacteria.

The *in vitro* selection technique of phage display was proposed for initial screening of peptide sequences interacting with subtilin to identify bacterial proteins interacting with subtilin that could be responsible for subtilin specificity. However, subtilin isolated previously from *Bacillus subtilis* 6633 by acetone-butanol precipitation had resulted in the isolation of subtilin that was very unstable, with loss of chemical activity observed in less than a day at room temperature. In this work, subtilin was isolated from *B. subtilis* LH45 using hydrophobic interaction chromatography, that resulted in subtilin that was stable even after being placed at room temperature for 2 d. Subtilin thus isolated also retained biological activity after four months of storage at –20°C. The stability of subtilin could be attributed to different factors. It is possible that using the acetone-butanol precipitation for subtilin isolation also resulted in precipitation of certain proteases that degraded subtilin. Another possibility is that the strain *B. subtilis* LH45 engineered to produce subtilin did not produce subtilin-degrading proteases. Using the hydrophobic interaction chromatographic method for subtilin isolation in addition to using the modified strain *B. subtilis* LH45 to produce subtilin probably enabled the

isolation of subtilin without proteases which would account for the increased stability of subtilin. The isolation of stable subtilin now facilitated several experiments involving subtilin that could then be compared with nisin, since subtilin and nisin are thought to possess similar mechanisms of action on account of being structural analogs. For instance, subtilin appears to be more effective at inhibiting *B. cereus* cells than nisin, as shown in Results, Part V, V-2. Since *B. cereus* and *B. anthracis* are genetically very closely related, and Coughlin *et al*. showed that formulations containing nisin, chelator, detergent, and alcohol inhibited growth of spores and vegetative cells of a test strain of *B. anthracis* (11), the above observations indicate that subtilin, like nisin, could potentially be used to combat *B. anthracis* as well. The isolation of stable subtilin demonstrated in this work enables the testing of this possibility. Stable subtilin was also isolated in this work from a cellulose column by eluting using hydrophobic conditions. This method of isolation of stable subtilin from a cellulose column points towards a new and easy method of large-scale isolation of subtilin from bacterial cultures.

Phage display experiments were then performed with subtilin to identify peptide targets of subtilin. Phage display is a powerful technique used to identify peptide ligands for a variety of target molecules such as enzymes, antibodies, cell receptors, etc. (70), (18). Phage display experiments of subtilin identified a 12-mer peptide sequence with a KTTLL motif that is characteristic of ATP binding cassette (ABC) proteins, including the initiation factor IF-2 (~78 kDa) that is involved in protein synthesis at the initiation stage. Another protein that was identified with one mismatch to the KTTLL motif was the elongation factor Tu (~43 kDa) involved in protein synthesis at the elongation stage. The identification of these two factors as possible subtilin-binding proteins is interesting in

that the elongation factor Tu was also identified as the protein target of sublancin (78). Sublancin with one dehydro residue, is another type A lantibiotic like subtilin which has three dehydro residues. Interestingly, other antibiotics containing dehydro residues such as thiostrepton and micrococcin, also inhibit protein synthesis by interfering with the function of elongation factor G (EF-G) and initiation factor IF-2 (6). This points to the possibility that inhibition of protein synthesis by type A lantibiotics such as subtilin, nisin and sublancin might be another mechanism of their antimicrobial effect, in addition to pore formation. Inhibition of protein synthesis by subtilin could perhaps be a secondary mechanism of antimicrobial action in vegetative cells, while the primary mechanism of action is pore formation in cell membranes leading to cell lysis.

Analysis of the KTTLL motif also resulted in the identification of ABC transporters similar to glutamine, anion transport and iron transport ABC transporters. The KTTLL motif is conserved among ABC transporters and forms part of the ATP binding cassette domain in ABC transporters (12). This suggests that subtilin could be binding to the ATP binding region and inhibiting ABC transporters present in the cell membrane. Binding of subtilin to ABC transporters is a likely possibility since nisin naturally binds to NisT, an ABC transporter that facilitates transport of nisin into the extracellular medium as part of nisin biosynthesis and secretion (see Fig. 4) (68). Nisin, subtilin and epidermin also bind to other membrane-bound ABC transporters (NisGEF, SpaIFG and EpiFEG, respectively) that are involved in providing immunity to the producer organism against the secreted lantibiotic (55). Binding of subtilin to specific ABC transporters in the cell membrane of susceptible bacteria would thus contribute to the specificity of antimicrobial action of subtilin.

Phage display studies were then followed by *in vivo* studies performed to isolate and identify subtilin-binding and nisin-binding proteins from intact bacterial cells to confirm the phage display results. Isolation of bacterial proteins binding to subtilin or nisin followed by identification of these subtilin-binding and nisin-binding bacterial proteins would then provide an insight into the specificity and antimicrobial mechanism of action of subtilin and nisin. Subtilin-binding bacterial proteins were isolated by applying the cell lysate of *B. cereus* and *B. subtilis* 168 cells reacted with biotinylated subtilin onto a monomeric avidin column. Bacterial proteins interacting both covalently and non-covalently with subtilin were isolated from both the *B. cereus* and *B. subtilis* samples. Of the bacterial proteins interacting covalently with subtilin, proteins corresponding to ~78 kDa and ~43 kDa were of particular interest, since the phage display results identified initiation factor IF-2 (~78 kDa) and elongation factor Tu (~ 43 kDa) as possible bacterial protein targets of subtilin.

To detect bacterial proteins that nisin interacts with, nisin was fluorescently labeled with fluorescein and reacted with *B. subtilis* 168 cells. Nisin, like subtilin, also bound both covalently and noncovalently to bacterial proteins. Several bacterial proteins covalently bound to fluorescein-nisin (F-N) were detected using a Storm Imager and also by immuno blotting. Both subtilin and nisin were shown to interact covalently with bacterial proteins. This indicated that the dehydro residues of subtilin and nisin were probably involved in the covalent interaction of subtilin and nisin with target proteins. The electrophilic dehydro residues of subtilin and nisin are capable of reacting with free nucleophilic groups in bacterial protein targets, probably a –SH group in a Cys residue, or a –OH group in Ser or Thr.

Addition of subtilin or nisin to a –SH group appears to be a more likely possibility. Morris *et al.* reported that nisin inhibited the reactivity of bacterial membrane sulfhydryl groups toward sulfhydryl agents, suggesting that the membrane sulfhydryl groups might be the biological target of nisin in its antimicrobial activity (51). Also, Rose *et al.* reported that when glutathione, a tripeptide with a free –SH group, is reacted with nisin, the number of glutathione molecules that can add on to nisin or nisin variant is dependent on the number of dehydro residues in nisin (60). This indicated that the dehydro residues of nisin are the sites of addition of glutathione to nisin. Further, experiments performed where nisin was reacted with Cys and monitored by NMR showed a decrease in the peak intensity of the dehydro residues (1). Another good reason in favor of the possibility of addition of nisin to a –SH group is that this occurs naturally during the formation of lanthionine or β-methyl-lanthionine residues in lantibiotics, when the dehydroalanine or dehydrobutyrine residue reacts with neighboring Cys residues to form lanthionine or β-methyl-lanthionine residues (24).

Covalent attachment of antibiotic to its target protein is seen in only a few other antibiotics such as fosfomycin (46) and thiostrepton (9). Thiostrepton, a peptide antibiotic with three dehydro alanines and one dehydrobutyrine, binds covalently to the Cys residue of its target protein TipAS through its dehydro alanine residue (9). In view of these observations, it is reasonable to propose that subtilin and nisin bind covalently to the –SH group of Cys residues in target proteins through their dehydro residues. A possible mechanism of covalent attachment of subtilin to bacterial proteins is proposed in Fig. 32.
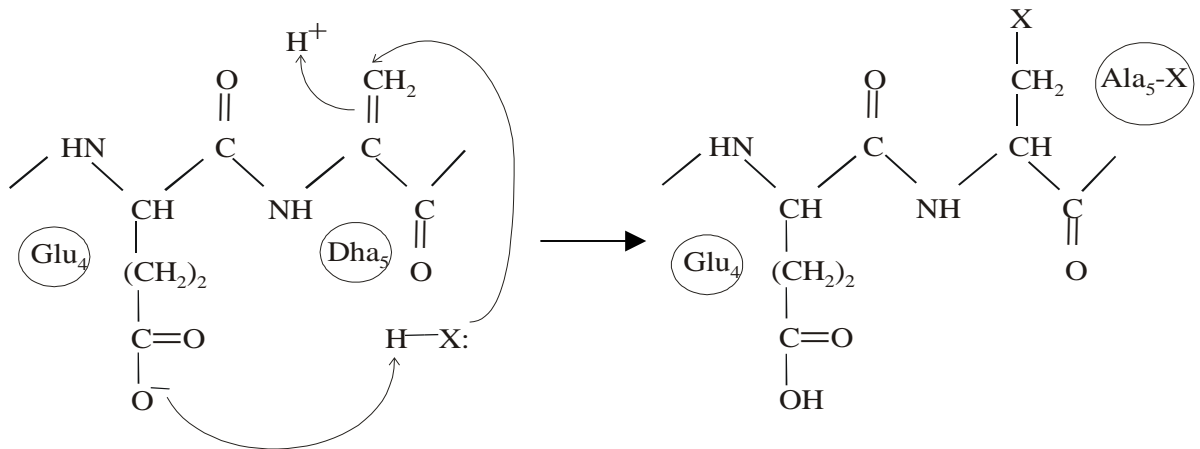
**Figure 32**. **Possible mechanism of covalent attachment of subtilin to bacterial proteins**. The electrophilic dehydro alanine residue (Dha$_5$) in subtilin is shown to react with a free nucleophilic group present in a bacterial protein. The carboxyl group of Glu$_4$ in subtilin is capable of behaving as a general base to remove a proton from a potential nucleophile such as a free -SH group in the Cys residue of a bacterial protein. The nucleophile can then attack the methylene group of Dha$_5$ in a Michael-type addition reaction resulting in covalent attachment of subtilin to the bacterial protein.

To isolate and identify bacterial proteins interacting with nisin, affinity chromatography was employed. Several different immunoaffinity columns with anti-FITC antibodies were then used to isolate bacterial proteins bound to fluorescein-nisin (F-N). However, when F-N was applied to the immunoaffinity column and eluted using low pH, it was difficult to elute the F-N sample completely from the immunoaffinity column. Other elution conditions including high salt and denaturing conditions (8 M Guanidine-HCl and 1% SDS) were also used, but the high salt and the 8 M Gu-HCl failed to elute any F-N from the column, although the 1% SDS eluted a small amount of F-N from the column. When bacterial proteins bound to F-N were applied to the immunoaffinity column and eluted using low pH, this resulted in the elution of a very low

amount of a protein of ~70 kDa size. Attempts were made to elute a sufficiently large amount of the ~70 kDa protein from the anti-FITC column so as to enable identification of the nisin-binding bacterial protein using trypsin digestion in conjunction with tandem mass spectrometry. However, it was difficult to elute the bound protein sample from the column completely. A similar problem was observed with sublancin, another type A antibiotic, when immunoaffinity chromatography was employed to isolate sublancin-binding bacterial proteins. A control experiment performed to elute $^{35}$S-sublancin from an anti-sublancin antibody column using low pH failed to elute $^{35}$S-sublancin completely from the column (59). It is possible that nisin and sublancin bind very tightly to components of the immunoaffinity column which results in low elution of nisin or sublancin from the column.

Future experiments can attempt to perform 2-D gel analysis of the bacterial proteins interacting with fluorescein-nisin to facilitate the isolation and identification of nisin-binding bacterial proteins using tandem mass spectrometry. This would help in understanding the specificity and antimicrobial mechanism of action of nisin and subtilin, since nisin and subtilin are structural analogs and possess a similar mechanism of action. This knowledge should prove useful in the design of structural variants of gene-encoded subtilin and nisin that can be more effectively targeted against bacterial pathogens.

# References

1.  **Balgley, B.** 2001. Ph.D. Thesis. Characterization of the dehydro residues of nisin, and construction and characterization of structural analogs of the lantibiotic sublancin. University of Maryland, College Park, MD.

2.  **Banerjee, S. and J. N. Hansen**. 1988. Structure and expression of a gene encoding the precursor of subtilin, a small protein antibiotic. Journal of Biological Chemistry **263**:9508-9514.

3.  **Bendayan, M.** 2000. A review of the potential and versatility of colloidal gold cytochemical labeling for molecular morphology. Biotechnic and Histochemistry **75**:203-242.

4.  **Breukink, E., I. Wiedemann, C. van Kraaij, O. P. Kuipers, H. Sahl, and B. de Kruijff**. 1999. Use of the cell wall precursor lipid II by a pore-forming peptide antibiotic. Science **286**:2361-2364.

5.  **Brotz, H., G. Bierbaum, K. Leopold, P. E. Reynolds, and H. G. Sahl**. 1998. The lantibiotic mersacidin inhibits peptidoglycan synthesis by targeting lipid II. Antimicrobial Agents and Chemotherapy **42**:154-60.

6.  **Cameron, D. M., J. Thompson, P. E. March, and A. E. Dahlberg**. 2002. Initiation factor IF2, thiostrepton and micrococcin prevent the binding of elongation factor G to the *Escherichia coli* ribosome. Journal of Molecular Biology **319**:27-35.

7.  **Chan, W. C., B. W. Bycroft, M. L. Leyland, L. Y. Lian, and G. C. Roberts**. 1993. A novel post-translational modification of the peptide antibiotic subtilin: isolation and characterization of a natural variant from *Bacillus subtilis* A.T.C.C. 6633. Biochemistry Journal **291**:23-27.

8.  **Chan, W. C., H. M. Dodd, N. Horn, K. Maclean, L. Y. Lian, B. W. Bycroft, M. J. Gasson, and G. C. Roberts**. 1996. Structure-activity relationships in the peptide antibiotic nisin - role of dehydroalanine. Applied and Environmental Microbiology **62**:2966-2969.

9.  **Chiu, M. L., M. Folcher, P. Griffin, T. Holt, T. Klatt, and C. J. Thompson**. 1996. Characterization of the covalent binding of thiostrepton to a thiostrepton-induced protein from *Streptomyces lividans*. Biochemistry **35**:2332-2341.

10. **Cole, J. L. and J. C. Hansen**. 1999. Analytical ultracentrifugation as a contemporary biomolecular research tool. Journal of Biomolecular Techniques **10**:163-176.

11. **Coughlin, R., L. Connelly, J. H. Crabb, and A. Turetsky**. 2003. Effects of nisin formulations on *Bacillus anthracis*, *megaterium*, and *cereus*. [Webpage] Available at http://www.asmbiodefense.org/2003monabs.asp.

12. **Croop, J. M.** 1998. Evolutionary relationships among ABC transporters, p. 101-116. *In* S. V. Ambudkar and M. M. Gottesman (eds.), Methods in enzymology. ABC transporters: Biochemical, cellular and molecular aspects. Academic Press, Inc., San Diego.

13. **de Vos, W. M., O. P. Kuipers, J. R. Vandermeer, and R. J. Siezen**. 1995. Maturation pathway of nisin and other lantibiotics: Posttranslationally modified antimicrobial peptides exported by Gram-positive bacteria. Molecular Microbiology **17**:427-437.

14. **Driessen, A. J. M., H. W. van den Hooven, W. Kuiper, M. van de Kamp, H.-G. Sahl, R. N. H. Konings, and W. N. Konings**. 1995. Mechanistic studies of lantibiotic-induced permeabilization of phospholipid vesicles. Biochemistry **34**:1606-1614.

15. **Durchschlag, H.** 1986. Specific volumes of biological macromolecules and some other molecules of biological interest, p. 45-128. *In* H.-J. Hinz (ed.), Thermodynamic data for biochemistry and biotechnology. Springer-Verlag, Germany.

16. **Entian, K.-D. and W. M. De Vos**. 1996. Genetics of subtilin and nisin biosynthesis. Biosynthesis of lantibiotics. Antonie van Leeuwenhoek **69**:109-117.

17. **Feeney, R. E., J. A. Garibaldi, and E. M. Humphreys**. 1948. Nutritional studies on subtilin formation by *Bacillus subtilis*. Archives of Biochemistry and Biophysics **17**:435-445.

18. **FitzGerald, K.** 2000. In vitro display technologies - new tools for drug discovery. Drug Discovery Today **5**:253-258.

19. **Gao, F. H., T. Abee, and W. N. Konings**. 1991. Mechanism of action of the peptide antibiotic nisin in liposomes and cytochrome *c* oxidase-containing proteoliposomes. Applied and Environmental Microbiology **57**:2164-2170.

20. **Gill, S. C. and P. H. von Hippel**. 1989. Calculation of protein extinction coefficients from amino acid sequence data. Analytical Biochemistry **182**:319-326.

21. **Hansen, J. C., J. Lebowitz, and B. Demeler**. 1994. Analytical centrifugation of complex macromolecular systems. Biochemistry **33**:13155-13163.

22. **Hansen, J. N.** 1993. The molecular biology of nisin and its structural analogs, p. 93-120. *In* D. Hoover and L. Steenson (eds.), Bacteriocins of lactic acid bacteria. Academic Press, New York.

23. **Hansen, J. N.** 1994. Nisin as a model food preservative, p. 69-93. *In* F. M. Clydesdale (ed.), CRC Critical Reviews in Food Science and Nutrition. CRC Press, Inc., Boca Raton, Florida.

24. **Hansen, J. N.** 1997. Nisin and related antimicrobial peptides, p. 437-470. *In* W. R. Strohl (ed.), Biotechnology of antibiotics. Marcell Dekker, Inc., New York.

25. **Helgason, E., O. A. Okstad, D. A. Caugant, H. A. Johansen, A. Fouet, M. Mock, I. Hegna, and A.-B. Kolsto**. 2000. *Bacillus anthracis*, *Bacillus cereus*, and *Bacillus thuringiensis* - one species on the basis of genetic evidence. Applied and Environmental Microbiology **66**:2627-2630.

26. **Henrikson, K. P., S. H. Allen, and W. L. Maloy**. 1979. An avidin monomer affinity column for the purification of biotin-containing enzymes. Analytical Biochemistry **94**:366-370.

27. **Hunt, D. F., J. R. Yates III, J. Shabanowitz, S. Winston, and C. R. Hauer**. 1986. Protein sequencing by tandem mass spectrometry. Proceedings of the National Academy of Sciences, USA **83**:6233-6237.

28. **Jack, R., G. Bierbaum, C. Heidrich, and H. G. Sahl**. 1995. The genetics of lantibiotic biosynthesis. Bioessays **17**:793-802.

29. **Jack, R. W. and G. Jung**. 1998. Natural peptides with antimicrobial activity. Chimia **52**:48-55.

30. **Jack, R. W. and H. G. Sahl**. 1995. Unique peptide modifications involved in the biosynthesis of lantibiotics. Trends in Biotechnology **13**:269-278.

31. **Jung, G.** 1991. Lantibiotics - ribosomally synthesized biologically active polypeptides containing sulfide bridges and $\alpha,\beta$–didehydroamino acids. Angewandte Chemie **30**:1051-1068.

32. **Kleinkauf, H. and H. von Dohren**. 1984. Peptide antibiotics, p. 283-307. *In* H. Pape and H. J. Rehm (eds.), Biotechnology, Microbial products II. VCH Verlagsgesellschaft mbH, Weinheim, Germany.

33. **Kordel, M., F. Schuller, and H. G. Sahl**. 1989. Interaction of the pore forming-peptide antibiotics Pep 5, nisin and subtilin with non-energized liposomes. Federation European Biochemical Society Letters **244**:99-102.

34. **Kotra, L. P., J.-P. Samama, and S. Mobashery**. 2002. $\beta$–lactamases and resistance to $\beta$–lactam antibiotics, p. 123-159. *In* K. Lewis, A. A. Salyers, H. W. Taber, and R. G. Wax (eds.), Bacterial resistance to antibiotics. Marcel Dekker, Inc., New York.

35. **Kuipers, O. P., G. Bierbaum, B. Ottenwalder, H. M. Dodd, N. Horn, J. Metzger, T. Kupke, V. Gnau, R. Bongers, P. van den Bogaard, H. Kosters, H. S. Rollema, W. M. de Vos, R. J. Siezen, G. Jung, F. Gotz, H.-G. Sahl, and M. J. Gasson**. 1996. Protein engineering of lantibiotics. Antonie van Leeuwenhoek **69**:161-170.

36. **Kunst, F., N. Ogasawara, I. Moszer, A. M. Albertini, G. Alloni, V. Azevedo, M. G. Bertero, P. Bessieres, A. Bolotin, S. Borchert, R. Borriss, L. Boursier, A. Brans, M. Braun, S. C. Brignell, S. Bron, S. Brouillet, C. V. Bruschi, B. Caldwell, V. Capuano, N. M. Carter, S. K. Choi , J. J. Codani, I. F. Connerton, A. Danchin, and *et al*.** 1997. The complete genome sequence of the gram-positive bacterium *Bacillus subtilis*. Nature **390**:249-256.

37. **Kussmann, M., E. Nordhoff, H. Rahbek-Nielsen, S. Haebel, M. Rossel-Larsen, L. Jakobsen, J. Gobom, E. Mirgorodskaya, A. Kroll-Kristensen, L. Palm, and P. Roepstorff**. 1997. Matrix-assisted laser desorption/ionization mass spectrometry sample preparation techniques designed for various peptide and protein analytes. Journal of Mass Spectrometry 593-601.

38. **Laemmli, U. K.** 1970. Cleavage of structural proteins during the assembly of the head of bacteriophage T4. Nature **227**:680-685.

39. **Laue, T. M.** 1995. Sedimentation equilibrium as thermodynamic tool, p. 427-452. *In* M. L. Johnson and G. K. Ackers (eds.), Methods in Enzymology, Energetics of biological macromolecules. Academic Press, New York, USA.

40. **Link, A. J., J. Eng, D. M. Schieltz, E. Carmack, G. J. Mize, D. R. Morris, B. M. Garvik, and J. R. Yates III**. 1999. Direct analysis of protein complexes using mass spectrometry. Nature Biotechnology **17**:676-682.

41. **Liu, W.** 1992. Ph.D. Thesis. Studies of the antimicrobial mechanism of subtilin by site-directed mutagenesis and elucidation of chemical, physical and antimicrobial properties of nisin. University of Maryland, College Park, MD.

42. **Liu, W. and J. N. Hansen**. 1990. Some chemical and physical properties of nisin, a small-protein antibiotic produced by *Lactococcus lactis*. Applied and Environmental Microbiology **56**:2551-2558.

43. **Liu, W. and J. N. Hansen**. 1991. Conversion of *Bacillus subtilis* 168 to a subtilin producer by competence transformation. Journal of Bacteriology **173**:7387-7390.

44. **Liu, W. and J. N. Hansen**. 1992. Enhancement of the chemical and antimicrobial properties of subtilin by site-directed mutagenesis. Journal of Biological Chemistry **267**:25078-25085.

45. **Liu, W. and J. N. Hansen**. 1993. The antimicrobial effect of a structural variant of subtilin against outgrowing *Bacillus cereus* T spores and vegetative cells occurs by different mechanisms. Applied and Environmental Microbiology **59**:648-651.

46. **Marquardt, J. L., E. D. Brown, W. S. Lane, T. M. Haley, Y. Ichikawa, C. H. Wong, and C. T. Walsh**. 1994. Kinetics, stoichiometry, and identification of the reactive thiolate in the inactivation of UDP-GlcNAc enolpyruvoyl transferase by the antibiotic fosfomycin. Biochemistry **33**:10646-10651.

47. **Moll, G. N., G. C. K. Roberts, W. N. Konings, and A. J. M. Driessen**. 1996. Mechanism of lantibiotic-induced pore-formation. Antonie van Leeuwenhoek **69**:185-191.

48. **Moll, G., J. Clark, W. Chan, B. Bycroft, G. Roberts, W. Konings, and A. Driessen**. 1997. Role of transmembrane pH gradient and membrane binding in nisin pore formation. Journal of Bacteriology **179**:135-140.

49. **Morency, H., M. Mota-Meira, G. LaPointe, C. Lacroix, and M. C. Lavoie**. 2001. Comparison of the activity spectra against pathogens of bacterial strains producing a mutacin or a lantibiotic. Canadian Journal of Microbiology **47**:322-331.

50. **Morris, S. L. and J. N. Hansen**. 1981. Inhibition of *Bacillus cereus* spore outgrowth by covalent modification of a sulfhydryl group by nitrosothiol and iodoacetate. Journal of Bacteriology **148**:465-471.

51. **Morris, S. L., R. C. Walsh, and J. N. Hansen**. 1984. Identification and characterization of some bacterial membrane sulfhydryl groups which are targets of bacteriostatic and antibiotic action. Journal of Biological Chemistry **259**:13590-13594.

52. **Nes, I. F. and J. R. Tagg**. 1996. Novel lantibiotics and their pre-peptides. Antonie van Leeuwenhoek **69**:89-97.

53. **Neu, H. C.** 1992. The crisis in antibiotic resistance. Science **257**:1064-1072.

54. **Noren, K. A. and C. J. Noren**. 2001. Construction of high-complexity combinatorial phage display peptide libraries. Methods **23**:169-178.

55. **Otto, M., A. Peschel, and F. Gotz**. 1998. Producer self-protection against the lantibiotic epidermin by the ABC transporter EpiFEG of Staphylococcus epidermidis Tu3298. FEMS Microbiol Lett **166**:203-11.

56. **Otvos, L. Jr, I. O, M. E. Rogers, P. J. Consolvo, B. A. Condie, S. Lovas, P. Bulet, and M. Blaszczyk-Thurin**. 2000. Interaction between heat shock proteins and antimicrobial peptides. Biochemistry **39**:14150-14159.

57. **Paik, S. H., A. Chakicherla, and J. N. Hansen**. 1998. Identification and characterization of the structural and transporter genes for, and the chemical and biological properties of, sublancin 168, a novel lantibiotic produced by *Bacillus subtilis* 168. Journal of Biological Chemistry **273**:23134-23142.

58. **Ralston, G.** 1993. Introduction to Analytical Ultracentrifugation. Beckman Instruments, Inc., California, USA.

59. **Rodriguez, V. W.** 1999. Ph.D. Thesis. The characterization of the downstream border of the subtilin operon in *Bacillus subtilis* LH45; and an investigation of the cellular target of the lantibiotic sublancin produced by *Bacillus subtilis* 168. University of Maryland, College Park, MD.

60. **Rose, N. L., P. Sporns, H. M. Dodd, M. J. Gasson, F. A. Mellon, and L. M. McMullen**. 2003. Involvement of dehydroalanine and dehydrobutyrine in the addition of glutathione to nisin. Journal of Agricultural and Food Chemistry **51**:3174-78.

61. **Ruhr, E. and H. G. Sahl**. 1985. Mode of action of the peptide antibiotic nisin and influence on the membrane potential of whole cells and on cytoplasmic and artificial membrane vesicles. Antimicrobial Agents and Chemotherapy **27**:841-5.

62. **Sahl, H.-G., R. W. Jack, and G. Bierbaum**. 1995. Biosynthesis and biological activities of lantibiotics with unique post-translational modifications. European Journal of Biochemistry **230**:827-853.

63. **Sahl, H. G., M. Kordel, and R. Benz**. 1987. Voltage-dependent depolarization of bacterial membranes and artificial lipid bilayers by the peptide antibiotic nisin. Archives of Microbiology **149**:120-124.

64. **Sambrook, J., E. F. Fritsch, and T. Maniatis**. 1989. Molecular cloning. A laboratory manual. Second Edition. Cold Spring Harbor Lab Press, Cold Spring Harbor.

65. **Saris, P. E. J., T. Immonen, M. Reis, and H.-G. Sahl**. 1996. Immunity to lantibiotics. Antonie van Leeuwenhoek **69**:151-159.

66. **Schagger, H. and G. von Jagow**. 1987. Tricine-sodium dodecyl sulfate-polyacrylamide gel electrophoresis for the separation of proteins in the range from 1 to 100 kDa. Analytical Biochemistry **166**:368-379.

67. **Schuller, F., R. Benz, and H. G. Sahl**. 1989. The peptide antibiotic subtilin acts by formation of voltage-dependent multi-state pores in bacterial and artificial membranes. European Journal of Biochemistry **182**:181-186.

68. **Siegers, K., S. Heinzmann, and K. D. Entian**. 1996. Biosynthesis of lantibiotic nisin. Posttranslational modification of its prepeptide occurs at a multimeric membrane-associated lanthionine synthetase complex. Journal of Biological Chemistry **271**:12294-12301.

69. **Siezen, R. J., O. P. Kuipers, and W. M. de Vos**. 1996. Comparison of lantibiotic gene clusters and encoded proteins. Antonie van Leeuwenhoek **69**:171-184.

70. **Smith, G. P. and J. K. Scott**. 1993. Libraries of peptides and proteins displayed on filamentous phage, p. 228-257. *In* R. Wu (ed.), Methods in enzymology. Recombinant DNA Part H. Academic Press, Inc., San Diego.

71. **Stevens, K. A., B. W. Sheldon, N. A. Klapes, and T. R. Klaenhammer**. 1991. Nisin treatment for inactivation of *Salmonella* species and other gram-negative bacteria. Applied and Environmental Microbiology **57**:3613-3615.

72. **Stoffels, G., A. Guthmundsdottir, and T. Abee**. 1994. Membrane-associated proteins encoded by the nisin gene cluster may function as a receptor for the lantibiotic carnocin UI49. Microbiology **140**:1443-1450.

73. **Stoffels, G., J. Nissen-Meyer, A. Gudmundsdottir, K. Sletten, H. Holo, and I. F. Nes**. 1992. Purification and characterization of a new bacteriocin isolated from a *Carnobacterium* sp. Applied and Environmental Microbiology **58**:1417-1422.

74. **Strohl, W. R.** 1997. Industrial antibiotics: Today and the future, p. 1-47. *In* W. R. Strohl (ed.), Biotechnology of antibiotics. Marcell Dekker, Inc., New York.

75. **van Belkum, M. J., J. Kok, G. Venema, H. Holo, I. F. Nes, W. N. Konings, and T. Abee**. 1991. The bacteriocin lactococcin A specifically increases permeability of lactococcal cytoplasmic membranes in a voltage-independent, protein-mediated manner. Journal of Bacteriology **173**:7934-7941.

76. **van den Hooven, H. W., C. A. Spronk, M. van de Kamp, R. N. Konings, C. W. Hilbers, and F. J. van de Van**. 1996. Surface location and orientation of the lantibiotic nisin bound to membrane-mimicking micelles of dodecylphosphocholine and of sodium dodecylsulphate. European Journal of Biochemistry **235**:394-403.

77. **Vestling, M. M., C. M. Murphy, and C. Fenselau**. 1990. Recognition of trypsin autolysis products by high-performance liquid chromatography and mass spectrometry. Analytical Chemistry **62**:2391-2394.

78. **Villaruz, A. E. C.** 2002. Ph.D. Thesis. Studies in the antimicrobial mechanism of the lantibiotics nisin and sublancin, and a *Bacillus subtilis* 168 expression system that displays the lantibiotic antimicrobial peptide sublancin on the cell surface. University of Maryland, College Park, MD.

79. **Wiedemann, I., E. Breukink, C. van Kraaij, O. P. Kuipers, G. Bierbaum, B. de Kruijff, and H. G. Sahl**. 2001. Specific binding of nisin to the peptidoglycan precursor lipid II combines pore formation and inhibition of cell wall biosynthesis for potent antibiotic activity. Journal of Biological Chemistry **276**:1772-9.

80. **Wilson, D. R. and B. B. Finlay**. 1998. Phage display: applications, innovations, and issues in phage and host biology. Canadian Journal of Microbiology **44**:313-329.

81. **Yamada, S., M. Sugai, H. Komatsuzawa, and A. Matsumoto**. 2001. Suppressed localization of a major autolysin on *Staphylococcus aureus* treated with tetracycline. Journal of Electron Microscopy **50**:359-64.

82. **Zahner, H. and H.-P. Fiedler**. 1995. The need for new antibiotics: Possible ways forward, p. 67-84. *In* P. A. Hunter, G. K. Darby, and N. J. Russell (eds.), Fifty years of antimicrobials: Past perspectives and future trends. Cambridge University Press, Great Britain.

83. **Zuber, P., M. M. Nakano, and M. A. Marahiel**. 1993. Peptide antibiotics, p. 897-916. *In* A. L. Sonenshein, J. A. Hoch, and R. Losick (eds.), *Bacillus subtilis* and other Gram-positive bacteria: Biochemistry, physiology and molecular genetics. American Society for Microbiology, Washington, D.C.